EVALUATION OF AMBIENT PARTICULATE MATTER (PM) SAMPLER PERFORMANCE THROUGH WIND TUNNEL TESTING

A Thesis

by

ABHINAV GUHA

Submitted to the Office of Graduate Studies of
Texas A&M University
in partial fulfillment of the requirements for the degree of

MASTER OF SCIENCE

May 2009

Major Subject: Biological and Agricultural Engineering

EVALUATION OF AMBIENT PARTICULATE MATTER (PM) SAMPLER PERFORMANCE THROUGH WIND TUNNEL TESTING

A Thesis

by

ABHINAV GUHA

Submitted to the Office of Graduate Studies of
Texas A&M University
in partial fulfillment of the requirements for the degree of

MASTER OF SCIENCE

Approved by:

Chair of Committee,	Bryan W. Shaw
Committee Members,	William B. Faulkner
	Dennis O' Neal
	Calvin B. Parnell
Head of Department,	Gerald Riskowski

May 2009

Major Subject: Biological and Agricultural Engineering

ABSTRACT

Evaluation of Ambient Particulate Matter (PM) Sampler Performance Through Wind Tunnel Testing. (May 2009)

Abhinav Guha, B.E., Mumbai University, India

Chair of Advisory Committee: Dr. Bryan W. Shaw

Previous studies have demonstrated that EPA approved federal reference method (FRM) samplers can substantially misrepresent the fractions of particles being emitted from agricultural operations due to the relationship between the performance characteristics of these samplers and existing ambient conditions. Controlled testing in a wind tunnel is needed to obtain a clearer understanding and quantification of the performance shifts of these samplers under varying aerosol concentrations, wind speeds and dust types.

In this study, sampler performance was tested in a controlled environment wind tunnel meeting EPA requirements for particulate matter (PM) sampler evaluation. The samplers evaluated included two low-volume PM_{10} and Total Suspended Particulate (TSP) pre-separators. The masses and particle size distributions (PSDs) obtained from the filters of tested samplers were compared to those of a collocated isokinetic sampler. Sampler performance was documented using two parameters: cut-point (d_{50}) and slope. The cut-point is the particle diameter corresponding to 50% collection efficiency of the pre-separator while the slope is the ratio of particle sizes corresponding to cumulative collection efficiencies of 84.1% and 50% ($d_{84.1}/d_{50}$) or 50% and 15.9% ($d_{50}/d_{15.9}$) or the

square root of 84.1% and 15.9% ($d_{84.1}/d_{15.9}$). The test variables included three levels of wind speeds (2-, 8-, and 24-km/h), five aerosol concentrations varying from 150 to 1,500 $\mu g/m^3$ and three aerosols with different PSDs (ultrafine Arizona Road Dust (ARD), fine ARD and cornstarch).

No differences were detected between the performance of the flat and louvered FRM PM_{10} samplers ($\alpha = 0.05$). The mean cut-point of both the PM_{10} samplers was 12.23 μm while the mean slope was 2.46. The mean cut-point and slope values were statistically different from the upper limit of EPA-specified performance criteria of 10.5 μm for the cut-point and 1.6 for the slope. The PM_{10} samplers over-sampled cornstarch but under-sampled ultrafine and fine ARD. The performance of the dome-top TSP sampler was close to the isokinetic sampler, and thus it can be used as a reference sampler in field sampling campaigns to determine true PM concentrations. There were large variations in the performance of the cone-top TSP samplers as compared to the isokinetic sampler. Dust type and wind speed along with their interaction had an impact on sampler performance. Cut-points of PM_{10} samplers were found to increase with increasing wind speeds. Aerosol concentration did not impact the cut-points and slopes of the tested samplers even though their interaction with dust types and wind speeds had an impact on sampler performance.

ACKNOWLEDGMENTS

First and foremost, sincere gratitude goes to my thesis advisor, Dr. Bryan W. Shaw, for supporting me financially over the course of my graduate study in the Department of Biological and Agricultural Engineering (BAEN) at Texas A&M University. His guidance and constant encouragement were always strong motivators. I would like to thank Dr. William B. Faulkner for supervising the project and providing the necessary tools to execute the experiments. His mentoring taught me to think more analytically and address scientific problems better. I greatly appreciate his painstaking reviews of my thesis drafts and his valuable suggestions, which I believe have largely improved my ability to write a science/research paper. I would also like to thank Dr. Calvin B. Parnell who guided me during my decision to transfer to the Air Quality group in the BAEN department. He has always advised students with great wisdom and is a great teacher.

Several family members and friends have supported me through this challenging endeavor. My brother Abhishek's perseverance and dedication towards his family is something I really appreciate; I cannot forget his valuable advice on academic pursuits. My sister-in-law, Trupti, has been a messiah clearing my doubts concerning statistical analysis and has always been willing to discuss all research issues, even though my research is very foreign to her interests. I can't thank her enough. My friends Chintan and Moshika have always been willing to listen to me and help me out with my research. They have been my pillars of support during the last six months when I was toiling

really hard. Their words of inspiration meant a whole lot more during those tough times. My uncle, Debashish Bose, is a father figure to both me and my brother. His generosity, words of wisdom and unflinching support to pursue our dreams make us indebted to him in so many ways.

Lastly, sitting several miles away is our mother, Reena Guha, who has made unbelievable sacrifices and adjustments since our father's demise to make sure we get the best of education and opportunities in life. Mom, we love you and I just want to let you know that slowly but surely, we are approaching our better years.

TABLE OF CONTENTS

Page

LIST OF FIGURES

LIST OF TABLES

Page

CHAPTER I

INTRODUCTION

An important piece of environmental legislation came into effect in the US in 1970 when the Clean Air Act Amendments (CAAA) were passed by the Congress (Cooper and Alley, 2002). This law provided the federal government the authority to clean up air pollution in the US through the actions of the US Environmental Protection Agency (EPA) which came into being the same year. The 1970 CAAA also required EPA to set National Ambient Air Quality Standards (NAAQS) for pollutants considered harmful to public health and welfare (USEPA, 1996). The NAAQS are a two-tiered regulatory standard composed of primary and secondary standards. The former are aimed at protecting public health (especially the health of "sensitive" population groups) while the secondary standards are aimed at protecting public welfare and preventing harmful effects such as reduced visibility, irritation to skin, and damage to animals, crops, vegetation and buildings. In 1971, EPA promulgated NAAQS for six criteria pollutants known to cause adverse health effects and adopted the primary and secondary standards as the upper limits of permissible pollutant concentrations which, if exceeded, would lead to unacceptable air quality (Federal Register, 1971). The original NAAQS for particulate matter (PM) was set for total suspended particulate (TSP) with the 24-hour primary standard set at 260 $\mu g/m^3$ and the 24-hour secondary standard at 150 $\mu g/m^3$. EPA has modified the PM standard several times over the years based on new evidence

---

This thesis follows the style of *Transactions of the ASABE*.

relating health risks to PM.

The current PM NAAQS regulates two categories of PM: $PM_{2.5}$, comprised of particles with an aerodynamic equivalent diameter (AED) less than or equal to 2.5 µm, and PM_{10} comprised of particles with an AED of 10 µm or less. In 2006, EPA modified the primary $PM_{2.5}$ standard from the original daily mean of 65 µg/m^3 to 35 µg/m^3 (98th percentile) while the annual standard was retained at 15 µg/m^3 (arithmetic mean) (CFR, 2006a). EPA uses PM_{10} as an indicator of the concentration of particles with an AED less than or equal to 10 µm but greater than 2.5 µm, known as inhalable coarse particles (PM_c or PM_{coarse}). In 2006, the primary 24-hour PM_{10} standard of 150 µg/m^3 (99th percentile) was reaffirmed in order to gather more data about measured PM_c concentrations which may lead to promulgation of a concentration standard for PM_c in the future. EPA, however, revoked the annual PM_{10} standard since available health evidence did not suggest a substantial link between long-term exposure to PM_{10} and health concerns (CFR, 2006a). The secondary standards of both $PM_{2.5}$ and PM_{10} are equivalent to the primary standards.

EPA has granted authority to state air pollution regulatory agencies (SAPRAs) to regulate air emissions including that of PM. The 1977 CAAA instituted the new source review (NSR) permitting program for stationary sources emitting regulated pollutants. NSR is a pre-construction permitting program designed to ensure that air quality in a particular region is not degraded significantly by the addition of new or modified sources of pollution. It also ensures that pollutant emissions from a new source will not contribute to an area being deemed as non-attainment for any criteria pollutant. An area

is designated as "non-attainment" for $PM_{2.5}$ or PM_{10} if there are multiple violations of the PM NAAQS leading to reduction of permissible emission limits/standards for all sources of PM in that area. Some SAPRAs use the property line concentrations of PM at a facility to determine if they are in compliance even though the use of NAAQS as a property line concentration limit is not encouraged by EPA.

There are a number of methods by which a source can demonstrate compliance with permit requirements. One method is monitoring of ambient air through gravimetric sampling near a source using EPA-approved Federal Reference Method (FRM) samplers or Federal Equivalent Method (FEM) samplers. A sampling methodology is designated as FRM or FEM through the provisions of 40 CFR, Part 53 (CFR, 2006b). EPA designates those PM_{10} samplers which meet the requirements specified in 40 CFR, Part 53, Subpart D and meet additional specifications set forth in 40 CFR, Part 50, Appendix J (CFR, 2006c) as FRM samplers. Appendix J specifies a measurement principle based on extracting an air sample from the atmosphere with a sampler that incorporates inertial separation of PM_{10} followed by collection of the particles on a filter over a 24-hour period. For a sampler to qualify as a FEM sampler, it must meet the performance specifications set forth in 40 CFR, Part 53, Subpart D and demonstrate comparability to a reference method as required by 40 CFR, Part 53, Subpart C (CFR, 2006d).

Size selective PM samplers are employed to measure PM_{10} concentrations. A PM_{10} pre-separator is assumed to have performance characteristics that can be described by a cumulative lognormal probability distribution with a cut-point (d_{50}) and a slope. EPA has defined the performance criteria for FRM PM_{10} samplers. A FRM PM_{10}

sampler is required to have a cut-point (d_{50}) of 10±0.5 μm and a slope of 1.5±0.1 (CFR, 2001). The cut-point of a sampler is defined as the particle diameter at which 50% of the particles of that size penetrate the pre-separator of the sampler and are deposited on the filter while the other half do not (Hinds, 1999). The slope of a sampler is the slope of the lognormal collection efficiency curve of the pre-separator and is defined as the ratio of the particle sizes corresponding to collection efficiencies of 84.1% and 50% ($d_{84.1}/d_{50}$) or 50% and 15.9% ($d_{50}/d_{15.9}$) or the square root of the ratio of ($d_{84.1}/d_{15.9}$) (Hinds, 1999). A particle size distribution (PSD) is a distribution of particles by volume, mass or number. For regulatory purposes, a PSD based on mass distribution is used. Most ambient aerosols are represented by PSDs which are lognormal in nature and characterized by a mass median diameter (MMD) and geometric standard deviation (GSD) (Hinds, 1999).

Most size-selective PM samplers rely on a pre-separator inlet consisting of an impactor plate to allow particles of a desired size to penetrate the sampler and collect on a filter while preventing non-desired particles from penetrating the sampler and reaching the filter. These impactors work by rapidly changing the air flow direction, which results in particles with a large momentum continuing on their path and impacting onto a plate (Figure 1). The efficiency of a size-selective sampler to remove particles from the air stream drawn into the sampler and prevent them from penetrating to the filter is described by a fractional efficiency curve (FEC). A PM sampler's FEC combined with the idealized ambient PSD can be used to determine the expected mass density distribution of the sampled aerosol on the sampler filter (Buser et al., 2007a). No size selective sampler is capable of allowing 100% of all particles below a given size to

penetrate while rejecting 100% of all the particles above that size. In addition, impacted particles may bounce, or as the layer of particles on the impaction surface increases, some of the particles may begin to blow off and deposit onto the filter, leading to sampling errors.

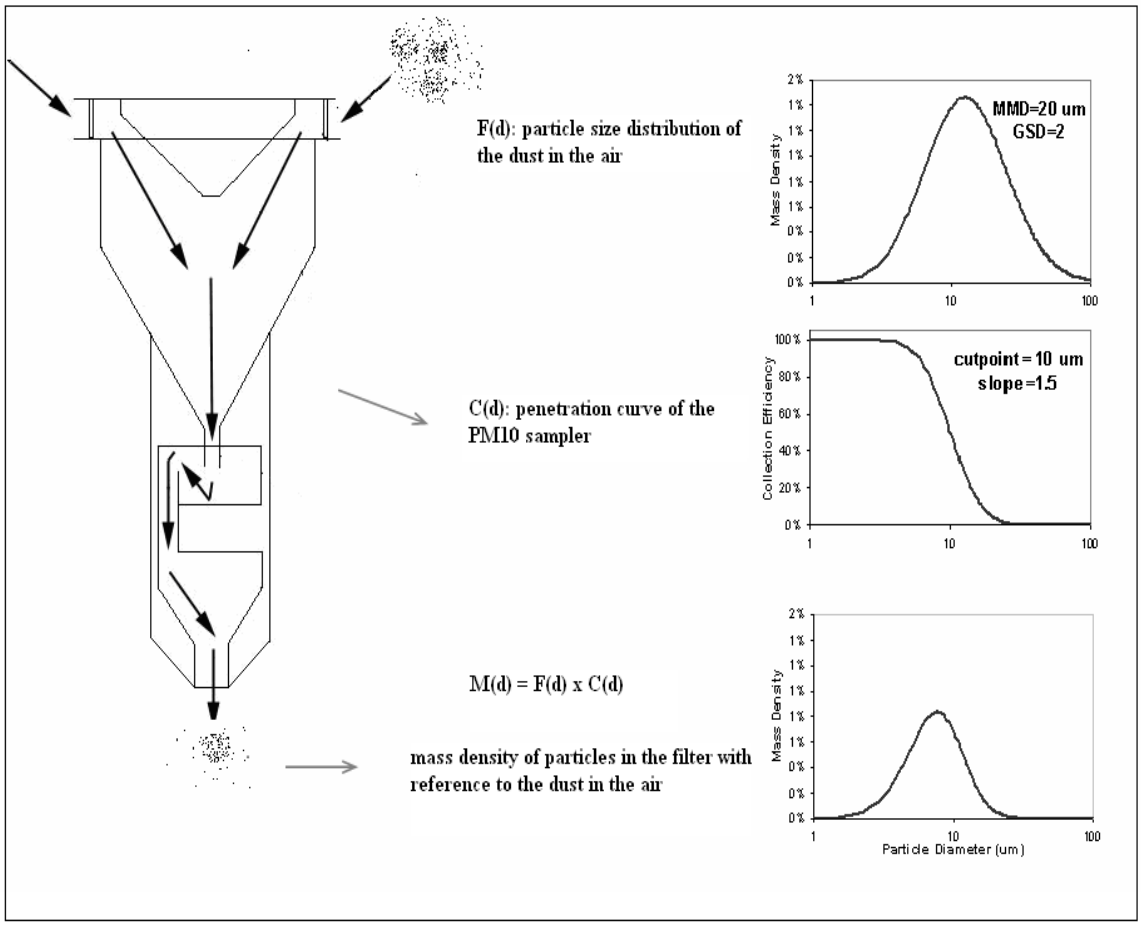

Figure 1. Illustration of interaction of particle size distribution and sampler's performance characteristics of a typical PM_{10} inlet (Chen, 2007).

When sampling with a FRM PM_{10} sampler, some particles larger than 10 µm penetrate the sampler inlet and are collected on the filter while some particles smaller

than 10 µm do not penetrate the pre-separator and are rejected. Hence the term "measured PM_{10}" is nominal since it includes a mass of particles larger than 10 µm and excludes a mass of particles smaller than 10 µm (Buser et al., 2007a). However, PM_{10} and $PM_{2.5}$ are defined as all particles with an AED less than or equal to 10 and 2.5 µm, respectively (USEPA, 1996). A common assumption made in the regulatory community is that the mass of particles within the size range of interest captured by the pre-separator is equal to the mass of particles larger than the size range of interest that penetrates the pre-separator and is collected on the filter. Figure 2A and 2B illustrate this assumption.

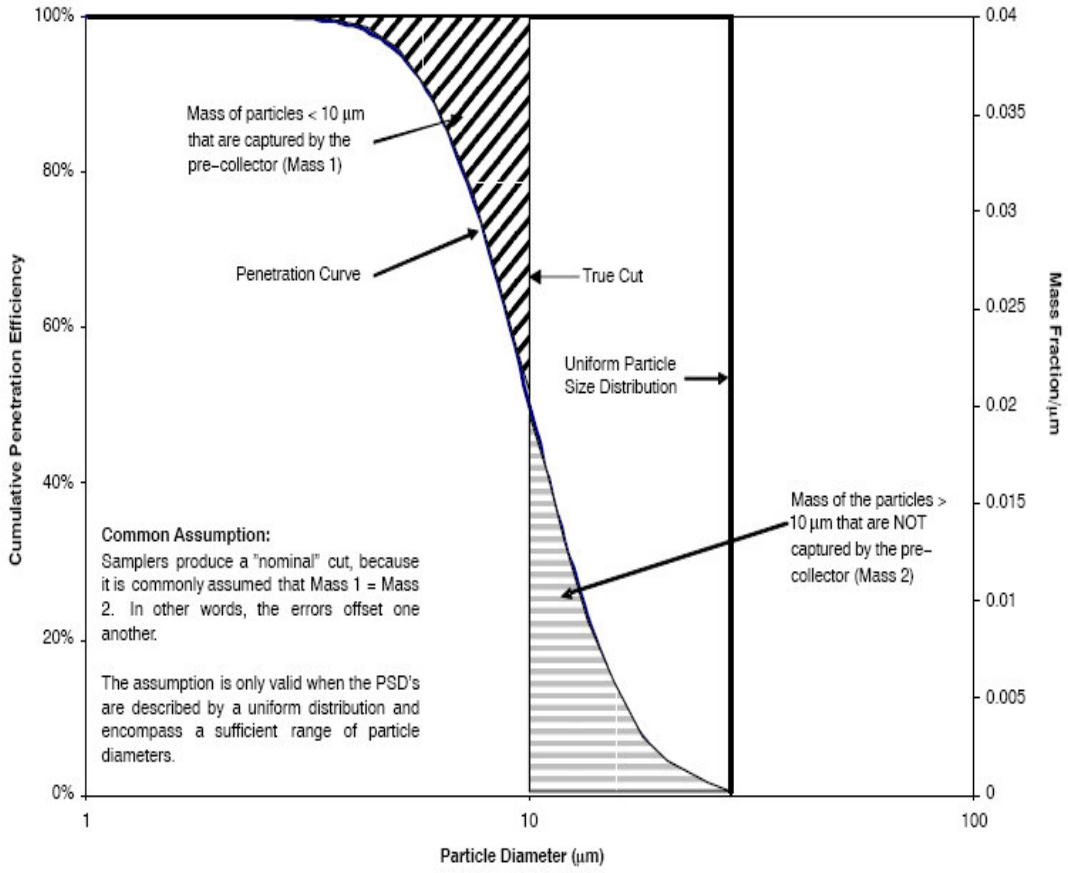

Figure 2A. PM_{10} sampler nominal cut (Buser et al., 2007a)

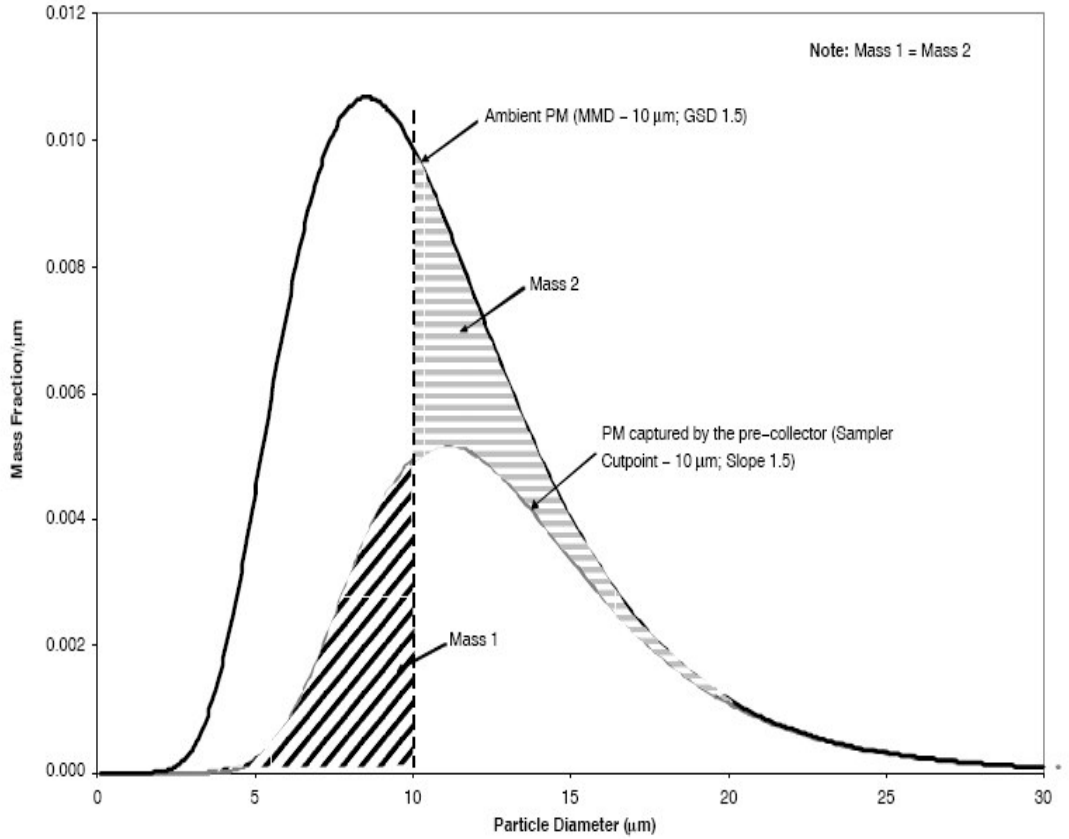

Figure 2B. PM_{10} sampler nominal cut for a uniform PSD (Buser et al., 2007a)

Ambient PSDs are represented by a lognormal distribution. However, the deviation of the PSD characteristics of the aerosols from the theoretical cut-point of PM_{10} samplers may introduce a source of bias in the aforementioned assumption when sampling in rural conditions (Buser et al., 2007a). For PSDs of aerosols commonly encountered in rural conditions, if the MMD of the ambient dust is smaller than the cut-point of the sampler, the mass of particles smaller than 10 µm that does not reach the filter (Mass 1) is greater than the mass of particles larger than 10 µm that penetrates the pre-separator (Mass 2) and reaches the filter (Figure 3). This is a case of a FRM PM_{10} sampler under-sampling bias.

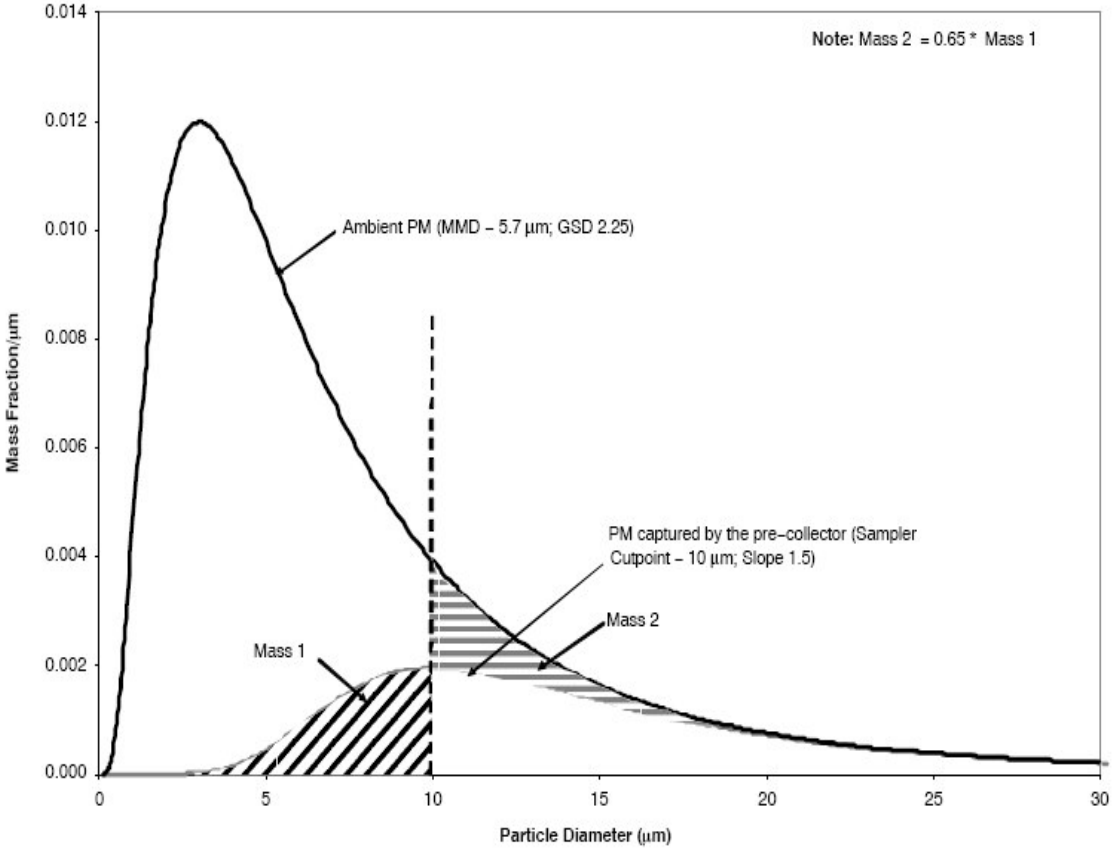

Figure 3. Under-sampling of urban dust (Buser et al., 2007a)

When the MMD of the ambient dust being sampled is larger than the cut-point of the sampler, the mass of particles smaller than 10 µm that does not reach the filter (Mass 1) is less than the mass of particles greater than 10 µm that penetrates the pre-separator (Mass 2) and is deposited on the filter (Figure 4). Thus, in this case, over-sampling of PM_{10} occurs. As the MMD of the dust in the air and the cut-point of a sampler diverge, the amount of under-sampling or over-sampling error increases (Buser et al., 2007b).

Buser et al. (2007b), using a theoretical analysis, reported that PM_{10} sampler measurements could be 139% to 343% higher than the true PM_{10} concentration even if the pre-separator operates within FRM performance standards when sampling PM with a

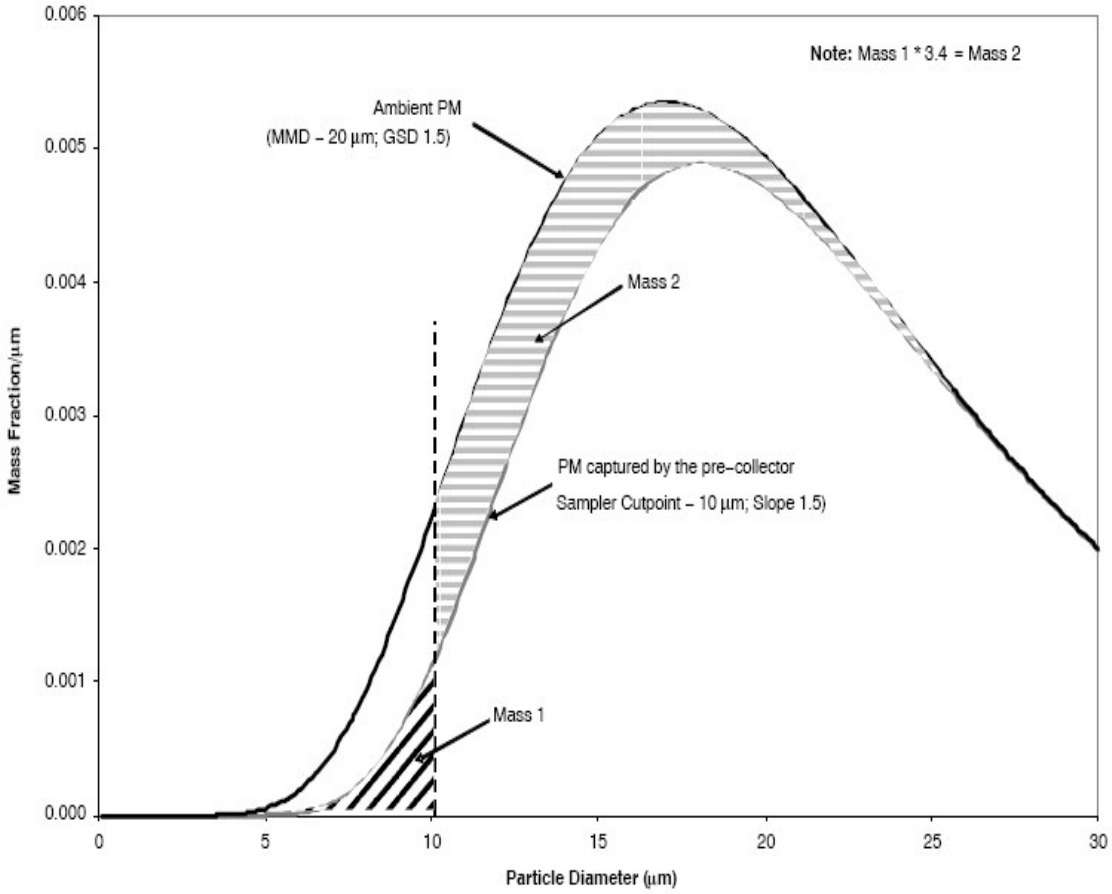

Figure 4. Over-sampling of rural dust (Buser et al., 2007a)

MMD of 20 µm and GSDs of 2.0 and 1.5, respectively. Using an empirical approach, Wang et al. (2005) documented an increase in FRM PM_{10} pre-separator cut-points with decreasing MMD of dusts. Deviations of the cut-point beyond the permitted range due to fluctuating wind and aerosol concentrations have also been reported (Ono et al., 2000). Inertial particle bounce and surface overloading of the samplers may also impact the sampler performance (Vanderpool et al., 2001). The shift of sampler performance characteristics may lead to additional under-sampling or over-sampling errors when measuring PM concentrations for regulatory purposes. Furthermore, biases in measured

concentrations of $PM_{2.5}$ and PM_{10} may lead to compounding of errors and uncertainties during determination of PM_c concentrations which could be a part of the NAAQS in the near future as suggested by EPA.

Agricultural sources of PM, which include anthropogenic sources of organic dusts, are characterized by relatively larger and broader PSDs as compared to PSDs of PM from urban sources. According to Parnell et al. (1986), a typical MMD for a rural aerosol would be about 12 to 16 μm while Redwine and Lacey (2001) reported PM from agricultural sources to be characterized by a lognormal distribution with MMD ranging from 15 to 25 μm AED (Table 1) and geometric standard deviation (GSD) ranging from 1.5 to 2.0. A typical MMD of urban PM is around 5.7 μm (USEPA, 1996).

Table 1. Particle size distributions of agricultural dusts.

Dust source	MMD[a](μm)	GSD[b]	Source
Almond harvesting	18.5	2.1	Capareda et al. (2005)
Cotton gin	23	1.8	Faulkner et al. (2007)
Beef cattle feed yard	20	2.2	Faulkner et al. (2007)
Open lot dairy	15	2.1	Faulkner et al. (2007)
Broiler building fan exhaust	24	1.6	Lacey et al. (2003)

[a] MMD = mass median diameter; [b] GSD = geometric standard deviation.

The concentrations of PM_{10} obtained from property line sampling of ambient air using FRM or FEM samplers may be incorporated by SAPRAs to regulate industries, issue permits and decide penalties or operating fees. The aforementioned sampler bias issues raise questions about the fairness of the methods used for determining regulatory compliance. Until recently agricultural industries were exempt from a vast number of air quality regulations. This was mostly due to the small size of most of these operations,

resulting in these industries being minor sources of PM, and the rural, sparsely populated location of many agricultural industries. But with increasing urban sprawl, many agricultural operations like cotton gins, feed mills, grain elevators, dairy operations and harvesting operations are becoming subject to air quality regulations. Furthermore, as urban growth continues to encroach on lands that have historically been used in agricultural production, increasing the proximity of agricultural operations to human dwellings, there is an increasing call for air quality regulations regarding agricultural operations like concentrated animal feeding operations (CAFOs), which may emit large quantities of PM. Due to interaction of PSD and sampler characteristics, existing PM samplers used by SAPRAs and EPA can substantially misrepresent the fractions of particles within the size ranges of interest in agricultural operations. If these erroneous concentrations are applied to regulation of agricultural operations, it will place an undue economic burden on many agricultural industries to come into compliance with current standards.

While many publications have pointed to problems with federally-approved sampling protocols and samplers (e.g. Ono et al., 2000; Wang et al., 2005), it is difficult to compare the performance characteristics of the samplers in these studies to quantify the shifts in sampler performance because environmental conditions and the PSD of sampled PM in each case are different and often undocumented. Controlled testing is needed to accurately characterize the performance of various FRM and FEM PM samplers operating in the presence of PM characterized by larger particles, as is typical of PM emitted from agricultural industries. Furthermore, previous studies have indicated

a strong relationship between shifts of cut-point and ambient wind speeds (Ono et al., 2000), and shifts in $PM_{2.5}/PM_{10}$ concentration ratios towards smaller values have been observed with increasing ambient PM_{10} concentrations (Cowherd, 2005). The shift of $PM_{2.5}/PM_{10}$ concentration ratios could be due to increased agglomeration of coarse particles as opposed to finer particles on the impactor plates of the sampler pre-separator at higher aerosol concentrations. Such a shift could lead to errors in PM_c calculations. In order to determine the suitability of current regulatory sampling protocol followed by SAPRAs and EPA, effects of variations of wind speed, ambient PM concentrations and PSDs of aerosols on the performance of these PM samplers should be quantified through controlled testing.

Objectives

The goal of this research was to evaluate the performance of FRM PM_{10} and low-volume TSP samplers under controlled conditions. The designs of the TSP samplers are based on application guidelines for a high-volume TSP sampler as mentioned in 40 CFR Part 50, Appendix B (CFR, 1987). The performance evaluation was conducted by observing the sampler cut-points and slopes under controlled conditions through wind tunnel testing. Specifically the objectives of this research were:

1. Empirically investigate the performance of two FRM PM_{10} samplers operating in the presence of poly-dispersed PM having various PSDs at different aerosol concentrations and wind speeds.

2. Empirically determine if the concentrations and PSDs from testing of low-volume TSP samplers can be used for determining true PM_{10} and $PM_{2.5}$ concentrations by performing collocated testing of TSP and isokinetic samplers in the wind tunnel.

CHAPTER II

LITERATURE REVIEW

The results of PM sampling determine whether an area or a source meets EPA and state regulatory standards for PM, and hence the PM collected by these samplers should be representative of the aerosols present in the ambient air around the sampler. A number of studies have investigated the performance characteristics of FRM and FEM samplers under various field conditions. Ono et al. (2000) reported that there were systematic differences in the measurements of EPA-approved FRM PM_{10} samplers and FEM Tapered Element Oscillating Microbalance (TEOM) samplers for the same location and time period. The authors reported that dichotomous, Graseby and Wedding samplers measured lower PM_{10} concentrations than TEOM samplers while sampling fugitive dust with high PM_c concentrations. They linked this observation to a decrease in cut-point due to higher wind speeds and decreasing cleanliness of the inlet as indicated by previous studies. McFarland et al. (1984) reported that cut-points for the Graseby and Wedding PM_{10} samplers decreased to 8.3 and 8.0 μm, respectively, at high wind speeds of 48 km/h while the cut-point of Wedding samplers decreased to 6.6 μm when the inlet was dirty. Ono et al. (2000) also found that the PM_{10} pre-separators' collection efficiency for smaller particles was affected under significant loading of larger particles.

Pargmann (2001) tested three kinds of $PM_{2.5}$ samplers (Well Impactor Ninety Six (WINS), Sharp Cut Cyclone (SCC) and high-volume $PM_{2.5}$) with aerosols having PSDs with MMDs of 17.1, 17.3 and 8.4 μm. The author found that all samplers had

oversampling biases ranging from 51% for the WINS separator (for MMD = 8.4 µm) to 1,771% for the SCC separator (for MMD = 17.3 µm) when compared to the true $PM_{2.5}$ concentrations, which were derived from TSP samplers by multiplying the mass fraction of PM below 2.5 µm with the TSP concentration. This bias was observed to increase with increasing aerosol MMD. Shifts of cut-point and slope of the three samplers were also reported. Pargmann (2001) concluded that $PM_{2.5}$ samplers used to monitor actual $PM_{2.5}$ concentrations in ambient air will not perform accurately in agricultural environments with MMDs higher than 10 µm.

Wang et al. (2005) carried out sampling tests with Graseby-Andersen FRM PM_{10} samplers in presence of cornstarch, fly ash and alumina by collocating them with low-volume TSP samplers. These low-volume TSP inlets were designed and built at Texas A&M University (Wanjura et al., 2003). The design of these low-volume TSP samplers was based on EPA's engineering design parameters for high-volume TSP samplers, listed in EPA 40 CFR Part 50, Appendix B (CFR, 1987). The cut-point of the FRM high-volume TSP sampler is reported to be around 45 µm with a slope of 1.5 (McFarland and Ortiz, 1983). Wanjura et al. (2003) reported that there was no difference ($\alpha = 0.05$) between the measured concentrations by the low-volume TSP samplers and the FRM high-volume TSP sampler for corn starch ($p = 0.787$) and fly ash ($p = 0.281$) while for alumina ($p = 0.037$) there was a difference in the mean concentrations. Wang et al. (2005) found that PM_{10} samplers over-sampled when exposed to ambient PM having MMD values larger than 10 µm AED, and they under-sampled when exposed to ambient PM having MMD values smaller than 10 µm AED. The authors also reported shifts of

performance characteristics (i.e. cut-point and slope) indicating that the cut-point increased as the PM MMD decreased. The authors, however, reported that there was a considerable horizontal and vertical gradient in the concentrations measured by the TSP samplers in their test chamber. The authors did not control the wind speed for their tests. Buser et al. (2008) used FRM PM_{10} samplers to monitor dust emissions from a south Texas cotton gin. The MMD and GSD of the PM collected on the TSP filters were 13.4 ±1.51 µm and 2.0 ± 0.11, respectively. They calculated ranges of cut-point and slope from 13.8 to 34.5 µm and 1.7 to 5.6, respectively, which resulted in overestimation of true PM_{10} concentrations by 145% to 287%.

There is little literature pertaining to wind tunnel testing of samplers. The USEPA wind tunnel (Ranade et al., 1990) and most other wind tunnel studies (McFarland and Ortiz, 1984) aimed at either design modification of existing FRM samplers or evaluation of sampler performance. However, this evaluation was performed using mono-dispersed liquid or solid aerosols having particles of a particular size as opposed to poly-dispersed aerosols with a lognormal PSD which provided a better representation of ambient aerosols. In the past, wind tunnels have also been used to evaluate candidate samplers for FRM designation (McFarland et al., 1984, Wedding et al., 1985). Chen (2007) designed and fabricated a controlled environment sampler testing wind tunnel meeting EPA's requirements for velocity profile and PM concentration uniformity as per Title V document and 40 CFR, Part 53, Subpart D (CFR, 2006b). The wind tunnel had a vibration hopper to feed dust into the system and hence allowed PM samplers to be tested with poly-dispersed aerosols in order to observe the

interaction of PSD and sampler performance characteristics. Wind tunnel tests were also conducted at Midwest Research Institute for the Western Governors' Association Western Regional Air Partnership to propose a modified $PM_{2.5}/PM_{10}$ ratio from fugitive dust emissions for paved and unpaved roads (Cowherd, 2005). These wind tunnel tests were conducted over different aerosol concentrations generated using a fluidized bed injection system. The tests evaluated a number of FRM samplers operating at low-volume flow rates of 16.7 alpm (actual lpm) and tested various geologic sources of dust in the western part of the US. Among other conclusions, the authors found that increasing aerosol concentration decreased the calculated $PM_{2.5}/PM_{10}$ ratios and that the ratio was affected by the shape of the particles of the source dust as well.

Rationale and Significance

Previous EPA wind tunnel tests were primarily aimed at characterizing the performance of candidate samplers for purposes of FRM designation (Ranade et al., 1990). The effect of varying aerosol concentrations on sampler performance was not determined in EPA tests. Wind tunnel testing, for the purpose of this research, permitted simulation of agricultural and urban conditions through the choice of poly-disperse aerosols with PSDs similar to those found in agricultural or urban conditions, respectively. Sampler testing was conducted using low-volume flow rate samplers whose performance characteristics were evaluated. The samplers were tested with three aerosols having distinct PSDs at three wind speeds (2-, 8-, and 24-km/h) and five

ambient aerosol concentrations ranging from 150 to 1,500 $\mu g/m^3$. The wind tunnel enabled reproducible test conditions as opposed to field testing of samplers.

"True PM_{10}" is considered to be that fraction of PM which includes all particles smaller than 10 µm in the air stream that is being sampled. True PM_{10} concentrations in the wind tunnel were determined using the PSD of aerosols sampled by an isokinetic probe by multiplying the mass fraction of PM smaller than 10 µm with the PM concentration measured by the isokinetic sampler. The TSP sampler can serve as a reference sampler in ambient sampling campaigns if the dust which is collected on the filter of the TSP sampler is representative of the ambient dust in terms of both PSD and mass concentration. When these conditions are fulfilled, a TSP sampler can be utilized with particle size analysis to measure true PM_{10} or $PM_{2.5}$ concentrations. This evaluation is important since isokinetic samplers can only be used when ambient wind speed and direction are known and constant, which rarely occurs except under controlled testing conditions. The TSP samplers in the wind tunnel study were collocated with the isokinetic sampler. The wind tunnel tests were used to determine the validity of using low-volume TSP samplers as a field reference sampler for determination of true PM_{10} concentrations which can address the issue of PM_{10} sampler errors and sampling bias. The results of this research lay the groundwork for understanding sampler performance in rural environments making the equitable regulation of air pollution from agricultural industries possible. The expected shifts of sampler cut-point and slope characteristics will enable researchers and scientists to determine true PM_{10} concentrations which may lead to more accurate and fair regulation.

CHAPTER III

METHODOLOGY

Dust Wind Tunnel

The dust wind tunnels designed for aerosol studies, and particularly for PM sampler evaluation, are required by EPA to attain aerosol concentrations and wind speeds similar to those encountered in ambient environment. The wind tunnel used in this study was designed and fabricated by researchers at the Center for Agricultural Air Quality Engineering and Science (CAAQES) at Texas A&M University. The wind tunnel conforms to EPA performance standards for uniformity of wind velocity and aerosol concentration specified in 40 CFR Part 53, Subpart D (CFR, 2006b) (Table 2).

Table 2. EPA requirements for the performance of wind tunnels for evaluating PM_{10} samplers (CFR, 2006b) .

Parameter		PM_{10} Requirement
Air Velocity	*Uniformity*	±10% for 2, 8 and 24 km/h
	Measurement	1) Minimum of 12 test points 2) Monitoring techniques: precision ≤ 2% ; accuracy ≤ 5%
Aerosol Concentration	*Uniformity*	±10% of the mean.
	Measurement	No less than 5 evenly spaced isokinetic samplers The sampling zone shall have a horizontal dimension not less than 1.2 times the width of the test sampler at its inlet opening and a vertical dimension not less than 25 centimeters
Particle size	*Measurement*	Accuracy ≤ 0.15 µm; size resolution ≤ 0.1 µm

Figure 5 is a schematic of the overhead view of the wind tunnel. The centrifugal fan (1) (PLR206, New York Blower Company, Willowbrook, IL, USA) is equipped with a variable frequency drive to regulate the speed of the fan. The wind tunnel body is located on an elevated platform to minimize vibration effects. The fan blows air up through a vertical transmission duct which leads to a horizontal pre-mixing duct (2). The transition box (3) functions as an elbow to create turbulence while the dust feeder (Wright Dust Feeder II, BGI Inc, MA, USA) is installed on top of the feeding duct (4). The feed point is such that the dust enters the chamber against the direction of flow of air to increase turbulent mixing. The inflow duct opens out to the GTPS mixing chamber which contains a belt-drive, axial fan (Dayton 3C613, 36 in propeller diameter, Dayton Co., Dayton, OH, USA). The air coming out of the GTPS chamber passes through the 1 m x 1 m flow-stabilizing duct (6). At the end of this duct is the test chamber (7), which has an expanded cross sectional area to avoid wall effects and to permit testing of multiple PM samplers simultaneously. The air coming out of the test chamber passes through a 90º exhaust elbow (8) which directs the flow out through an exhaust fan on the roof (9).

The dust feeder (WDF II, BGI Inc, Waltham, MA, USA) is equipped with a carbide blade to cut through the dust contained in a tightly packed cylindrical container. Prior to a test, the dust was packed and the dust-packed container mounted on the feeder. The feeder has a broad range of output from 0.0026 to 60 g/h of unit density dust

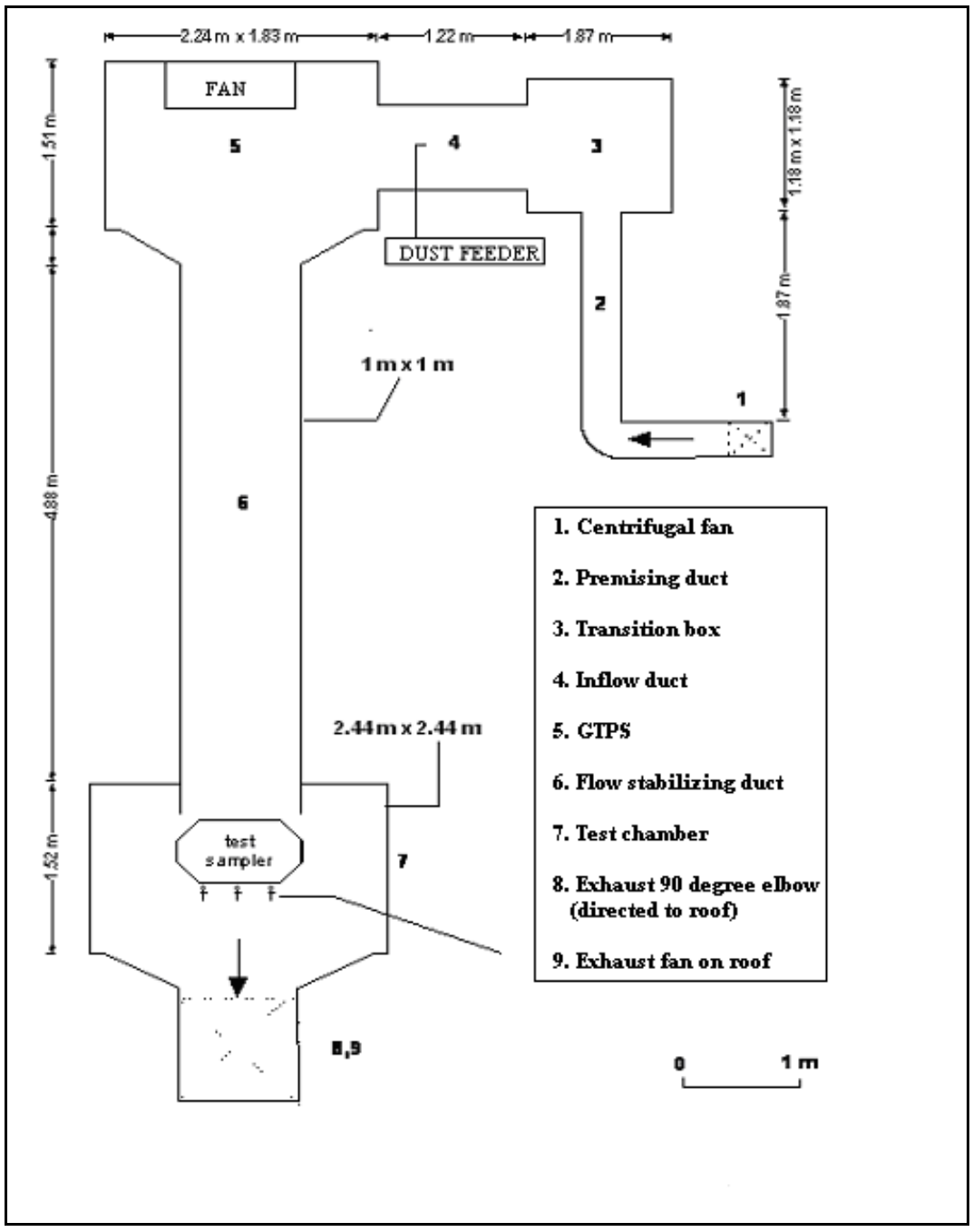

Figure 5. Schematic of the modified wind tunnel.

Wind Tunnel Performance Assessment Tests

Velocity Profile

The velocity in the sampler test chamber of the wind tunnel was measured using an air velocity transducer (TSI 8455, TSI Inc., Shoreview, MN, USA) with a precision of 0.01 m/s and an accuracy of ±0.5% of full scale of the selected range. The uniformity of wind speed was evaluated by recording wind speed values at all points along a hypothetical 16-point grid in the test chamber. The 16-point grid divided the 1 m x 1 m flow stabilizing duct evenly into a 4 x 4 grid. The grid plane was located at the entrance to the test chamber at the end of the flow-stabilizing duct.

For uniformity tests, the centrifugal fan was turned on and the frequency of the drive increased until the velocity transducer reading was within ±10% of target flow velocity. For each of the sixteen grid positions, velocities were recorded every two seconds by the transducer for five minutes and then averaged. The coefficient of variation (COV) of the mean velocities at all sixteen points was determined. The maximum and minimum deviation of velocity at a grid-point from the mean was also determined. For velocity uniformity tests at 8 and 24 km/h, the exhaust fan was turned on while the exhaust fan was turned off for 2 km/h velocity uniformity tests as it generated wind speeds in excess of 2 km/h. For all three tests, the maximum and minimum velocity was found to be within 10% of the average velocity at all grid-points. The COV was found to be <10% for tests at all three wind speeds. The results of the

tests showed that the EPA velocity requirements for dust wind tunnels were satisfied for the wind tunnel used in this study (Table 3).

Table 3. Velocity uniformity of wind tunnel.

Wind speed (km/h)	Coefficient of variation (COV) (%)	Deviation from the mean	
		Maximum (%)	Minimum(%)
2	7.434	9.91	9.02
8	4.328	6.33	9.07
24	5.124	8.64	9.25

Concentration Profile

Concentration uniformity tests were performed in the wind tunnel to evaluate its conformity to EPA performance specifications for dust wind tunnels. Gravimetric sampling with nine isokinetic samplers was carried out simultaneously to determine aerosol concentrations in a hypothetical 9-point grid (dividing the 1 m x1 m flow-stabilizing duct into a 3 x 3 grid). The isokinetic inlets, with different opening diameters for the three wind speeds, were machined conically from aluminum with 47 mm filter holders and were fitted into stainless steel probes which were fitted into a rack. The probes allowed the sampler grid to be positioned at the entrance of the test chamber. The isokinetic samplers blocked only 0.28% of the total sampling area on the vertical cross section.

The filters used for collecting the sampled dust were 47 mm polytetrafluoroethylene (PTFE) filters (Zefluor PTFE membrane, 2 µm pore size, Pall Corp, East Hill, NY, USA). The filters were weighed on a precision analytical balance (XS205 Dual Range, 0-81 g, readability: 0.01 mg, Mettler Toledo, Columbus, OH, USA). The filter weighing protocol is located in Appendix A. Each filter was weighed three times before and after sampling, and the mean weights were calculated. If the standard deviation of the three weights was greater than 30 µg, the filter was re-weighed until the standard deviation of the three weights was less than 30 µg.

Pre-weighed 47 mm PTFE filters were placed in each of the isokinetic sampling probes. Concentration tests were performed over the three EPA-specified wind speeds of 2-, 8-, and 24-km/h with corn starch. All nine isokinetic inlets were connected to low-volume sampling systems placed outside the wind tunnel that drew air at a volume flow-rate of approximately 1 m^3/h. The set up and function of the sampling system has been described in the section "PM sampling system." Dust was fed into the wind tunnel at a target concentration of 500 µg/m^3. Test durations for the three velocities varied from 2 to 4 h to collect a minimum of 1 mg of dust on each filter. After the tests, the filters were post-weighed and the net difference of weights divided by the total volume of air sampled to determine TSP concentrations. The COVs of aerosol concentrations for the three wind speeds were less than 10% while the deviation of concentration from the mean was slightly higher than 10% for concentration tests at 24 km/h but below 10% for tests at 2 and 8 km/h (Table 4).

Table 4. Concentration uniformity of corn starch in wind tunnel.

Wind speed (km/h)	Coefficient of variation (COV) (%)	Deviation from the mean	
		maximum(%)	minimum(%)
2	5.453	7.92	9.02
8	6.753	8.71	8.99
24	7.465	13.2	0.924

Test Dusts

PM sampling tests were carried out in the presence of poly-disperse aerosols as opposed to mono-disperse aerosols used in EPA wind tunnel tests (Ranade et al., 1990). Recent wind tunnel studies (Kenny et al., 2005; Witschger et al., 1997) used poly-dispersed aerosols primarily because: 1) they represented more accurately the kind of aerosols encountered in the real world environment during PM sampling and 2) the experimental procedure associated with the use of mono-dispersed aerosols was more tedious and expensive.

Urban PM has an MMD around 5.7 μm (USEPA, 1996) while rural aerosols have MMDs around 15 μm or larger (Faulkner et al., 2007). This study intended to simulate urban and rural environments through the choice of aerosols with MMDs ranging from 5 to 20 μm AED. After examining the physical properties and limitations of use, three dusts were selected for the wind tunnel tests: ultrafine ARD (MMD = 5.3 μm AED, GSD = 1.6), fine ARD (MMD = 12 μm AED, GSD = 1.7) and corn starch (MMD = 17.1 μm AED, GSD = 1.5). Prior to use, both varieties of ARD were heated to 105°C for an

hour and kept in a desiccator. This action reduced the moisture content in dusts and prevented caking problems in the feeder. Corn starch was kept in the desiccator without heating since corn starch particles show excessive binding properties when heated to 105ºC leading to caking problems.

The particle densities of all aerosols were determined using a pycnometer (AccuPyc II 1330, Micromeritics, Norcross, GA, USA). The particle density analysis protocol is located in Appendix B. The aerosols had particle densities of 2.7 g/cm^3 (ultrafine ARD and fine ARD) and 1.5 g/cm^3 (cornstarch). The shape factor of a particle relates the drag on an irregular particle to the drag on a spherical particle of the same volume (Hinds, 1999). A perfectly spherical particle will have a shape factor of 1.0. The test dusts for this study were imaged under an analytical-grade scanning electron microscope (SEM) (Figure 6; JEOL-JSM 6400, JEOL USA Inc, Peabody, MA, USA). Based on the near-spherical images of corn starch particles, Wang et al., (2005) assumed the shape factor of corn starch as 1.00. Since the SEM images of cornstarch particles are not strictly spherical, the shape factor of cornstarch was assumed as 1.05. The shape factor of ARD (angular particles) was assumed as 1.4 based on sharp and angular SEM images of ARD particles and literature on shape factor of quartz-type particles (Hinds, 1999).

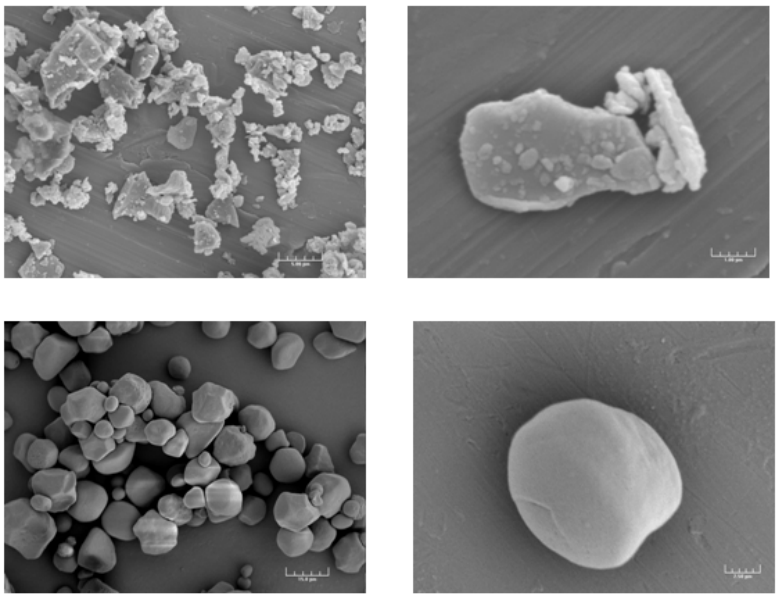

Figure 6. SEM images of ARD (top left, top right) and corn starch (bottom left, bottom right).

Isokinetic Sampling System

An isokinetic sampling system was used as a reference sampler to sample air loaded with dust particles. Isokinetic sampling ensured that the sampled particles from the moving air stream were representative of the particles of concern in terms of concentration and size distribution. The system consisted of conical, isokinetic sampling inlets machined from aluminum with nominal inlet nozzle diameters of 19.8-, 10.2-, and 7.4-mm for the three test wind speeds of 2-, 8-, and 24-km/h, respectively. However, to achieve isokinetic sampling at a target flow rate of 1 m^3/h, the nominal inlet nozzle diameters should have been 25.2-, 12.6-, and 7.4-mm for the aforementioned wind speeds, respectively. Hence the isokinetic inlets in this study were slightly anisokinetic.

Mathematical calculations and statistical tests to determine the underestimation of concentrations indicated that the sampling errors due to anisokinetic sampling of the three aerosols were negligible and that an assumption of isokinetic conditions was fairly true for this study. Appendix C describes the evaluation of sampling error and underestimation of concentration due to differences in the dimensions of the isokinetic inlets. The inlets fit onto 47 mm filter holders which were attached to the isokinetic probes and installed in the same vertical plane as PM_{10} and TSP samplers. Air entering the inlet was drawn through a pump (M161-AT-AA1, Air Dimensions Inc, USA) and a mass flow controller (MFC) (FMA5420-12VDC, Omega Inc, Stamford, CT, USA). LabView was used to control the MFC. The real time values of temperature, velocity and pressure were obtained every millisecond and the two-second average of these parameters used to calculate the required mass flow rate of air. This required mass flow rate was compared to the actual mass flow rate which was then adjusted by the MFC to maintain isokinetic conditions. The MFC thus automatically adjusted for the decreased air flow arising from loading of filters and kept the volume flow rate constant at 1 m^3/h.

Particulate Matter (PM) Sampler Inlets

The performance of two variants of PM_{10} sampler inlets, namely the Graseby-Anderson PM_{10} inlet (henceforth the flat-head PM_{10} inlet) and the BGI PM_{10} inlet (henceforth the louvered-head PM_{10} inlet), was evaluated. Collocated with the two PM_{10} samplers and the isokinetic sampler were two low-volume TSP samplers, one being the dome-top and the other being the cone-top TSP inlet (Figure 7). The TSP sampler designated by EPA as a FRM sampler operated on a high-volume basis with flow rates ranging between 66 and 102 m^3/h. These samplers were known to experience difficulties maintaining a constant flow rate while sampling in high concentrations due to the accumulation of particles on the filter leading to high, unsustainable pressure drops (Price and Lacey, 2003). To overcome this issue, dome-top TSP and cone-top TSP samplers, operating on a low-volume basis, were developed by researchers at CAAQES and the USDA-ARS Southwestern Cotton Ginning Research Laboratory at Mesilla Park, New Mexico. Since there were no EPA guidelines for low-volume TSP samplers, these TSP inlets were designed to conform to EPA specifications for high-volume TSP sampler inlets in 40 CFR, Part 50, Appendix B (CFR, 1987).

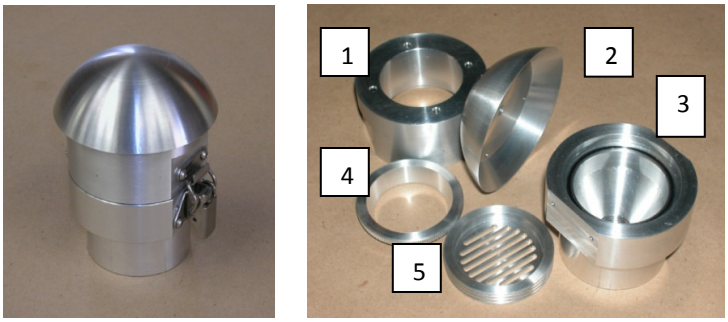

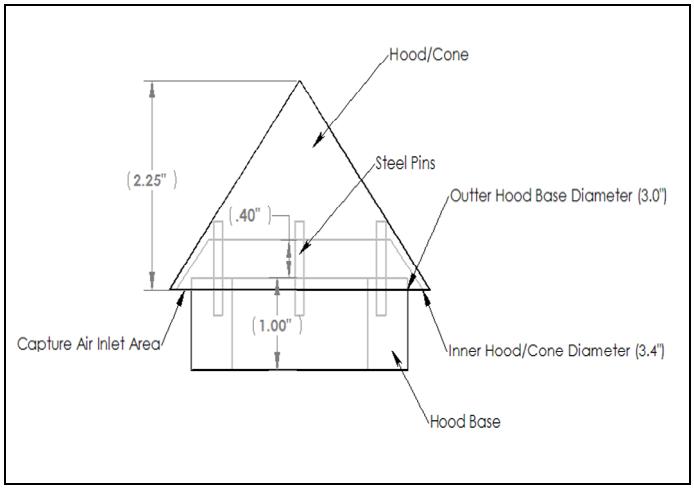

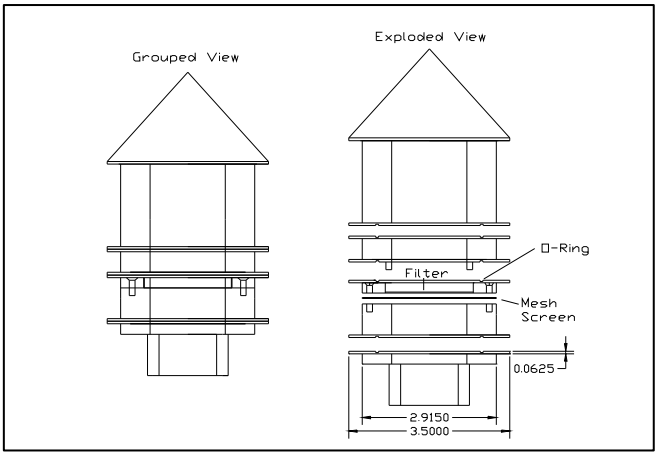

Figure 7. Dome-top TSP inlet (top left), exploded view of the cone-top TSP inlet (middle) and engineering drawing of the cone-top TSP inlet hood (bottom). The five components of the dome-top low-volume TSP inlet are shown disassembled (top right) : (1) upper barrel, (2) sampler cap, (3) lower barrel, (4) filter cassette top, and (5) filter cassette bottom.

Particulate Matter (PM) Sampling System

All the four sampler inlets were operated on a low-volume basis (1 m^3/h). The sampler inlets were connected through 0.95 cm (3/8 inch internal diameter) diameter tubing to sampler boxes. The sampler flow rate control boxes were designed at Texas A&M University and were placed outside the wind tunnel. Figure 8 illustrates the set-up of the low-volume PM_{10}/TSP sampling system.

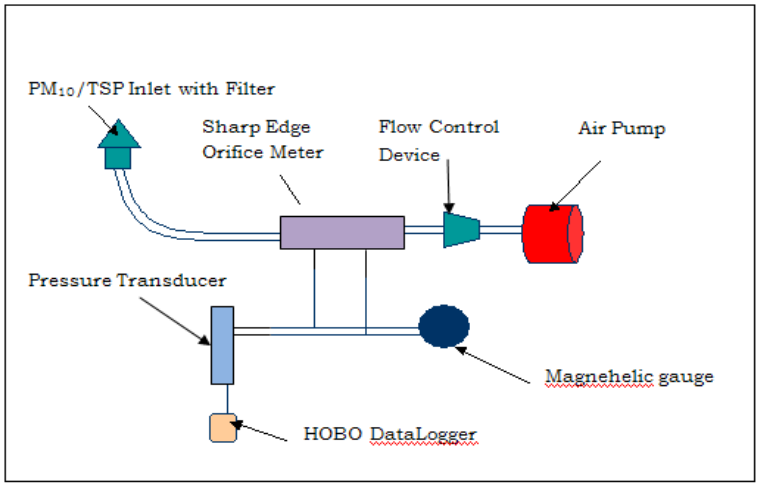

Figure 8. Low-volume PM_{10}/TSP sampler set up.

A 0.09 kW (1/8 hp) diaphragm pump (Thomas 917CA18, Thomas Pumps and Compressors, Sheboygan, WI, USA) provided air-flow, which was adjusted using a ball valve located downstream of the sampler filter. The air-flow rate was monitored using a sharp edge orifice plate. Appendix D describes the calibration of the orifice meter. The pressure drop across the orifice plate was monitored using a differential pressure transducer (PX 274-05DI, Omega Engineering Inc, Stamford, CT, USA) and checked visually with a magnehelic gauge (2005, range: 0- 5.0 inch of water, Dwyer Instruments,

Michigan City, IN, USA) . Appendix E describes the calibration of the differential pressure transducer. A data logger (HOBO U12-006, 4-20 mA, Onset Corp, Pocasset, MA, USA) recorded the current output of the transducer every two seconds, and this output was converted to differential pressure using the pressure transducer calibration equations. The temperature and relative humidity of air during each test were recorded using a thermal anemometer (TSI 8386, Accuracy: 0.3˚C, 3 % RH, TSI Inc, Berkshire, UK) while the barometric pressure was determined by a pressure sensor (7400 Davis Perception II, Davis Instruments, Hayward, CA, USA). Equations 1 and 2 were used to calculate the flow rate of sampled air:

$$Q = 1.252 \times 10^4 \times K \times \sqrt{\frac{1}{1-\beta^4}} \times D_o^2 \times \sqrt{\frac{P_w}{\rho_a}} \quad (1)$$

$$\beta = \frac{D_o}{D_p} \quad (2)$$

where:

Q = volumetric flow rate of air, (m^3/h),

K = orifice meter constant, (dimensionless),

β = velocity of approach factor, (dimensionless),

D_o = orifice diameter, (m),

P_w = pressure drop across the orifice plate, (mm of H_2O),

ρ_a = density of air, (kg/m^3), and,

D_p = inlet diameter, (m).

The density of the air was calculated using equations 3 and 4:

$$\rho_a = \frac{P_b - P_{wv}}{0.0028 \times (273 + t_{db})} + \frac{P_{wv}}{0.0046 \times (273 + t_{db})} \quad (3)$$

$$P_{wv} = \frac{RH}{100} * P_s \quad (4)$$

where:

P_b = barometric pressure, (atm),

P_{wv} = water vapor pressure, (atm),

t_{db} = dry bulb temperature, (°C),

RH = relative humidity, (%), and,

P_s = saturated water vapor pressure, (atm).

The value of P_s was determined from steam tables (Wilhelm et al., 2005) on the basis of the t_{db} and converted to appropriate SI units. An analysis of systematic uncertainty of the volumetric flow-rate of the low volume PM sampling system was performed and is described in Appendix F. The systematic uncertainty in the flow rate measurement was found to be 16.6%.

Experimental Design

The quartet of PM sampler inlets and the isokinetic sampler inlet were placed in one vertical plane in the test chamber and sampled aerosols fed into the wind tunnel by the dust feeder. Figure 10 shows an example arrangement of the samplers in the test chamber. The positions of the sampler inlets were randomized for each test. A randomized complete block design with replication as the blocking factor was adopted,

with three replications comprised of 45 tests each. Tests were conducted over three wind speeds of 2-, 8- , and 24-km/h, aerosol concentrations of 150-, 300-, 500-, 1000-, and 1500-µg/m^3, and with three aerosols (ultrafine ARD, fine ARD and cornstarch). Test durations were determined on the basis of aerosol concentration and the minimum mass of dust required on a filter to ensure a successful PSD analysis (1 mg). The duration of each test was 7-, 3.5-, 2-, 1-, and 0.67-h for 150-, 300-, 500-, 1000-, and 1500-µg/m^3 concentrations, respectively.

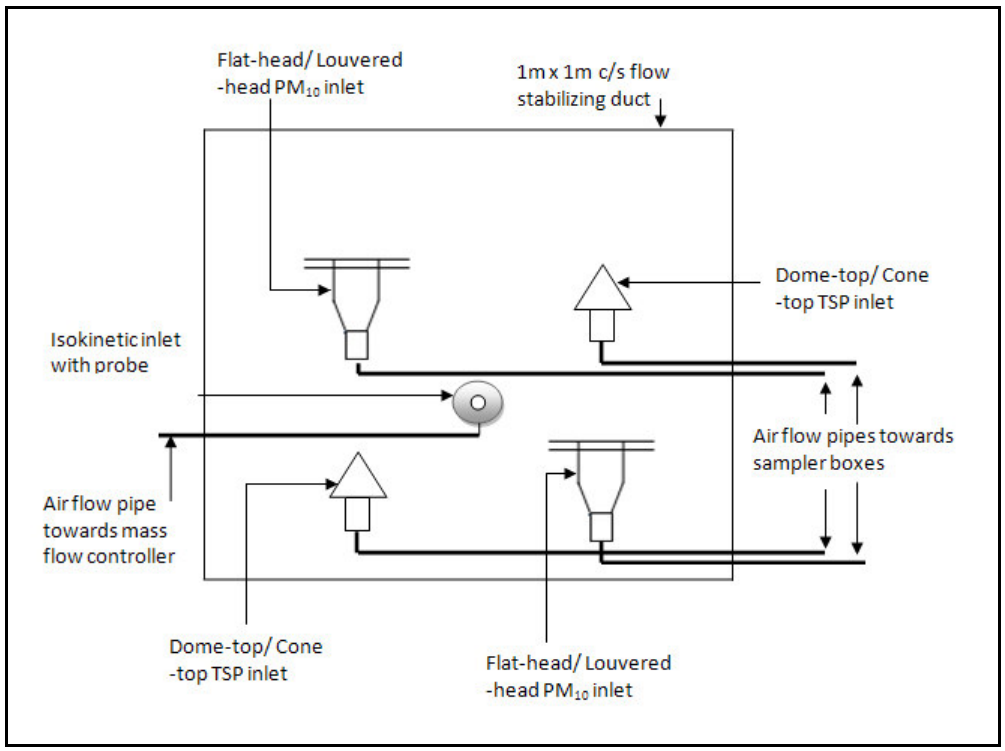

Figure 9. Front view schematic of the test chamber with the isokinetic sampler inlet and PM_{10} and TSP sampler heads arranged in a random square pattern.

Wind Tunnel Testing Protocol

Pre-experimental Preparation

Before each test, the centrifugal fan and exhaust fan were turned on at the maximum drive frequency (60 Hz), which generated wind speeds of around 30 km/h to blow away any dust which had accumulated due to settling from the previous test. All four sampler inlets, the isokinetic inlets, and the filter holder assembly were cleaned using paper towels dampened with alcohol. The sampler inlets were then installed in the test chamber as per a random grid order generated prior to every new test.

Depending upon the wind speed at which a test was conducted, the isokinetic inlet with the corresponding nozzle diameter was fit into a probe in the center of the chamber cross-section. The full-scale range of the velocity transducer was re-set before each test depending on the wind speed. Five clean, numbered, pre-weighed filters were placed in the sampler cassettes of the four test samplers and the isokinetic inlet. Log sheets were maintained to record the filter numbers being placed in each of the five samplers. The values of the temperature, relative humidity and barometric pressure were recorded and the density of air determined using eq.3.

Wind Tunnel Testing

The centrifugal and exhaust fans were turned on, and the speed of the centrifugal fan was adjusted to achieve the desired wind speed in the tunnel. When the test wind speed was achieved, the dust feeder was turned on along with the compressed air supply. For any combination of wind speed and target aerosol concentration, the motor speed of

the feeder was determined from manufacturer-provided calibration charts. The pressure of the compressed air supply was maintained between 55 and 172 kPa (8 and 25 psig) to avoid disruption and collapse of the compressed dust cake inside the feeder container. All five sampler pumps were then turned on. The pressure drop across each orifice plate was determined from the pressure drop versus density charts obtained during orifice meter calibration. This pressure drop was manually set on the magnehelic gauge using a ball valve. The data loggers were launched at the start of every new test to begin logging the current output of the pressure transducer. The test start and end times were noted in log sheets. During the test, the magnehelic gauge was read occasionally and the pressure drop adjusted back to the starting value in case of a visually-evident change in pressure drop across the orifice meter. To stop the test, the feeder and compressed air supply were turned off first, followed by the centrifugal and exhaust fans. Finally, all the pumps were turned off and the data loggers stopped.

Post-experimental Protocol

The filters were removed from the sampler inlets, placed in petri-dishes and taken to an air conditioned chamber to condition for a minimum of 24 hours before post-weighing. The logger data was transferred to a computer. The pressure drop-versus-current output equations generated during calibration of each pressure transducer were used to determine the average pressure drop over the test. This pressure drop was then used to calculate the volumetric flow rate using eq. 1.

Concentration and PSD Analysis

The weight differential from each filter was divided by the total volume flow of air passed through the filter in a given test to determine the concentration of PM collected by each sampler for each test (eq. 5 and 6).

$$C = \frac{\Delta M}{V} \tag{5}$$

$$V = Q \times t \tag{6}$$

where:

C = concentration of PM on filter, (μg/m^3),

ΔM = mass of PM on filter, (μg),

V = total volume of air sampled, (m^3),

Q = volume flow rate, (m^3/h), and,

t = test duration, (h).

A particle size analysis of the PM from each filter was carried out using a Malvern Mastersizer (Hydro SM2000, Malvern Instruments Ltd, Worcestershire, UK) to determine the PSD of the PM. The particle sizing protocol is described in Appendix G. The analysis yielded the volume fractions of particles ranging from 0.1 to 200 μm over 100 logarithmically-sized bins. The generated PSDs were converted from equivalent spherical diameter (ESD) to AED using equation 7.

$$AED = ESD \times \sqrt{\frac{\rho}{\rho_w \times \chi}} \tag{7}$$

where:

ρ = particle density, (g/cm^3),

χ = particle shape factor, (dimensionless), and,

ρ_w = density of water = 1, (g/cm^3).

Data Analysis

The PSD of a poly-dispersed dust can be best represented by a mono-modal lognormal distribution characterized by a MMD and a GSD (Hinds, 1999). The lognormal mass density distribution of most ambient dusts can be expressed according to equation 8.

$$f(d_p, MMD, GSD) = \frac{1}{d_p \ln GSD \sqrt{2\pi}} \exp\left[\frac{-(\ln d_p - \ln MMD)^2}{2(\ln GSD)^2}\right] \quad (8)$$

where:

f (d_p, MMD, GSD) = lognormal mass density function, (decimal),

d_p = particle diameter, (μm),

MMD = mass median diameter of distribution, (μm), and

GSD = geometric standard deviation of distribution, (dimensionless).

Since the dust collected on the isokinetic sampler filter is expected to be representative of the ambient dust in the wind tunnel, the PSD generated from the Malvern Mastersizer analysis of isokinetic filters was treated as the lognormal mass density distribution of the test dust, hereafter referred to as the ambient PSD (f_{amb}). The dust collected on the filter of a size-selective PM_{10} sampler was known as measured PM and the distribution represented by f_{PM10}.

Equation 9 expresses the lognormal collection efficiency density function of a PM pre-separator.

$$CE\left(d_p, d_{50}, slope\right) = \frac{1}{d_p \ln(slope)\sqrt{2\pi}} \exp\left[\frac{-\left(\ln d_p - \ln d_{50}\right)^2}{2(\ln(slope))^2}\right] \quad (9)$$

where:

$CE(d_p, d_{50}, slope)$ = collection efficiency of pre-separator for a particle with diameter d_p, (decimal),

d_{50} = cut-point of sampler (μm), and

slope = slope of sampler FEC (dimensionless).

Sampler performance was documented using two parameters: cut-point and slope. These two parameters define a sampler's fractional efficiency curve (FEC) which describes the efficiency of a size selective sampler to remove particles from the air stream drawn into the sampler and prevent them from penetrating to the filter. The FEC is expressed by the lognormal cumulative distribution function for the collection efficiency as:

$$FEC(a, d_{50}, slope) = \int_0^a CE(d_p, d_{50}, slope) dd_p \quad (10)$$

where:

$FEC(a, d_{50}, slope)$ =collection efficiency for particles having diameters less than a, (decimal),and,

a = diameter of particle at which collection efficiency is being calculated, (μm).

The efficiency of a size selective sampler to allow penetration of the pre-separator by particles of a given size and collect them on a filter is described by the sampler penetration curve (Buser et al., 2002). The penetration efficiency is defined as:

$$P_{PM10}(a, d_{50}, slope) = 1 - FEC(a, d_{50}, slope) \quad (11)$$

where:

$P_{PM10}(a,d_{50}, slope)$ = penetration efficiency of PM_{10} pre-separator for a particle with diameter d_p, (decimal).

The expected PM_{10} concentrations of each particle size range on a sampler filter can be determined by combining equations 8 and 11 into equation 12.

$$C_{PM10(expected),i}(MMD, GSD, d_{50}, slope) = C_{amb}\int_{a_i}^{b_i}\left(f_{amb}(d_p, MMD, GSD)P_{PM10}(d_p, d_{50}, slope)\right)dd_p \quad (12)$$

where:

$C_{PM10(expected),i}$ = expected mass concentration of PM_{10} from the size selective sampler filter of a particle size range with upper bin diameter b_i and lower bin diameter a_i, ($\mu g/m^3$), and,

C_{amb} = ambient PM concentration collected on isokinetic filter, ($\mu g/m^3$).

The measured PM_{10} concentration of each particle size range was determined from the measured PM_{10} concentration and the PSD captured on the size-selective PM sampler filter as in equation 13.

$$C_{PM10(measured),i}(MMD,GSD) = C_{PM10}\int_{a_i}^{b_i}\left(f_{PM10}\left(d_p, MMD_{PM10}, GSD_{PM10}\right)\right)dd_p \quad (13)$$

where:

$C_{PM10(measured),i}$ = measured mass concentration of PM_{10} of a particle size d_p on the size-selective sampler filter with upper bin diameter b_i and lower bin diameter a_i, ($\mu g/m^3$),

C_{PM10} = measured PM concentration collected on size-selective PM_{10} filter, ($\mu g/m^3$),

MMD_{PM10} = mass median diameter of dust collected on PM_{10} filter, (μm), and,

GSD_{PM10} = geometric standard deviation of dust collected on PM_{10} filter, (dimensionless).

The difference between the measured and expected concentrations of PM_{10} of each particle size bin (i) is represented by a quantity J_i.

$$J_i = C_{PM10(measured),i} - C_{PM10(expected),i} \quad (14)$$

$$K = \sum_{i=0}^{n} J_i^2 \quad (15)$$

If the measured and expected PM_{10} concentrations are close to being equal then the quantity J (and therefore K) will tend towards a value of zero. When the concentrations and PSDs of the dust collected on the isokinetic filters and size selective PM_{10} filters were known, the quantity J for each particle size bin was determined, squared and the sum of squares for n bin sizes (K) minimized to obtain "best fit" values of cut-points and slopes of the PM_{10} FEC (eq.9). The constraints applied during minimization of differences were: cut-point (upper limit = 200 µm, lower limit = 1 µm)

and slope (upper limit = 20, lower limit = 1). This methodology was used to determine the "best fit" cut-points and slopes of both PM_{10} and TSP samplers, respectively.

Statistical Analysis

Exploratory data analysis was performed on the cut-points, slopes and aerosol concentrations of the samplers from each test as well as on the PSD characteristics of the dust obtained from the sampler filters. The 'Descriptives' function in SPSS (SPSS 16.0, SPSS Inc., Chicago, IL USA) was used to determine the means, standard deviations and mean standard errors of the individual data sets. The standardized residuals (z-res) were derived by subtracting the population mean from the individual raw scores and then dividing the difference by the population standard deviation. The z-res observations with values greater than 3 and less than -3 were considered outliers and excluded from further analysis. An outlier is an observation that lies outside the overall pattern of a distribution (Moore and McCabe, 1999). Outliers may represent faulty data, erroneous procedures, or wrong assumptions about the distribution of data and can abnormally influence the results of statistical tests conducted on a data set. For determining outliers in the case of concentrations, the 'Regression' function in SPSS was used to determine standardized residuals and leverage values. A leverage value indicates the potential of an independent variable to influence the dependent variable. Data points with more than six times the mean leverage value and absolute standardized residual values greater than three were excluded from the analysis. After the outliers were excluded, the 'Descriptives' command in SPSS was used to check for the skewness and kurtosis values for all data

sets. Values of skewness and kurtosis less than an absolute value of two indicated fairly normal data distribution.

To study the effect of the three independent variables (dust type, wind speed and aerosol concentration) on the dependent variables (cut-point and slope) of the PM_{10} and TSP samplers, a 3x3x5 model factorial analysis of variance (ANOVA) test was conducted in SPSS with null hypotheses ($\alpha = 0.05$) that dust type, wind speed and aerosol concentration and their interaction effects do not have any effect on the cut-points and slopes of PM_{10} samplers or TSP samplers. The p-value of the effects of the various independent parameters on the performance characteristics of samplers was determined before any further analysis and compared with the α value to determine if the null hypothesis can be rejected. All statistical tests performed in the analysis mentioned hereafter were conducted at the 0.05 level of significance.

An independent one sample t-test using the 'Compare Means' function in SPSS was used to determine if the means of cut-points and slopes of both PM_{10} samplers were within EPA's performance criteria of 10 ± 0.5 µm and 1.5 ± 0.1 for cut-point and slope, respectively, at various test conditions. T-tests were also conducted to see if the cut-points of TSP samplers were different from the reported value of 45 µm. Analysis of variance (ANOVA) tests were conducted on the cut-points, slopes and measured PM_{10} concentrations from the two PM_{10} samplers using the 'General Linear Model' function in SPSS with the null hypothesis ($\alpha = 0.05$) that the cut-points, slopes and measured PM_{10} concentrations from both samplers not different. Similar ANOVA tests were used to test the null hypothesis ($\alpha = 0.05$) that the cut-points, slopes and measured TSP

concentration of both TSP samplers were not different. ANOVA tests were conducted on the MMDs and GSDs of the dust collected on filters of isokinetic samplers, the dome-top TSP sampler and cone-top TSP sampler with the null hypothesis ($\alpha = 0.05$) that the MMDs and GSDs from the three samplers were not different. Means were compared using the Least Significant Difference (LSD) pair-wise multiple comparison test. A regression analysis was carried out to compare measured TSP and isokinetic concentrations.

Measured PM_{10} concentrations from the flat-head and louvered-head PM_{10} samplers were compared to the true PM_{10} concentrations. True PM_{10} was determined by multiplying the mass fraction of particles below 10 µm with the aerosol concentration from the isokinetic sampler. The mean measured PM_{10} concentrations were obtained for tests conducted with the three dust types. The sampling error was determined by subtracting the true PM_{10} concentrations from the measured PM_{10} concentrations and then dividing the difference by the true PM_{10} concentration before converting to percentage value. In this manner the over-sampling or under-sampling rates were determined. T-tests were used to determine if these sampling errors were different from 0.0% ($\alpha = 0.05$). True $PM_{2.5}$ and true PM_{10} concentrations determined from the TSP sampler PSD and aerosol concentration by the above mentioned method for tests with cornstarch were compared to the true $PM_{2.5}$ and true PM_{10} concentrations determined from the isokinetic sampler by evaluating their sampling errors. The sampling errors determined the suitability of either of the TSP samplers to act as a reference sampler in rural conditions.

Follow-up ‘post-hoc’ tests were conducted in SPSS and ‘estimated marginal means’ of the interactions determined to explore the nature of interaction between dust types, wind speeds and aerosol concentrations on the performance characteristics of PM_{10} and TSP samplers. A stepwise linear regression test was conducted using the ‘Regression’ function in SPSS to correlate the three independent variables to the dependent variables (cut-point and slope). Prior to running the regression, dust type was coded as a categorical variable so that it could be entered directly into the regression model and meaningfully interpreted. The regression was then performed by entering the predictor variables representing dust type, wind speed and concentration into the regression model.

CHAPTER IV

RESULTS AND DISCUSSION

Prior to collecting data for the second replication, it was observed that the internal parts of the dust feeder were being worn away by the abrasive actions of the test dusts. After replacing equipment and making changes recommended by the dust feeder manufacturer, a set of ten tests in the second replicate were conducted with ultrafine Arizona Road Dust while maintaining the internal randomization of sampler order to ensure proper operation of the feeder mechanism. Following the successful ten test evaluation of the dust feeder mechanism, the random experimental order of the experimental plan was followed for the remainder of the second replicate and the last replicate. A deviation from the experimental plan may have reduced the effective sample size for the tests which could have reduced the statistical power of the tests below adequacy levels. Due to this deviation from the experimental plan, statistical analysis and conclusions of this thesis should be considered cautiously.

The skewness and kurtosis values suggested that performance characteristics to be tested were fairly normally distributed apart from the PM10 sampler slopes (Table 5).

Table 5. Skewness and kurtosis results to check for normal distribution of data.

Parameter	Skewness	Kurtosis
Flat-head PM_{10} sampler cut-point	0.592	-0.397
Louvered-head PM_{10} sampler cut-point	0.388	-0.858
Dome-top TSP sampler cut-point	0.509	0.204
Cone-top TSP sampler cut-point	0.601	-0.251
Flat-head PM_{10} sampler slope	2.849	2.116
Louvered-head PM_{10} sampler slope	1.170	2.141
Dome-top TSP sampler slope	0.763	-0.075
Cone-top TSP sampler slope	0.746	0.417

Cut-points and Slopes of PM_{10} Inlets

The EPA performance criterion for FRM and FEM PM10 samplers allows a cut-point value of 10±0.5 µm and a slope value of 1.5±0.1 (CFR, 2001). The sampler cut-points of flat-head PM_{10} samplers ranged from 5.5 to 25.7 µm with a mean value and mean squared error (MSE) of 12.2 µm and 0.4 µm, respectively. The PM_{10} sampler cut-point of the louvered PM_{10} sampler ranged from 5.4 to 22.4 µm with a mean value and MSE of 12.2 µm and 0.4 µm, respectively. No outliers were detected for either of the PM_{10} sampler cut-points. The PM_{10} sampler slopes for the flat-head PM_{10} sampler ranged from 1.1 to 8.5 with a mean and MSE of 2.4 and 0.1, respectively, while the PM_{10} sampler slopes for the louvered-head PM_{10} sampler ranged from 1.2 to 5.8 with a mean and MSE of 2.5 and 0.1, respectively. There were three outliers in each of the PM_{10} sampler slope data sets having standardized residuals with an absolute value of more than three. These points were excluded from the analysis. The calculated cut-points of both FRM PM_{10} samplers showed a wide variation beyond EPA's specified tolerances.

Effects of Ambient Parameters on Performance Characteristics of Samplers

The results of factorial ANOVA, to determine if the effects of independent variables on the performance characteristics of PM_{10} and TSP samplers were statistically significant, have been presented in Tables 6 and 7, respectively. The results of the test indicated that dust type ($p < 0.0005$) had a statistically significant effect on cut-points of all test samplers and slopes of PM_{10} samplers while slopes of TSP samplers were not affected by dust type. Changes in wind speed had statistically significant effects on the cut-points of PM_{10} samplers and slopes of TSP samplers ($p < 0.0005$). The effect of aerosol concentration on the dependent variables was not statistically significant in most cases ($p > 0.05$) apart from cone-top TSP sampler slope ($p = 0.019$). The interaction of dust type and wind speed had statistically significant effect on cut-points and slopes of all the four test samplers ($p < 0.003$). The interaction of dust type and concentration had statistically significant effect on sampler cut-points but not slopes apart from dome-top TSP sampler slope. The interaction of wind speed and aerosol concentration was found not to affect TSP sampler cut-points and flat-head PM_{10} sampler slopes ($p > 0.05$).

Table 6. Significance values of factorial ANOVA tests on PM_{10} samplers to determine effects of parameters on dependent variable.

Parameter	Dependent Variable			
	Flat PM_{10} cut-point	**Flat PM_{10} slope**	**Louvered PM_{10} cut-point**	**Louvered PM_{10} slope**
Dust type	< 0.0005	< 0.0005	< 0.0005	< 0.0005
Wind speed	< 0.0005	0.149	< 0.0005	0.310
Concentration	0.684	0.319	0.718	0.445
Dust * Wind speed	< 0.0005	< 0.0005	< 0.0005	< 0.0005
Dust * Concentration	< 0.0005	0.584	< 0.0005	0.099
Wind speed * Concentration	0.007	0.103	0.01	0.003
Dust * Wind speed * Concentration	< 0.0005	0.829	< 0.0005	0.337

Table 7. Significance values of factorial ANOVA tests on TSP samplers to determine effects of parameters on dependent variable.

Parameter	Dependent Variable			
	Dome TSP cut-point	**Dome TSP slope**	**Cone TSP cut-point**	**Cone TSP slope**
Dust type	< 0.0005	0.062	< 0.0005	0.366
Wind speed	0.549	< 0.0005	0.930	0.018
Concentration	0.061	0.299	0.209	0.019
Dust * Wind speed	0.001	0.003	< 0.0005	< 0.0005
Dust * Concentration	0.004	0.040	< 0.0005	0.533
Wind speed * Concentration	0.292	0.003	0.381	< 0.0005
Dust * Wind speed * Concentration	0.054	0.074	0.231	0.051

Variation of Performance Characteristics of FRM PM_{10} Samplers by Dust Type

The results of t-tests performed on the cut-points and slopes of both FRM PM_{10} samplers with different dust types are listed in Tables 8 and 9. T-tests results indicated that cut-points of both PM_{10} samplers were different and larger than the upper limit of the cut-point (10.5 μm) when sampling ultrafine ARD ($p < 0.0005$) and corn starch ($p = 0.023$; $p = 0.012$). An ANOVA test indicated that the cut-points of both PM_{10} samplers were different from each other for all the three dust types. In the presence of a smaller MMD aerosol like ultrafine ARD (representative of an urban environment), the cut-points were larger than those obtained when sampling a larger MMD aerosol like cornstarch (representative of rural environment). The shift of cut-points to values beyond 10.5 μm would shift the FEC to the right in Figure 3 and thus Mass 1 may further increase over Mass 2 leading to additional under-sampling of dusts with MMDs less than 10 μm (Mass 1 >> Mass 2). When sampling fine ARD, the cut-points of both PM_{10} samplers were within EPA's tolerances (Tables 8 and 9). The wide variation of PM_{10}

sampler cut-points, as indicated by the range (5.43 to 18.25 µm) and the large mean squared errors (MSEs), resulted in the means of calculated cut-points below 9.5 µm compensating calculated cut-points above 10.5 µm. Hence the mean PM_{10} sampler cut-point for fine ARD was within EPA performance standards even though results of individual tests were outside the allowable performance limits.

A clear cut-point trend was not observed in this study as a function of dust type even though the mean cut-point for ultrafine ARD (smaller MMD aerosol) was larger than cornstarch (larger MMD aerosol). In contrast, Wang et al. (2005) found that cut-points increased with decreasing MMD of aerosols. The tests conducted by Wang et al. (2005), however, did not include cases with aerosols having MMDs less than the theoretical cut-point of a PM_{10} sampler (10 µm) and included two aerosols with nearly equal MMDs (10.58 and 10.38 µm, respectively). Hence it cannot be conclusively stated that a decreasing trend in cut-points really existed in the study by Wang et al. (2005).

The mean slope for both PM_{10} samplers for tests with all dust types was different from EPA performance criteria of 1.5 ±0.1 ($p < 0.002$; Tables 8 and 9). No visible trends were observed within mean slope values.

Table 8. Results of one sample independent t-test and ANOVA on performance characteristics of flat PM_{10} sampler with different aerosols.

	Flat PM_{10} cut-point			Flat PM_{10} slope		
Dust type	Mean(µm)[c]	MSE[a]	p-value[b]	Mean(µm)	MSE[a]	p-value[d]
Ultra-fine ARD	14.7x	0.7	< 0.0005	1.9	0.1	0.001
Fine ARD	10.2y	0.5	0.674	2.7	0.1	< 0.0005
Cornstarch	11.7z	0.7	0.023	2.3	0.1	< 0.0005

[a] MSE = Mean Squared Error; [b] Test value = 10.5 µm; [c] No differences were detected (α = 0.05) between means in the same column followed by the same letter; [d] Test value = 1.6.

Table 9. Results of one sample independent t-test and ANOVA on performance characteristics of louvered PM_{10} sampler with different aerosols.

	Louvered PM_{10} cut-point			Louvered PM_{10} slope		
Dust type	Mean(µm)	MSE[a]	p-	Mean(µm)	MSE[a] (µm)	p-value[d]
Ultra-fine ARD	14.6x	0.6	< 0.0005	2.0	0.1	< 0.0005
Fine ARD	10.2y	0.5	0.821	2.9	0.1	< 0.0005
Cornstarch	12.0z	0.8	0.012	2.3	0.1	< 0.0005

[a] MSE = Mean Squared Error; [b] Test value = 10.5; [c] No differences were detected (α = 0.05) between means in the same column followed by the same letter; [d] Test value = 1.6.

Variation of Performance Characteristics of FRM PM_{10} Samplers by Wind Speed

The results of t-tests performed on the cut-points and slopes of both FRM PM_{10} samplers at different wind speeds are listed in Tables 10 and 11. The PM_{10} cut-point results for tests at 2 km/h were not different from the upper limit of 10.5 µm for both samplers ($p = 0.449$; $p = 0.916$). For tests conducted at 8 and 24 km/h, cut-points of both samplers were larger than the upper limit of allowed cut-point ($p < 0.002$). Since an increasing trend in PM_{10} sampler cut-points was observed for both samplers, an ANOVA test was conducted in SPSS to test whether the means of cut-points calculated at the three wind speeds were different from each other. The results indicated that the three cut-points were different for both flat and louvered PM_{10} samplers ($p = 0.043$, 0.018, respectively). PM_{10} sampler cut-points increased with an increase in the wind speed at which a test was conducted.

In contrast, McFarland et al. (1984) indicated that cut-points of FRM high-volume samplers decreased at increased wind speeds of 48 km/h. Such a trend was not seen for the data in this study. A high-volume sampler draws about 66 to 100 times the

mass of ambient air and aerosol in the same period of time as a low-volume sampler does. This tends to rapidly make the inlet and impactor plate of the sampler dirty. The drop in cut-points reported by McFarland et al. (1984) may be more a function of the "dirtiness" of samplers rather than effect of wind speed. The accumulated aerosol, arising from heavy loading and prolonged use without cleaning, will lead to high surface roughness and viscosity of the oil-coated surface which will trap the large particles in the impactor (Ono et al., 2000). Thus the accumulation of larger particles in the pre-separator may have shifted the penetration curve to the left in Figure 1 thus shifting the cut-point towards smaller diameters. A decrease in the cut-point of the Wedding sampler to 6.6 μm when the inlet was dirty was reported at 8 km/h (McFarland et al., 1985) while a dirty SA-321A sampler was reported to have a cut-point of 8.0 μm (Rodes et al., 1985). This indicates that wind speed was not necessarily responsible for the decrease in cut-points of dirty samplers as reported by McFarland et al. (1984).

The mean slope for both PM_{10} samplers for tests at all wind speeds was different from EPA performance criteria of 1.5±0.1 ($p < 0.002$; Tables 10 and 11). No visible trends were observed within mean slope values.

Table 10. Results of one sample independent t-test and ANOVA on performance characteristics of flat PM_{10} sampler at different wind speeds.

Wind	Flat PM_{10} cut-point			Flat PM_{10} slope		
Speed(km/h)	Mean(μm)[c]	MSE[a]	p-value[b]	Mean(μm)	MSE[a]	p-value[d]
2	10.1x	0.5	0.449	2.4	0.1	< 0.0005
8	12.3y	0.6	0.002	2.2	0.1	< 0.0005
24	13.6z	0.8	0.001	2.3	0.2	0.002

[a] MSE = Mean Squared Error; [b] Test value = 10.5 μm; [c] No differences were detected (α = 0.05) between means in the same column followed by the same letter; [d] Test value = 1.6.

Table 11. Results of one sample independent t-test and ANOVA on performance characteristics of louvered PM_{10} sampler at different wind speeds.

Wind	Louvered PM_{10} cut-point			Louvered PM_{10} slope		
Speed(km/h)	Mean(µm)[c]	MSE[a]	p-value[b]	Mean(µm)	MSE[a]	p-value[d]
2	10.4x	0.5	0.916	2.6	0.1	< 0.0005
8	12.4y	0.5	< 0.0005	2.3	0.1	< 0.0005
24	13.6z	0.8	0.001	2.3	0.2	0.001

[a] MSE = Mean Squared Error; [b] Test value = 10.5; [c] No differences were detected (α = 0.05) between means in the same column followed by the same letter; [d] Test value = 1.6.

Variation of Performance Characteristics of FRM PM_{10} Samplers by Aerosol Concentration

Mean cut-points of both PM_{10} samplers were different from the upper limit of allowed cut-point for tests conducted at 150-, 300- and 500-µg/m^3 while there were no differences in the mean cut-points at 1000 and 1500 µg/m^3 (Tables 12 and 13). The mean slope for both PM_{10} samplers at all aerosol concentrations was different and larger than the EPA performance criteria of 1.5±0.1 ($p < 0.003$; Tables 12 and 13). No visible trends were observed within mean slope values. The ANOVA tests indicated that at certain levels of aerosol concentrations there were no differences in the mean cut-points.

Table 12. Results of one sample independent t-test and ANOVA on performance characteristics of flat PM_{10} sampler at different concentrations.

Aerosol concentration	Flat PM_{10} cut-point			Flat PM_{10} slope		
(µg/m^3)	Mean	MSE[a](µm)	p-value[b]	Mean(µm)	MSE[a](µm)	p-value[d]
150	12.1x	0.6	0.010	2.3	0.1	< 0.0005
300	12.5y	0.7	0.006	2.1	0.1	0.003
500	12.2x	0.9	0.050	2.2	0.1	< 0.0005
1000	12.1x	1.2	0.193	2.5	0.2	<0.0005
1500	12.1x	1.4	0.279	2.5	0.2	< 0.0005

[a] MSE = Mean Squared Error; [b] Test value = 10.5 µm; [c] No differences were detected (α = 0.05) between means in the same column followed by the same letter; [d] Test value = 1.6.

Table 13. Results of one sample independent t-test and ANOVA on performance characteristics of louvered PM_{10} sampler at different concentrations.

Aerosol concentration ($\mu g/m^3$)	Louvered PM_{10} cut-point			Louvered PM_{10} slope		
	Mean(µm)[c]	MSE[a](µm)	pvalue[b]	Mean(µm)	MSE[a](µm)	p-value[d]
150	12.1w	0.6	0.011	2.2	0.1	< 0.0005
300	12.7x	0.7	0.005	2.2	0.1	< 0.0005
500	12.8x	0.9	0.014	2.4	0.1	< 0.0005
1000	11.5y	1.0	0.324	2.7	0.2	< 0.0005
1500	11.9z	1.3	0.315	2.5	0.2	< 0.0005

[a] MSE = Mean Squared Error; [b] Test value = 10.5; [c] No differences were detected (α = 0.05) between means in the same column followed by the same letter; [d] Test value = 1.6

Cut-points and Slopes of TSP Inlets

The cut-point of the dome-top TSP sampler ranged from 12.6 to 45.0 µm with a MSE of 0.6 µm. The cut-point of the cone-top TSP sampler ranged 12.8 to 64.2 µm with a MSE of 1.0 µm. Two outlier points were excluded from the analysis for both TSP samplers. The slope of the dome-top TSP sampler ranged from 1.0 to 2.7 with a MSE of 0.04. The slope of the cone-top TSP sampler ranged from 1.1 to 3.0 with a MSE of 0.04. One outlier point each was excluded from the slope values for both TSP samplers. The mean cut-points of both TSP samplers (28.2 ±1.1 and 33.0±1.9 µm) were different and smaller than the reported value of 45 µm for all aerosol types, wind speeds and aerosol concentrations ($p < 0.01$; Tables 14, 15 and 16).

Table 14. Results of one sample independent t-test and ANOVA on TSP sampler cut-points with different aerosols.

	Dome-top TSP			Cone-top TSP		
Dust type	Mean(µm)[c]	MSE[a](µm)	pvalue[b]	Mean(µm)[c]	MSE[a](µm)	p-value[b]
Ultrafine ARD	24.8x	0.6	< 0.0005	24.7x	0.7	< 0.0005
Fine ARD	31.2y	0.9	< 0.0005	40.1y	1.7	0.006
Cornstarch	28.9z	1.0	< 0.0005	33.5z	1.4	< 0.0005

[a] MSE = Mean Squared Error; [b] Test value = 45 µm; [c] No differences were detected (α = 0.05) between means in the same column followed by the same letter.

Table 15. Results of one sample independent t-test and ANOVA on TSP sampler cut-points at different wind speeds.

Wind	Dome-top TSP			Cone-top TSP		
Speed(km/h)	Mean(µm)[c]	MSE[a](µm)	p-value[b]	Mean(µm)[c]	MSE[a](µm)	p-value[b]
2	27.8x	0.9	< 0.0005	32.5x	1.5	< 0.0005
8	29.8y	1.0	< 0.0005	35.4y	1.9	< 0.0005
24	26.4z	0.9	< 0.0005	31.4z	1.8	< 0.0005

[a] MSE = Mean Squared Error; [b] Test value = 45 µm; [c] No differences were detected (α = 0.05) between means in the same column followed by the same letter.

Table 16. Results of one sample t-tests and ANOVA on TSP sampler cut-points at different concentrations.

Aerosol concentration	Dome-top TSP			Cone-top TSP		
(µg/m^3)	Mean(µm)[c]	MSE[a](µm)	pvalue[b]	Mean(µm)	MSE[a](µm)	p-value[c]
150	25.8x	1.0	< 0.0005	32.8x	1.8	< 0.0005
300	28.7y	1.1	< 0.0005	32.0x	1.6	< 0.0005
500	26.3x	1.1	< 0.0005	34.0y	2.4	<0.0005
1000	28.0y	1.1	< 0.0005	30.6z	1.9	< 0.0005
1500	31.4z	1.7	< 0.0005	30.7z	1.6	<0.0005

[a] MSE = Mean Squared Error; [b] Test value = 45 µm; [c] No differences were detected (α = 0.05) between means in the same column followed by the same letter.

Performance Comparison within PM_{10} and TSP Inlets

ANOVA tests were conducted to compare the performance of the two PM_{10} samplers. The results are presented in Table 17. No differences were detected between the cut-points and the slopes of the two samplers ($p = 0.992$; 0.544, respectively). There were no differences in the PM_{10} concentration measurements for tests at each of the five test concentrations ($p > 0.05$). Thus the performance of the two PM_{10} samplers was concluded to be similar under all conditions tested. The similarity in performance characteristics of the two PM_{10} samplers in spite of the fact that the mean cut-points while sampling ultrafine ARD and cornstarch and mean slopes while sampling all the three aerosols for both samplers were outside EPA's tolerances point towards the inherent errors arising in performance characteristics of PM_{10} samplers due to the sampling methodology required by the EPA.

Table 17. ANOVA results from comparison of flat-head and louvered-head PM_{10} samplers.

	Flat PM_{10}	Louvered PM_{10}	Significance (p-value)
Cut-point	11.8	11.9	0.992
Slope	2.3	2.4	0.544
PM_{10} Conc. (150 µg/m^3)[a]	113	109	0.734
PM_{10} Conc. (300 µg/m^3) [a]	222	213	0.658
PM_{10} Conc. (500 µg/m^3) [a]	360	367	0.857
PM_{10} Conc. (1000 µg/m^3) [a]	639	688	0.988
PM_{10} Conc. (1500 µg/m^3) [a]	967	945	0.913

[a] Values in parentheses indicate target TSP concentrations.

The results of ANOVA tests on performance characteristics of TSP samplers are presented in Table 18. Differences were detected in the cut-points and slopes between

the two TSP samplers ($p < 0.0005$, 0.001, respectively). The mean TSP concentrations calculated for tests at all the five test concentrations were different ($p < 0.05$). The results indicated that the performance characteristics of the two TSP samplers were different for all conditions. The cut-points of cone-top TSP samplers were consistently higher than the cut-points of dome-top TSP samplers for all data values compared.

Table 18. ANOVA results from comparison of dome-top and cone-top TSP samplers.

	Dome-top	Cone-top	Significance (p-value)
Cut-point	27.9	32.1	< 0.0005
Slope	1.71	1.9	0.001
TSP Conc.(150 µg/m^3)[a]	193	138	< 0.0005
TSP Conc. (300 µg/m^3) [a]	365	274	< 0.0005
TSP Conc. (500 µg/m^3) [a]	605	452	< 0.0005
TSP Conc. (1000 µg/m^3) [a]	1108	890	0.035
TSP Conc. (1500 µg/m^3) [a]	1433	1067	0.035

[a] Values in parentheses indicate target TSP concentrations.

Performance Comparison of Collocated Isokinetic and TSP Inlets

The MMDs and GSDs of both TSP sampler PSDs determined from the samplers were compared to the MMDs and GSDs of isokinetic PSDs, respectively, through an ANOVA test. The TSP sampler concentrations and isokinetic concentrations were compared through a linear regression. The results of the ANOVA tests and linear regression on dome-top TSP and cone-top TSP samplers have been presented in Tables 19 and 20, and in Tables 21 and 22, respectively. In general, the PSDs captured by the dome-top TSP sampler were similar to those from the isokinetic sampler except for the

GSDs obtained from fine ARD where the mean was different (p = 0.002) (Table 19). Increase in the MMD of the sampled aerosol did not bring about any noticeable difference in the performance of the TSP sampler and the isokinetic sampler.

The results of the regression analysis of dome-top TSP with isokinetic concentrations indicated that the concentrations were highly correlated (Table 20). A slope of unity and intercept of zero indicates that the dome-top TSP sampler captured identical TSP concentrations as the isokinetic sampler. The 95% intercept confidence intervals (CIs) for tests with ultrafine and fine ARD included zero while the intercept of cornstarch did not. The intercept CIs increased with increasing MMD of dust while the slope coefficients decreased with increasing MMDs and were less than unity for all cases. The 90% CIs for the slope did not include unity for all three aerosol conditions either. The intercept and slope CIs indicated that isokinetic TSP concentrations were linearly related to but were higher than the dome–top TSP concentrations.

Table 19. ANOVA results from comparison of isokinetic sampler and dome-top TSP sampler[a].

Dust	Parameter	Isokinetic	Dome-top TSP	Significance(p-value)
Ultrafine ARD	MMD[b]	4.7x	4.7x	0.754
	GSD[c]	2.1x	2.1x	0.093
Fine ARD	MMD[b]	8.7x	8.0x	0.198
	GSD[c]	2.9x	2.6y	0.002
Cornstarch	MMD[b]	16.4x	15.1x	0.051
	GSD[c]	1.9x	1.9x	0.367

[a] No differences were detected (α = 0.05) between means in the same row followed by the same letter.
[b] MMD = Mass Median Diameter
[c] GSD = Geometric Standard Deviation.

Table 20. Regression results of dome-top TSP concentrations with isokinetic concentrations.

Dust	$R^{2[a]}$	Parameter	$B^{[b]}$	95% CI[c] for B	
				Lower Bound	Upper Bound
Ultrafine	0.90	Intercept (μg/m^3)	28	-70	127
		Slope	0.75	0.67	0.83
Fine ARD	0.85	Intercept (μg/m^3)	72	-33	177
		Slope	0.76	0.65	0.86
Cornstarch	0.73	Intercept (μg/m^3)	128	41	214
		Slope	0.61	0.49	0.74

[a] Correlation coefficient; [b] Unstandardized coefficient; [c] Confidence interval.

Unlike the comparison with dome-top TSP samplers, differences at $\alpha = 0.05$ significance level were detected when comparing the PSDs captured by the cone-top TSP sampler with those from the isokinetic sampler (Table 21). The differences in the MMDs collected by the cone-top TSP sampler as compared to the isokinetic sampler while sampling fine ARD and cornstarch (agricultural dust) were statistically significant ($p < 0.0005$; 0.002, respectively). Though the correlation coefficients of regression on concentrations indicated a reasonably high correlation, low slope CIs compared to unity meant that the cone-top TSP samplers captured a lower concentration of TSP than isokinetic samplers (Table 22). The cone-top TSP sampler was thus concluded to be non-representative in capturing ambient aerosols and was considered unsuitable for use as a reference sampler in urban as well as rural conditions.

Table 21. ANOVA results from comparison of isokinetic sampler and cone-top TSP sampler[a].

Dust	Parameter	Isokinetic	Cone-top TSP	Significance (p-value)
Ultrafine ARD	MMD[b]	4.7x	4.6x	0.059
	GSD[c]	2.1x	2.1x	0.088
Fine ARD	MMD[b]	8.7x	6.6y	< 0.0005
	GSD[c]	2.9x	2.8x	0.681
Cornstarch	MMD[b]	16.4x	14.6y	0.002
	GSD[c]	1.9x	2.0y	< 0.0005

[a] No significant differences were detected ($\alpha = 0.05$) between means in the same row followed by the same letter.
[b] MMD = Mass Median Diameter
[c] GSD = Geometric Standard Deviation

Table 22. Regression results of dome-top TSP concentrations with isokinetic concentrations.

Dust	R^2[a]	Parameter	B[b]	95% CI[c] for B	
				Lower Bound	Upper Bound
Ultrafine	0.88	Intercept	60	-25	145
		Slope	0.58	0.51	0.65
Fine ARD	0.85	Intercept	59	-26	143
		Slope	0.59	0.51	0.67
Cornstarch	0.71	Intercept	78	21	135
		Slope	0.38	0.29	0.46

[a] Correlation coefficient; [b] Unstandardized coefficient; [c] Confidence interval

Sampling Errors of PM Samplers in Comparison to Reference Sampler

Results of sampling errors determined from the comparison of true and measured PM_{10} concentrations are presented in Table 23. The results indicate that both PM_{10} samplers over-sampled cornstarch (representing agricultural dust) while under-sampling ultrafine ARD (representing urban dust) and fine ARD (mean MMD < 10 µm) (Table 23). The results indicate that under-sampling or over-sampling error increased as the

MMD of the dust deviated from the theoretical cut-point of the PM_{10} sampler (10 µm). The differences in the measured and true PM_{10} concentrations were statistically significant for both PM_{10} samplers. T-test results indicated that all sampling errors were different from zero (a zero error would indicate no sampling error) for the three samplers for all aerosol types.

Table 23. Sampling errors of mean PM_{10} sampler concentrations with variation of aerosol MMD[a].

	Isokinetic		Flat PM_{10}		Louvered PM_{10}	
Dust type	MMD	True PM_{10} (µg/m^3)	Measured PM_{10} (µg/m^3)	Sampling Error (%) [b][c]	Measured PM_{10} (µg/m^3)	Sampling Error (%) [b][c]
Ultrafine ARD	4.7	861x	657y	-23.8	645y	-25.1
Fine ARD	9.0	463x	393y	-15.3	369y	-20.4
Cornstarch	16.4	157x	221y	40.8	223y	42.2

[a] No differences were detected ($\alpha = 0.05$) between means in the same row followed by the same letter; [b] Positive value indicates over-sampling while negative value indicates under-sampling; [c] All values are different from test value of 0.0% ($p < 0.0005$).

The suitability of the two TSP samplers when acting as a reference sampler in a typical agricultural environment was evaluated in order to address the issue of sampler bias in rural conditions. Since the regression of TSP concentrations indicated that TSP sampler concentrations were less than isokinetic concentrations (Tables 20 and 22), it was necessary to compare the true PM_{10} and $PM_{2.5}$ concentrations determined from the PSD and TSP concentrations obtained from the TSP samplers with those from the isokinetic sampler to determine if the true concentrations were different from each other ($\alpha = 0.05$). Hence, the means of true $PM_{2.5}$ and PM_{10} concentrations were determined for

each TSP sampler for tests with cornstarch (simulating agricultural aerosols) and compared to the true $PM_{2.5}$ and PM_{10} concentrations of the isokinetic sampler (Table 24).

Table 24. Sampling errors of mean true $PM_{2.5}$ and PM_{10} concentrations of TSP and isokinetic samplers for tests in an agricultural environment (cornstarch).

Sampler type	True $PM_{2.5}$ ($\mu g/m^3$)[a]	Sampling Error (%) [b][c]	True PM_{10} ($\mu g/m^3$) [a]	Sampling Error (%) [b][c]
Dome-top	35x	-3.9	160x	2.0
Cone-top	19y	-47.2a	87y	-44.2a
Isokinetic	37x	N/A[d]	157x	N/A[d]

[a] No differences were detected ($\alpha = 0.05$) between means in the same column followed by the same letter; [b] Positive value indicates over-sampling while negative rate indicates under-sampling; [c] Values followed by a letter are different from test value of 0.0% ($p < 0.05$); [d] N/A = Not Applicable.

The sampling error was different from zero ($p < 0.05$) and negative in magnitude for the true PM concentrations obtained from the cone-top TSP sampler indicating that cone-top TSP samplers under-sampled ambient PM. The cone-top TSP sampler had large under-sampling errors of 44 and 47% when measuring true PM_{10} and $PM_{2.5}$ concentrations, respectively. T-test results indicated that the sampling error was not different from zero ($p > 0.05$) for the true $PM_{2.5}$ and PM_{10} concentrations captured by the dome-top TSP sampler. The dome-top TSP sampler was concluded to perform suitably as a reference sampler due to the similarity of the PSD characteristics coupled with the similarity in true PM concentrations. Thus the dome-top TSP sampler can serve effectively as a reference sampler in agricultural environments while the cone-top TSP sampler should not be used as such.

Interaction Effects of Dust Type and Wind Speed

The interaction of dust type and wind speed had statistically significant effect on cut-points and slopes of all the four test samplers ($p < 0.003$). The PM_{10} cut-points were different by dust type at calm air conditions (2 km/h) and at high wind speeds (24 km/h) but there were no differences at 8 km/h. The PM_{10} sampler slopes and TSP sampler cut-points were different by dust type at all wind speed conditions ($p < 0.05$). The PM_{10} cut-points and slopes were different by wind speed for all the three aerosol types with the cut-points showing an increasing trend with increasing wind speeds for cornstarch and slopes showing a decreasing trend for ultrafine ARD and cornstarch. The TSP sampler cut-points were different by wind speed for higher MMD dusts like cornstarch and fine ARD but not for smaller MMD ultrafine ARD. Though the interaction of dust type and wind speed did not form any definite trend, the interactions produced p-values which were statistically significant at higher wind speeds but not for calm air conditions.

Interaction Effects of Dust Type and Aerosol Concentration

The interaction of dust type and concentration had statistically significant effects on all performance characteristics except PM_{10} sampler slopes and cone-top TSP sampler slope. The PM_{10} sampler cut-points and the dome-top and cone-top TSP sampler cut-points were different by dust type at all aerosol concentrations. The PM_{10} sampler cut-points were different by aerosol concentration for fine ARD but the differences in means were not statistically significant for ultrafine ARD and cornstarch. The dome top TSP sampler cut-points were different by aerosol concentration for aerosols with MMDs

resembling rural conditions (cornstarch) but not different for aerosols with urban MMDs (ultrafine ARD). For the cone-top TSP sampler cut-points, the differences were statistically significant by aerosol concentration for all the three aerosols. In general, the interaction of dust type and aerosol concentration seemed to affect the performance characteristics of higher MMD aerosols more than they affected the performance characteristics of a lower MMD aerosol like ultra-fine ARD.

Interaction Effects of Wind Speed and Aerosol Concentration

The interaction of wind speed and aerosol concentration did not result in a statistically significant effect on TSP sampler cut-points and flat-head PM_{10} sampler slopes ($p > 0.05$). The mean cut-points of both PM_{10} samplers were different by wind speed at all aerosol concentrations ($p < 0.05$) though the difference in means was large only at 500 $\mu g/m^3$ but not at low or high aerosol concentrations. The mean slope of the louvered-head PM_{10} sampler was different by wind speed at all aerosol concentrations while the mean slopes of both TSP samplers were different by wind speed at extreme values of aerosol concentrations (150-, 1000-, and 1500-$\mu g/m^3$) but not at middle aerosol concentrations. The sampler cut-points of both PM_{10} samplers were different by aerosol concentration at all the three wind speeds ($p < 0.05$) though the differences in means were more noticeable at higher wind speeds (8 and 24 km/h) than at calm air conditions (2 km/h). The louvered-head PM_{10} sampler slopes were different by aerosol concentration at a wind speed of 24 km/h but the differences were not statistically significant at lower wind speeds. The cone-top TSP sampler slopes were different by

aerosol concentration at extreme air conditions (2 and 24 km/h) while the differences were not statistically significant at 8 km/h. The dome-top TSP sampler slopes were not different by aerosol concentration at any of the three wind speeds ($p > 0.05$). In general, the effects of interactions of wind speed and aerosol concentration were observed to be statistically significant at higher wind speeds but not so during low wind speed conditions while the statistical significance of the effects at middle aerosol concentrations seemed coincidental.

Interaction Effects of Dust Type, Wind Speed and Aerosol Concentration

The interaction of the three predictor variables had statistically significant effects on PM_{10} sampler cut-points ($p < 0.0005$) but not on the PM_{10} sampler slopes ($p > 0.05$). The performance characteristics of the TSP samplers did not seem to be affected by the overall interaction of the predictor variables.

Linear Regression between Ambient Parameters and Performance Characteristics of Samplers

The results of regression on the performance characteristics of PM samplers to determine the linearity of the relationship with the ambient parameters has been presented in Tables 25 and 26. In general, aerosol type was determined to be the best predictor of the linear variability in sampler performance characteristics though it was not a good predictor in terms of the R^2-value. Although statistically significant, wind speed made little contribution to the linear variability of sampler cut-points and dome-top TSP sampler slope. Though aerosol concentration was entered as a predictor variable

for each case, the outcomes of the regression models suggested that variability in the sampler performance was not affected by variation in aerosol concentration. The small R^2 for all cases indicated that the regression model was weak in its ability to predict the variation in performance characteristics of the samplers (Table 25 and 26).

Table 25. Results of regression on cut-point of PM samplers.

Sampler Type	Prediction Variable	R^2	Increase in R^2	p-value
Flat-head PM_{10}	Dust type	0.165	0.165	0.001
	Wind speed	0.224	0.045	<0.0005
Louvered-head PM_{10}	Dust type	0.175	0.175	<0.0005
	Wind speed	0.225	0.056	0.004
Dome-top TSP	Dust type	0.233	0.233	<0.0005
	Wind speed	0.271	0.039	0.014
Cone-top TSP	Dust type	0.332	0.332	<0.0005
	Wind speed	--	--	--

Table 26. Results of regression on slope of PM samplers.

Sampler Type	Prediction Variable	R^2	Increase in R^2	p-value
Flat-head PM_{10}	Dust type	0.103	0.103	<0.0005
	Wind speed	--	--	--
Louvered-head PM_{10}	Dust type	0.139	0.139	<0.0005
	Wind speed	--	--	--
Dome-top TSP	Dust type	--	--	--
	Wind speed	0.125	0.125	<0.0005
Cone-top TSP	Dust type	0.036	0.036	0.036
	Wind speed	--	--	--

CHAPTER V

SUMMARY AND CONCLUSIONS

Cut-points of PM_{10} samplers deviated from their theoretical value when sampling aerosols having MMDs significantly different from the theoretical cut-points of the samplers. The shift in cut-point of the PM_{10} sampler while sampling ultra-fine ARD was larger than that when sampling cornstarch. Past studies found an increasing trend for cut-points with decreasing MMD (Wang et al., 2005). The mean cut-points fell within EPA's tolerances when sampling an aerosol with a mean MMD close to the theoretical cut-point of the PM_{10} sampler (i.e. fine ARD), but individual test results varied outside of the allowable range.

The mean cut-points of both PM_{10} samplers increased with increasing wind speed. This observation may be explained by the increased momentum of larger particles at higher wind speeds, which may carry these particles through the impactor plates and onto the filter. Their inclusion in the constitution of the filter PSD would shift the penetration curve to the right in Figure 1 indicating an increase in sampler cut-point. Additionally a larger number of heavier particles penetrating the pre-separator will lead to over-sampling of the ambient aerosol.

Mean slopes of both PM_{10} samplers showed a deviation from the EPA criteria of 1.5 ± 0.1 for all dust types and at all wind speeds, but no significant trends were observed. No trends in cut-point or slope were observed for tests at different aerosol concentrations. Factorial ANOVA tests indicated that aerosol concentration does not affect performance characteristics of the samplers apart from the slope of the cone-top TSP sampler.

The two PM_{10} (flat-head and louvered-head) samplers had similar performance characteristics over the entire test schedule in spite of those performance characteristics being outside EPA's tolerances. This indicated that variation in cut-points and slopes of PM_{10} samplers may not be due to design flaws of the samplers but instead due to inherent errors arising from the interaction of particle size characteristics of the sampled aerosol with the performance characteristics of the sampler. These errors may intensify based on the hypothesis that heavier particles penetrate the pre-separator and collect on the filter at higher wind speeds.

The PM_{10} samplers were found to over-sample cornstarch (simulating agricultural aerosols) and under-sample ultra-fine ARD (simulating urban aerosols). The results of this study show that shifts in sampler performance would shift the FEC and may exacerbate the over-sampling and under-sampling biases identified by Buser et al. (2007a). The over-sampling or under-sampling rates increased as the MMD of sampled aerosol deviated from the theoretical cut-point of a PM_{10} sampler.

The TSP (dome-top and cone-top) samplers had cut-points which were different and significantly lower than the reported cut-point for TSP samplers (45 μm). The dome–top TSP sampler captured similar PSDs as the isokinetic sampler. The TSP concentrations of the dome-top TSP sampler had a high positive correlation with TSP concentrations from the isokinetic sampler. The measured TSP concentrations, however, were less than those of isokinetic sampler. In an agricultural environment (represented by cornstarch), the true PM_{10} and $PM_{2.5}$ concentrations measured by the dome-top TSP sampler were similar to the true concentrations obtained from the isokinetic sampler in

spite of the dissimilar TSP concentrations. On the other hand, the cone-top TSP sampler had large differences in characteristics of captured PSDs and TSP concentrations as compared to isokinetic samplers. The true PM_{10} and $PM_{2.5}$ concentrations measured by the cone-top TSP sampler indicated that it has an under-sampling bias as compared to isokinetic sampler.

The interaction effects of dust type and wind speed as well as the interaction effects of aerosol concentration and wind speed were statistically significant at higher wind speeds while the interaction effects of dust type with aerosol concentration was statistically significant effects for higher MMD aerosols like cornstarch than for ultrafine ARD. Stepwise linear regression models are weak in their ability to explain the variability of performance characteristics of the test samples due to ambient parameters. Varying aerosol type explains the linear variation of the performance characteristics of samplers to a reasonable extent while changes in wind speed primarily affect the variation of sampler cut-points. Due to complex interaction between the three parameters and their unpredictable nature, it was not possible to quantify these changes conclusively through a linear regression and determine cut-point and slope trends.

The following generalized conclusions were drawn from this research:

- The performance characteristics (cut-point and slope) of both PM_{10} samplers were greatly affected by the environmental conditions like aerosol type, wind speed and aerosol concentration over the tests. The performance characteristics of the FRM PM_{10} samplers used in this study deviated beyond the EPA-specified performance criteria.

- FRM PM_{10} samplers will have an over-sampling bias or under-sampling bias when operating in rural and urban conditions, respectively.
- The dome-top TSP sampler can be used as an effective reference sampler in field sampling campaigns.
- The cone-top TSP sampler is not suited for use as a reference sampler.

REFERENCES

Buser, M. D., C. B. Parnell, Jr., B. W. Shaw, and R. E. Lacey. 2007a. Particulate matter sampler errors due the interaction of particle size and sampler performance characteristics: Background and theory. *Trans ASABE* 50(1): 221-228.

Buser, M. D., C. B. Parnell, Jr., B. W. Shaw, and R. E. Lacey. 2007b. Particulate matter sampler errors due the interaction of particle size and sampler performance characteristics: Ambient PM_{10} samplers. *Trans ASABE* 50(1): 229-240.

Buser, M. D., J. D. Wanjura, D. P. Whitelock, S. C. Capareda, B. W. Shaw, and R. E. Lacey. 2008. Estimating FRM PM_{10} matter performance characteristics using particle size analysis and collocated TSP and PM_{10} samplers: Cotton gins. *Trans ASABE* 51(2): 695-702.

Capareda, S. C., C. B. Parnell, B. W. Shaw, and J. D. Wanjura. 2005. Particle size distribution analyses of agricultural dusts and report of true PM_{10} concentrations. *Proc. 2005 American Society of Agricultural Engineers (ASAE) Conference.* Paper No. 054044. Tampa, Florida: ASAE.

Chen, J. 2007. Development of methodology to correct sampling errors associated with FRM PM_{10} sampler. Ph.D. Dissertation. College Station, TX: Texas A&M University, Department of Biological and Agricultural Engineering.

Code of Federal Regulations (CFR). 1987. Reference method for the determination of suspended particulate matter in the atmosphere (high volume method). 40 CFR, Part 50, Appendix B. Washington, D.C.: U.S. Government Printing Office.

Code of Federal Regulations (CFR). 2001. Ambient air monitoring reference and equivalent methods. 40 CFR, Part 53. Washington, D.C.: U.S. Government Printing Office.

Code of Federal Regulations (CFR). 2006a. National ambient air quality standards for particulate matter; final rule. 40 CFR, Part 50. Washington, D.C.: U.S. Government Printing Office.

Code of Federal Regulations (CFR). 2006b. Ambient air monitoring reference and equivalent methods. 40 CFR, Part 53, Subpart D. Washington, D.C.: U.S. Government Printing Office.

Code of Federal Regulations (CFR). 2006c. Reference method for the determination of particulate matter as PM_{10} in the atmosphere. 40 CFR, Part 50, Appendix J. Washington, D.C.: U.S. Government Printing Office.

Code of Federal Regulations (CFR). 2006d. Ambient air monitoring reference and equivalent methods. 40 CFR, Part 53, Subpart C. Washington, D.C.: U.S. Government Printing Office.

Cooper, C. D. and Alley, F. C. 2002. *Air Pollution Control: A Design Approach.* 3rd ed. Prospect Heights, IL: Waveland Press Inc.

Cowherd, Jr., C. 2005. Analysis of the fine fraction of particulate matter in fugitive dust. Final Report. Midwest Research Institute (MRI) Project No. 110397. MRI-AED\R110397-06.doc.

Faulkner, W. B., B. W. Shaw, R. E. Lacey. 2007. Coarse fraction aerosol particles: Theoretical analysis of rural versus urban environments. *Applied Engineering in Agriculture*. 23(2): 239-244

Federal Register. 1971, April 30. National primary and secondary ambient air quality standards. *Federal Register.* 36:8186-8201.

Hinds, W. C. 1999. *Aerosol Technology - Properties, Behavior, and Measurement of Airborne Particles*. 2nd ed. New York: John Wiley & Sons, Inc.

Lacey, R. E., J. S. Redwine and C. B. Parnell Jr. 2003. Particulate matter and ammonia emission factors for tunnel ventilated broiler production houses in the southern United States. *Transactions of the ASAE* 46(4): 1203-1214.

McFarland, A. R. and C. A. Ortiz. 1983. Evaluation of prototype PM-10 inlets with cyclonic fractionators . Paper No. 33.5 presented at the 76th Annual Meeting and Exposition of the Air Pollution Control Association , Atlanta , GA.

McFarland, A. R., C. A. Ortiz, and R. W. Bertch, Jr. 1984. A 10 µm cutpoint size selective inlet for hi-vol samplers. *Journal of Air Pollution Control Association.* 34(5): 544-547.

McFarland, A. R.and C. A. Ortiz. 1985. Sampling anomalies of the 40-CFM Wedding aerosol sampler. College Station, TX: Texas A&M University, Department of Civil Engineering.

Moore, D. S. and McCabe, G. P. 1999. *Introduction to the Practice of Statistics*. 3rd ed. New York, NY, W.H. Freeman, Inc.

Ono, D. M., E. Hardebeck, J. Parker and B. G. Cox. 2000. Systematic biases in measured PM_{10} values with US environmental protection agency-approved samplers at Owens Lake, California. *Journal of the Air & Waste Management Association* 50(7): 1144-1156.

Pargmann, A. R. 2001. Performance characteristics of $PM_{2.5}$ samplers in the presence of agricultural dusts. M.S. Thesis. College Station, TX: Texas A&M University, Department of Agricultural Engineering.

Parnell, C. B., D. D. Jones, R. D. Rutherford, and K. J. Goforth. 1986. Physical properties of five grain dust types. *Environmental Health Perspectives,* 66:183–188.

Price, J. E., R. E. Lacey. 2003. Uncertainty associated with the gravimetric sampling of particulate matter. ASAE Paper No. 034116. St. Joseph, MI: ASAE

Ranade, M. B. M. C. Woods, F. L. Chen, L. J. Purdue, and K. A. Rehme. 1990. Wind tunnel evaluation of PM_{10} samplers. *Aerosol Science Technology.* 13: 54-71.

Redwine, J. S. and R. E. Lacey. 2001. Concentration and emissions of ammonia and particulate matter in tunnel ventilated broiler houses under summer conditions in Texas. ASAE Paper No. 01-4095. St. Joseph, MI: ASAE.

Rodes, C. E., D. M. Holland, L. J. Purdue, and K. A. Rehme. 1985. A field comparison of PM10 inlets at four locations. *Journal of Air Pollution Control Association*. 35(4): 345-354.

U.S. Environmental Protection Agency (USEPA) 1996. Air quality criteria for particulate matter, Vols. I, II, and III. EPA-600/P-95/001 aF-cF.3v. Washington, DC: US Environmental Protection Agency, Office of Research and Development. Available at: http://www.epa.gov/ncea/archive/pdfs/partmatt/vol1/067v1fm.pdf.

Vanderpool, R. W., T. M. Peters, S. Natarajan, D. B. Gemmill, and R. W. Wiener, 2001. Evaluation of loading characteristics of the EPA WINS $PM_{2.5}$ separator. *Aerosol Sci. Tech*. 34(5):444-456.

Wang, L., J. D. Wanjura, C. B. Parnell, Jr., B. W. Shaw, and R. E. Lacey. 2005. Performance characteristics of low-volume PM_{10} sampler. *Trans ASAE* 48(2): 739-748.

Wanjura, J. D., C. B. Parnell Jr., B. W. Shaw, and R. E. Lacey. 2003. Design and evaluation of a low volume total suspended particulate sampler. *Proc. 2003 Beltwide Cotton Conference*: 2489-2496.

Wedding, J. B., M. A. Weigand, Y. J. Kim. 1985. Evaluation of the Sierra-Andersen 10 µm inlet for the high–volume sampler. *Atmos Environ*. 19. 539-542.

Wilhelm, L. R., Dwayne A. Suter, and Gerald H. Brusewitz. 2005. Psychrometrics. *Food & Process Engineering Technology*, 213-257. St. Joseph, Michigan: ASAE.

APPENDIX A

WEIGHING PROCEDURE FOR LOW-VOLUME SAMPLER FILTERS

The following procedure was used to weigh the filters used by the low-volume PM_{10}, TSP and isokinetic samplers. The procedures outlined below are based on the operating instructions in the operator manual of the analytical balance (XS205 Dual Range, range: 0-81 g, readability: 0.01 mg, Mettler Toledo, Columbus, OH, USA).

Preparing the Filters

Both new and loaded filters must be conditioned in an air conditioned room for 24 hours before weighing with the Mettler-Toledo XS205 balance. The conditions of temperature and relative humidity should be kept relatively constant.

Unloaded (new) low-volume sampler filters should be numbered using a permanent marker before weighing.

a. Write the filter number clearly on one side of the unloaded 47mm diameter filter.
b. Place the newly numbered filter in a new 50mm diameter petri-dish. Do not number the petri-dish.
c. Stack the petri-dishes loaded with numbered filters in order by filter number in stacks of 25.

Calibrating the Scale

Once the scale has been plugged into the electrical wall outlet for 30 minutes, press the <<On/Off>> button to turn the scale on. Calibrate the scale using the following steps.

1) Press and briefly hold (1-2 seconds) the <<1/10d / Cal>> button on the control panel to start the self-calibration routine.
2) The scale will perform the internal calibration routine. The routine is finished once the display message "cal done" appears. If the "abort" message appears during the calibration routine, press the <<C>> button to clear the scale control panel. Repeat step (1) until the calibration routine finishes successfully.
3) Tare the scale readout by pressing the <<O/T>> button.

Weighing a Batch of Filters

1) Open the scale weight spreadsheet on the computer next to the scale table to record the weights into. The XS205 weighing software is already installed on to this computer to enable direct weight tranbsfer from the balance.
2) Enter the number of the filters that are to be weighed into the spreadsheet.
3) Open the balance tray door and place the filter holder apparatus with anti-static tray onto the balance pan.
4) Close the balance tray door.
5) Tare the scale by pressing the <<O/T>> button.
6) Press the <<1/10 d>> button on the scale control panel to add one decimal place to the readout number range.
7) Open the balance tray door and place either the anti-static bag containing the 47mm numbered filter (for low volume sampler filter weighing) on the filter

holder apparatus. For low volume sampler filter weighing, weigh only the numbered filter not the filter and petri-dish combined.

8) Once the "o" symbol disappears from the readout, press the <<menu>> button. A three second countdown will begin.
9) Once the countdown has finished, the stable weight will appear on the readout. Hit the transfer button to automatically transfer the filter weight on to the spreadsheet.
10) Open the balance tray door and remove the low volume filter.
11) Close the balance tray door.
12) Tare the scale by pressing the <<O/T>> button.
13) Repeat steps 7 – 12 for a total of 3 weights before weighing a different filter.
14) Perform the weighing procedure for all of the numbered filters.

Assuring the Quality of the Filter Weights

The standard deviation of the filter weights calculated by the spreadsheet should be less than approximately 0.00003 grams. If the standard deviation of the three weights is above this value, re-weigh the filter until the standard deviation of the three weights is less than 0.00003 g. If the problem persists the scale may need to be recalibrated or allowed to "warm up" for about 10 minutes before weighing again.

Scale Technical Data

Model: Mettler-Toledo XS205

Readability: 0.01 mg

Max Capacity: 41 g

Repeatability: 0.02 mg

Linearity: 0.03 mg

References

Mettler- Toledo XS. 2003. *Operating instructions for Mettler – Toledo XS balances*. Columbus, OH, USA.

APPENDIX B

PROCEDURE TO DETERMINE DUST PARTICLE DENSITY

The following procedure was used to determine the particle density of the three dusts used (corn starch, fly ash, and aluminum oxide). The procedures outlined here are presented in the AccuPyc 1330 Pycnometer Operator's Manual (Micromeritics, 2000).

Equipment

1. AccuPyc 1330 Pycnometer (AccuPyc 1330 Pycnometer, Micromeritics Instrument Corp., Norcross, GA)

   Precision: Reproducibility typically to within ±0.01% of the nominal full-scale cell chamber volume. The nominal full scale cell chamber volume is the sample capacity. Reproducibility guaranteed to within ±0.02% of the nominal full-scale volume on clean, dry, thermally equilibrated samples.

   Accuracy: Accurate to within ±0.03% of reading plius 0.03% of the nominal full scale cell chamber volume.

   Sample Volume: 0.5 to 100 cm^3

2. Mettler-Toledo AG245 balance

   Readability: 0.01 mg

   Max Capacity: 41 g

   Repeatability: 0.02 mg

   Linearity: 0.03 mg

3. Calibration Standards

Two – 23/32" diameter Tungsten Carbide calibration balls calibrated with master balls calibrated by the NIST Test No. 821 25B 592-97 (Precision Ball and Gauge Co., Alvadore, OR).

Calibration Procedure

The pycnometer should be recalibrated anytime it is restarted. The following procedure should be followed to calibrate the pycnometer.

1. Check the calibration of the pycnometer by performing an analysis on the empty sample cup to see how close the average volume is to zero. If the volume returned is not within ±0.05% of full scale, recalibrate the pycnometer using the following procedure.

   When recalibrating the pycnometer, you should set up the calibration parameters so that 10 purges and 10 runs are performed. Perform the procedures in step #8 below before beginning the calibration routine.

2. Place an empty cup in the cell chamber.
3. Replace the cell chamber cap.
4. Press [ ] + [·] to begin the calibration procedure.
5. The following messages will be displayed:

   Volume of cal std: 1.0000 cm^3

   Enter the volume of the calibration standard used and press [ENTER].

   [Enter] to start [Escape] to cancel

Press [ENTER] to begin the calibration procedure. The pycnometer will beep 3 times once the first phase of the calibration is complete.

Insert cal std [Enter] to start

Insert the calibration standard in the cup in the cell chamber. Use both calibration balls for calibrating the 10 cm^3 pycnometer.

6. Replace the cell chamber cap and press [ENTER].
7. During each calibration and analysis procedure, the pycnometer automatically zeros the pressure transducer. This can be done manually by pressing [ ] + [0].
8. Entering the analysis and calibration parameters
    a. Press [ ] + [2] to display and edit the analysis and calibration parameters
    b. Press [CHOICE] until *Analysis Parameters* is displayed and press [ENTER].
    c. Enter the number of purges to be performed (10) and press [ENTER].
    d. Enter the purge fill pressure and press [ENTER]. The purge fill pressure should be 19.5 psig.
    e. Enter the number of runs to be performed (10) and press [ENTER].
    f. Enter the run fill pressure (19.5 psig) and press [ENTER].
    g. Enter the Equilibration Rate (0.005 psig/min) and press [ENTER].
    h. Enter no when asked *"Use run precision?"* and press [ENTER]

i. Enter the number "0.05" when asked "*Percent full scale?"* and press [ENTER]

j. Press [SAVE] to save the changes made and return to the display mode.

Performing an Analysis

The cell chamber and cap must be kept clean at all times. Use a lint-free cloth to wipe particles from the surfaces before performing an analysis.

1. Check the helium tank pressure on the regulator to make sure that it is above 200 psig. Lower tank pressures may cause inadequate sample saturation.
2. Set the regulator pressure to 2 psig above the user defined fill pressure for purging and running (see step 8 above). This pressure should be about 21.5 psig.
    a. Press [ ] + [1] to enter manual mode.
    b. Press [8] (expand) and [9] (vent) to open the expansion and vent valves. When the valves are open, the indicators above the keys are turned on.
    c. Press [7] (fill) to open the fill valve.
    d. Set the regulator pressure control knob on the tank to the desired pressure (21.5 psig).
    e. Press [7] (fill) to close the fill valve. Press [SAVE] to return to display mode.
3. Setting report options
    a. Press [ ] + [2].

b. Press [CHOICE] until *Report Options* is displayed and press [ENTER].

c. Select density and press [ENTER].

d. Select Yes for *Request Sample ID?* This option allows the user to enter a sample identification number containing 1 to 20 numbers and dashes.

e. Press [ENTER].

f. For *Transmission Format,* select single column.

g. The *Report Destination* should be set to display. Press [ENTER].

h. Press [SAVE].

4. Preparing the sample.

a. Keep the cap on the cell chamber except when actually inserting or removing a sample. If the chamber remains uncapped, temperature instability will occur which could affect analysis results.

b. Weigh the empty sample cup and record the weight on the log sheet.

c. Sieve a sample of the dust to be analyzed using a 100 micrometer screen mesh.

d. Place a quantity of the sample in the sample cup. Use as large a quantity of sample as possible. Try to fill the cup at least two-thirds full. Pack powders and fluffy materials (if permissible) to obtain maximum sample weight in the cup.

e. Dry the sieved sample in the sample cup according to the procedures outlined in the ASTM Designation: D 3173 – 00 (ASTM, 2000).

f. Once the sample has been dried and allowed to cool to room temperature in a desiccator, weigh the sample cup containing the dried sample.

g. Subtract the empty cup weight from the weight of the cup containing the dried sample to obtain the dried sample weight.

h. Remove the cell chamber cap.

i. Insert the sample cup with sample into the cell chamber.

j. Replace the cell chamber cap.

5. Starting the Analysis

   a. To start the analysis press [ ] + [4].

   b. Enter the sample ID and press [ENTER] when prompted.

   c. Enter the dried sample weight when prompted for the sample weight and press [ENTER]. The sample weight should be entered in grams.

   d. Press [ENTER] to begin the analysis.

6. Viewing the Analysis Results

   a. The pycnometer will beep three times when the analysis is complete. Remove the sample from the test chamber and press [CHOICE] to cycle through the error messages.

   b. Once all of the error messages have been displayed, the average density of the user defined number of runs is displayed on the display along with the deviation from the mean. Press [ENTER].

   c. When the *Reload* prompt is displayed, you may begin another operation.

References

Micromeritics Instrument Corp. 2000. AccuPyc 1330 Pycnometer Operator's Manual v3.xx. Norcross, GA: Micromeritics Instrument Corp.

ASTM. 2000. ASTM D 3173 – 00. Standard test method for moisture in the analysis sample of coal and coke. West Conshohocken, PA: ASTM.

APPENDIX C

EVALUATION OF SAMPLING ERROR DUE TO ANISOKINETIC SAMPLING

Isokinetic sampling ensures that the concentration and the size distribution of the aerosol entering the sampler inlet is the same as that in the flowing stream. When these conditions are not met, the sampling procedure is said to be anisokinetic. Anisokinetic sampling can take place under three conditions: firstly, when the probe is not aligned with the gas flow streamlines; secondly, when the velocity in the probe exceeds the stream velocity known as superisokinetic sampling; and thirdly, when the stream velocity exceeds the velocity in the probe known as subisokinetic sampling (Hinds, 1999).

In this study the three isokinetic inlets were designed to attain an isokinetic flow rate of 1 m^3/h when tested at wind speeds of 2-, 8-, and 24-km/h and were required to have inlet nozzle diameters of 25.2-, 12.6-, and 7.4-mm, respectively. However, due to oversight while designing them, the inlets designed for use at 2 and 8 km/h had inlet nozzle diameters of 19.8 and 10.2 mm, respectively, which caused the flow velocities in the inlet to be 3.2 and 12.2 km/h, respectively. This led to a case of superisokinetic sampling when the two mentioned inlets were used.

In superisokinetic sampling, some particles have so much inertia that they continue in a straight line as the gas curves into the inlet. These high inertia particles present in the original volume of air being sampled cannot follow the converging streamlines to enter the probe and are lost from the sample. Thus the true concentration of particles may be underestimated leading to sampling error if the numbers of particles left out of the sample are large.

The underestimation of concentration can be determined by the Belyaev and Levin (1974) equation.

$$\frac{C}{C_0} = 1 + \left(\frac{U}{U_0} - 1\right)\left(1 - \frac{1}{1 + (2 + 0.62U/U_o)Stk}\right) \quad \text{(C.1)}$$

where:

C = concentration of aerosols in the probe, ($\mu g/m^3$),

C_0 = concentration of aerosols in the free stream, ($\mu g/m^3$),

Stk = stokes number for the inlet,

U = gas velocity in the probe, (m/s), and,

U_0 = free stream velocity, (m/s),

The stokes number for the inlet can be calculated as

$$Stk = \tau \times U_0 / D_s \quad \text{(C.2)}$$

where:

Ds = inlet nozzle diameter, (m), and,

τ = relaxation time, (s).

The term relaxation time characterizes the time required for a particle to adjust its velocity to a new condition of forces. Relaxation time is affected by the temperature and

pressure of the surrounding gas. Relaxation time increases rapidly with the particle size because it is proportional to the square of diameter as shown in Table C.1.

Table C.1. Relaxation time for unit density particles at standard conditions

Particle diameter (μm)	Relaxation time (s)
0.01	7.0×10^{-9}
0.1	9.0×10^{-8}
1.0	3.5×10^{-6}
10.0	3.1×10^{-4}
100	3.1×10^{-2}

When $U/U_0 \approx 1$ or $Stk \approx 0$ the ratio $C/C_0 \approx 1$ and it can be safely assumed that the underestimation is negligible and that there is no sampling error arising due to the slight anisokinetic conditions. To evaluate whether the deviation of the test velocities from the target velocities brought about a significant error to the true concentration values, the relaxation times for the Arizona road dust (ARD) and cornstarch particles were determined utilizing Table C.1. The relaxation times were used to determine the Stokes number for the inlet for various particle sizes (AED) (equation C.2) and ultimately the concentration ratio using equation C.1 and presented in Table C.2.

Table C.2. Determination of underestimation of aerosol concentration due to anisokinetic sampling at 2 and 8 km/h.

Dust Type	**AED (μm)**	**Stoke Number**		**C/C_0**	
		2 km/h	**8 km/h**	**2 km/h**	**8 km/h**
Ultrafine ARD,	0.14	6.82×10^{-7}	5.29×10^{-6}	~ 1	~ 1
Fine ARD	1.39	2.65×10^{-4}	2.06×10^{-5}	~ 1	~ 1
	13.90	2.41×10^{-2}	0.182	0.98	0.94
	138.91	2.41	18.2	0.71	0.67
Corn Starch	0.12	3.78×10^{-6}	2.94×10^{-5}	~ 1	~ 1
	1.22	1.47×10^{-4}	1.14×10^{-3}	~ 1	~ 1
	12.15	1.3×10^{-2}	0.101	0.99	0.96
	121.51	1.3	10.1	0.73	0.68

After interpolation, on an average, 95% of all particles in an ultrafine ARD sample (MMD = 4.7 μm) and 90% of all particles in a fine ARD sample (MMD = 8.7 μm) were smaller than 13.9 μm which led to an underestimation of true concentration by less than 6% and could be considered negligible. The underestimation of true concentration was less than 10% for about 85% of the cornstarch particles (MMD = 16.4 μm). Thus, based on the values of concentration ratios at the two target wind speeds, the sampling error in either of the two isokinetic inlets in question was found to be negligible. On a theoretical basis, an assumption of isokinetic sampling was fairly true for the tests conducted using the two isokinetic inlets.

For experimental verification, an ANOVA comparison of the PSD characteristics and average TSP concentrations captured by the three isokinetic inlets operating at target wind speeds of 2-, 8-, and 24-km/h was performed (Table C.3).

Table C.3. ANOVA comparison of aerosol characteristics for tests conducted with three isokinetic inlets operating at target wind speeds of 2-, 8-, and 24-km/h.

Aerosol Characteristic	Ultrafine ARD	Fine ARD	Cornstarch
MMD	0.78	0.98	0.45
GSD	0.54	0.87	0.29
TSP Conc.	0.69	0.57	0.74

The isokinetic inlet operating at 24 km/h had an accurate dimension for nozzle diameter and comparison of its aerosol collection characteristics to the two inlets with inaccurate design would indicate if differences existed at the 95% significance level. The p-values suggested that there were no differences in the performance of the three

isokinetic inlets. Thus the isokinetic inlets operating at target wind speeds of 2 and 8 km/h did not underestimate the true concentration or capture non-representative samples of aerosols as compared to the isokinetic inlet operating at 24 km/h. hence the assumption of isokinetic test conditions held true for all the tests conducted in the study.

References

Hinds, W. C. 1999. *Aerosol technology - properties, behavior, and measurement of airborne particles*. 2nd ed. New York, NY, John Wiley & Sons, Inc.

Belyaev, S. P., and Levin, L. M., Techniques for collection of representative aerosol samples. *Journal of Aerosol Science*, 5, 325-338 (1974).

APPENDIX D

SHARP EDGE ORIFICE METER CALIBRATION PROCEDURE

The following procedure was used to calibrate the orifice meters used with the low volume TSP samplers.

Equipment

1. Omega Mass Flow Controller (Model: FMA5420-12VDC, Omega Inc, Stamford, CT, USA)

   Range: 0 – 20 slpm

   Accuracy: ±1.5% Full Scale (F.S.)

2. Electrical transformer for mass flow meter
3. Fluke multimeter (867B Graphical Multimeter)

   Accuracy: ±0.025% basic accuracy

4. Digital differential pressure gauge (Dwyer Series 475-1 Mark III digital manometer)

   Range: 0 – 19.99 in W.C.

   Accuracy: ±0.5% F.S. (15.6 – 25.6°C), ±1.5% F.S. (0 – 15.6 and 25.6 – 40°C)

5. Digital temperature, barometric pressure, and relative humidity sensor (Davis Perception II)
6. Needle valve
7. Compressed air source
8. 3 - 3 ft pieces of 3/8” diameter plastic tubing
9. 2 – 2 ft pieces of 1/8” diameter plastic tubing

10. 6 steel hose clamps

Setup

1. Connect the needle valve to the compressed air source using one piece of the plastic tubing.
2. Connect the open end of the needle valve to the upstream port on the mass flow meter using a piece of the plastic tubing.
3. Connect the downstream port of the mass flow meter to the upstream port on the orifice meter.

   **The upstream port of the orifice meter is on the side with the pressure tap furthest from the orifice plate*.

4. Plug the electrical transformer for the mass flow meter into the wall outlet and connect it to the mass flow meter.

   **The mass flow meter must be plugged in for 15 minutes before taking flow measurements*.

5. Connect the RS-232 cable to the communication port on the mass flow meter and tighten the holding screws.
6. Connect the multimeter leads to the free ends of the two wires of the RS-232 cable. Turn on the multimeter and set it to read in the 1 volt range.
7. Connect the positive pressure port of the digital manometer to the upstream pressure tap on the orifice meter with a piece of the 1/8” diameter tubing.

Connect the negative port to the downstream side with the other piece of 1/8" diameter tubing.

Procedure

1. Record the barometric pressure, temperature, and relative humidity from the Davis Perception II instrument onto the log sheet.
2. With no air flowing through the system, record the voltage from multimeter on the log sheet. This is the "zero flow voltage".
3. Turn on the differential pressure gauge and zero the readout by turning the small steel knob between the pressure ports. Set the readout units to be "in WC" by pressing the E/M button.
4. Turn the knob on the needle valve counter clockwise until the display on the multimeter reads 5.0 ± .05volts.
5. Record the actual voltage and differential pressure on the log sheet.
6. Turn the knob on the needle valve clockwise until the voltage reading is approximately 0.1V less than the previous reading.
7. Record the actual voltage and differential pressure on the log sheet.
8. Repeat steps 6 and 7 until the multimeter reads approximately 2.5 volts.
9. Once all of the readings have been taken, convert the voltage readings to flow readings using equation D.1.

$$Q = 4.0076(V) - 4.0076(V_Z) \qquad \text{(D.1)}$$

where:

Q = standard flow rate (standard liters per minute),

V = voltage reading (volts), and

V_Z = Zero flow voltage (volts).

The standard conditions of the air used by the mass flow meter are 21.1°C and 14.7 PSIA.

10. Calculate the K values for each flow/differential pressure point using equation D.2.

$$K = \frac{2.55 \times 10^{-2} \times Q}{D_o^2 \times \sqrt{1/(1-\beta^4)} \times \sqrt{\Delta P_T / \rho_a}} \quad \text{(D.2)}$$

$$\beta = D_o / D_p \quad \text{(D.3)}$$

where:

K = orifice meter constant, dimensionless,

Q = volumetric flow rate of air, m^3/h,

β = velocity of approach factor, dimensionless,

D_o = orifice diameter, m,

ΔP_T = Pressure drop across the orifice plate as measured by the pressure transducer, Pa

ρ_a = density of air, kg/m^3, and,

D_p = inlet diameter, m

11. The average of all the K values determined above is the K value for the orifice meter.

APPENDIX E

DIFFERENTIAL PRESSURE TRANSDUCER CALIBRATION PROCEDURE

The following procedure is used to determine the differential pressure (in W.C.) vs. output current (ma) for the differential pressure transducers used in the low-volume PM sampling systems.

Equipment

1. Differential pressure transducer (Omega PX274-30DI, Omega Engineering inc., Stamford, CT, USA)

   Accuracy: ±1% Full Scale (FS) (includes non-linearity, non-repeatability, and hysteresis)

   Operating Temperature: -18 to 80°C (0 – 175°F)

   Media Compatibility: Clean dry air or anyinert gas

   Environment: 10 to 90% RH non-condensing

   Supply voltage: 12 to 40 V_{dc}

   Output: 4 – 20 mA

   Supply Current: 20 mA maximum

   Load Impedance: 1.6 K ohms at 40 V_{dc} maximum

2. Electrical transformer for differential pressure transducer
3. Fluke multimeter (867B Graphical Multimeter)

   Accuracy: ±0.025% basic accuracy

4. Digital differential pressure gauge (Dwyer Series 475-1 Mark III digital manometer)

   Range: 0 – 19.99 in W.C.

   Accuracy: ±0.5% F.S. (15.6 – 25.6°C), ±1.5% F.S. (0 – 15.6 and 25.6 – 40°C)

5. Digital temperature, barometric pressure, and relative humidity sensor (Davis Perception II)
6. Air pressure generator (Beckman Air Comparison Pycnometer 93001, Beckman Instruments, inc., Irvine, CA)
7. 3 – 2ft pieces of 3/16" ID Tygon tubing
8. 1 - 3/16" OD plastic "T" connector for Tygon tubing
9. Wooden test stand

Procedure

1. Mount the pressure transducer vertically on the test stand with the pressure taps pointing downward.
2. Remove the two screws from the front face of the pressure transducer and pull off the front cover.
3. Connect the pressure generator to the plastic "T" using one piece of the Tygon tubing.
4. Connect one end of the "T" connector to the "+" port of the differential pressure gauge.

5. Connect the open end of the “T” connector to the “+” port of the differential pressure transducer.
6. Locate the “+” and “-“ terminals on the differential pressure transducer.
7. Connect the “+” terminal on the pressure transducer to the “+” terminal on the power transformer. Connect the “-“ terminal on the pressure transducer to the “-“ terminal on the power transformer.

   DO NOT PLUG THE TRANSFORMER INTO THE WALL AT THIS TIME!

8. Connect the multimeter in series with the pressure transducer and power transformer on the “-“ side as shown in figure E.1.

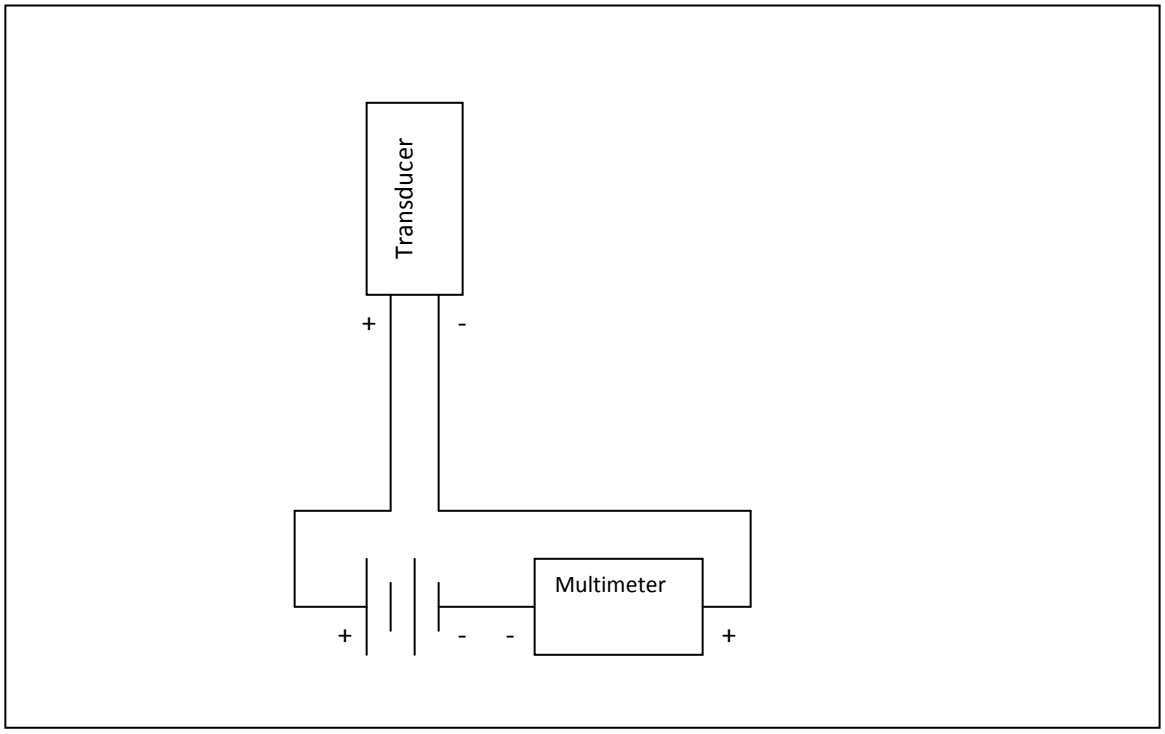

Figure E.1. Wiring schematic for calibrating the differential pressure transducers used with the low and high volume TSP samplers.

9. Locate the jumper settings for the 0 – 7.5 in W.C. range in the users guide for the PX274 and make sure that the jumpers are set correctly on the differential pressure transducer.
10. Plug the power transformer into the wall electrical outlet.
11. With no pressure applied to the "+" side of the differential pressure transducer, adjust the zero trimmer to obtain the desired low pressure output. The low pressure output should be as close to 4 mA as possible as read by the multimeter set to read in the mA range.
12. Record the low pressure reading from the differential pressure gauge (in W.C.) and the corresponding current output (mA) on the log sheet. Also record the temperature, relative humidity, and barometric pressure from the digital weather station.
13. Turn the knob on the pressure generator until the differential pressure gauge reads 0.5 in W.C. and record the corresponding current output from the differential pressure transducer.
14. Repeat step 13 over the operating range of 0 to 7.5 in W.C.
15. Once all of the differential pressure/output current data points have been taken, input them into a statistical software package (SPSS or SAS) and perform a linear regression analysis on the data. Obtain the linear regression equation coefficients and the coefficient of determination (R^2) from the statistical software output.

APPENDIX F

UNCERTAINTY ANALYSIS FOR THE VOLUMETRIC FLOW RATE OF A LOW-VOLUME SAMPLER

Systematic Uncertainty of Volumetric Flow Rate

Let A be a function of independent variables x_1 , x_2 , x_3,…., x_n. Now consider ω to be defined as the uncertainty in the measured or calculated value of each variable and ω_1 , ω_2 ,… ,ω_n be the uncertainties associated with each of the independent variables respectively. The resulting uncertainty in the value of Y can be calculated as a positive square root of the estimated variance, ω_Y^2 , from the following equations (Holman, 2001).

$$\omega_Y = +\sqrt{\omega_Y^2} \tag{F.1}$$

$$\omega_Y^2 = \left(\frac{\delta Y}{\delta x_1}\omega_1\right)^2 + \left(\frac{\delta Y}{\delta x_2}\omega_2\right)^2 + \cdots + \left(\frac{\delta Y}{\delta x_n}\omega_n\right)^2 \tag{F.2}$$

or, $$\omega_Y^2 = (\theta_1\omega_1)^2 + (\theta_2\omega_2)^2 + \cdots + (\theta_n\omega_n)^2 \tag{F.3}$$

where

θ = sensitivity coefficient.

To calculate the systematic uncertainty in the value of the volumetric flow rate (Q) during the PM sampling operation, the values of variances of individual variables should be calculated first. The volumetric flow rate is calculated from the pressure drop across the orifice meter using equation F.4 which is derived from Bernoulli's equation involving a corrective velocity of approach factor.

$$Q = 4 \times 10^3 \times K \times D_o^{\,2} \times \sqrt{1/(1-\beta^4)} \times \sqrt{\Delta P_T/\rho_a} \tag{F.4}$$

$$\beta = {}^{D_o}/_{D_p} \tag{F.5}$$

where:

Q = volumetric flow rate of air, m^3/h,

K = orifice meter constant, dimensionless,

β = velocity of approach factor, dimensionless,

D_o = orifice diameter, m,

ΔP_T = Pressure drop across the orifice plate as measured by the pressure transducer, Pa

ρ_a = density of air, kg/m^3, and,

D_p = inlet diameter, m

The variances associated with the measurement of each of the quantities on the right hand side (R.H.S) of equation F.5 can be calculated (equations F.6 through F.10) and then the uncertainty in measurement of Q determined using equation F.10.

$$\frac{\delta Q}{\delta K} = 4 \times 10^3 \times D_o{}^2 \sqrt{{}^{1}/_{1-\beta^4}} \times \sqrt{{}^{\Delta P_T}/_{\rho_a}} \tag{F.6}$$

$$\frac{\delta Q}{\delta \Delta P} = \frac{4\times 10^3 \times K \times D_o{}^2 \sqrt{{}^{1}/_{1-\beta^4}}}{\sqrt{\rho_a}} \times \frac{1}{2\times\sqrt{\Delta P_T}} \tag{F.7}$$

$$\frac{\delta Q}{\delta \rho_a} = \frac{4\times 10^3 \times K \times D_o{}^2 \sqrt{{}^{1}/_{1-\beta^4}}}{1} \times \frac{-1\times\sqrt{\Delta P_T}}{2\times \rho_a{}^{3}/_{2}} \tag{F.8}$$

$$\frac{\delta Q}{\delta D_o} = 4 \times 10^3 \times K \times \sqrt{\Delta P_T / \rho_a} \times \frac{2 \times D_o \times D_p{}^6}{(D_p{}^4 - D_o{}^4)^{3/2}} \quad \text{(F.9)}$$

$$\frac{\delta Q}{\delta D_p} = 4 \times 10^3 \times K \times \sqrt{\Delta P_T / \rho_a} \times \frac{-2 \times D_p \times D_o{}^6}{(D_p{}^4 - D_o{}^4)^{3/2}} \quad \text{(F.10)}$$

$$\omega_Q = \sqrt{\left(\left(\frac{\delta Q}{\delta K} \times \omega_K\right)^2 + \left(\frac{\delta Q}{\delta \Delta P_T} \times \omega_{\Delta P}\right)^2 + \left(\frac{\delta Q}{\delta \rho_a} \times \omega_{\rho_a}\right)^2 + \left(\frac{\delta Q}{\delta D_o} \times \omega_{D_o}\right)^2 + \left(\frac{\delta Q}{\delta D_p} \times \omega_{D_p}\right)^2\right)} \quad \text{(F.11)}$$

Density of air (ρ) and orifice meter constant (K) are dependent variables and their uncertainties should be determined separately considering them as a function of separate independent variables. The value of $\omega_{\rho a}$ and ω_K are determined using the principle equations F.12 and F.19.

$$\rho_a = \frac{P_b - P_{wv}}{287.05 \times (273 + t_{db})} + \frac{P_{wv}}{461.495 \times (273 + t_{db})} \quad \text{(F.12)}$$

$$P_{wv} = \frac{RH \times P_s}{100} \quad \text{(F.13)}$$

where:

ρ_a = density of air, kg/m^3 as measured during sampling test,

P_b = barometric pressure, Pa,

P_{wv} = water vapor pressure, Pa,

t_{db} = dry bulb temperature, °C,

RH = relative humidity, %, and,

P_s = saturated water vapor pressure, Pa.

The value of P_s can be determined from the steam table (Silver and Nydahl, 1977) on basis of the t_{db} and converted to appropriate SI units. The uncertainty in the air density value is calculated by taking partial differential of the air density w.r.t to all variables on R.H.S of equation F.12 (equation F.14 through F.17) to determine the individual variances and then calculating $\omega_{\rho a}$ (equation F.18).

$$\frac{\delta \rho_a}{\delta RH} = \frac{-1.32 \times 10^{-5} \times P_s}{(273 + t_{db})} \tag{F.14}$$

$$\frac{\delta \rho_a}{\delta P_s} = \frac{-1.32 \times 10^{-5} \times RH}{(273 + t_{db})} \tag{F.15}$$

$$\frac{\delta \rho_a}{\delta P_b} = \frac{3.48 \times 10^{-2}}{(273 + t_{db})} \tag{F.16}$$

$$\frac{\delta \rho_a}{\delta t_{db}} = \frac{\left(\left(1.32 \times 10^{-5} \times RH \times P_s\right) - \left(3.48 \times 10^{-2} \times P_b\right)\right)}{(273 + t_{db})^2} \tag{F.17}$$

$$\omega_{\rho_a} = \sqrt{\left(\left(\frac{\delta \rho_a}{\delta RH} \times \omega_{RH}\right)^2 + \left(\frac{\delta \rho_a}{\delta P_s} \times \omega_{P_s}\right)^2 + \left(\frac{\delta \rho_a}{\delta P_b} \times \omega_{P_b}\right)^2 + \left(\frac{\delta \rho_a}{\delta t_{db}} \times \omega_{t_{db}}\right)^2\right)} \tag{F.18}$$

The value of K is determined during calibration of orifice meter by rearranging equation F.4.

$$K = \frac{2.55 \times 10^{-5} \times Q}{D_0^2 \times \sqrt{1/(1-\beta^4)} \times \sqrt{\Delta P_m / \rho_a}} \tag{F.19}$$

where:

ΔP_m = pressure drop across the orifice plate as measured by a digital manometer, Pa.

The partial differential equations of K w.r.t independent variables are :

$$\frac{\delta K}{\delta Q_{MFC}} = \frac{2.55\times10^{-5}}{D_o^{\,2}\times\sqrt{1/(1-\beta^4)}\times\sqrt{\Delta P_m/\rho_c}} \tag{F.20}$$

$$\frac{\delta K}{\delta \Delta P} = \frac{2.55\times10^{-5}\times Q_{MFC}\times\sqrt{\rho_c}}{D_o^{\,2}\times\sqrt{1/(1-\beta^4)}} \times \frac{-1}{2\times\Delta P_m^{\,3/2}} \tag{F.21}$$

$$\frac{\delta K}{\delta \rho_c} = \frac{2.55\times10^{-5}\times Q_{MFC}}{D_o^{\,2}\times\sqrt{1/(1-\beta^4)}\times\sqrt{\Delta P}} \times \frac{1}{2\times\rho_c^{\,3/2}} \tag{F.22}$$

$$\frac{\delta K}{\delta D_o} = \frac{2.55\times10^{-5}\times Q_{MFC}}{\sqrt{\Delta P_m/\rho_c}} \times \frac{-2\times D_p^{\,2}}{D_o^{\,5}\times\left(D_p^{\,4}-D_o^{\,4}\right)^{3/2}} \tag{F.23}$$

$$\frac{\delta K}{\delta D_p} = \frac{2.55\times10^{-5}\times Q_{MFC}}{\sqrt{\Delta P_m/\rho_c}} \times \frac{2\times D_o^{\,2}}{D_p^{\,5}\times\left(D_p^{\,4}-D_o^{\,4}\right)^{3/2}} \tag{F.24}$$

The uncertainty in the value of orifice meter constant (K) can be determined by utilizing the calculated individual variances (equations F.20 through F.24) in equation F.25 to solve for ω_K.

$$\omega_K = \sqrt{\left(\left(\frac{\delta K}{\delta Q_{MFC}}\times\omega_Q\right)^2+\left(\frac{\delta K}{\delta \Delta P_m}\times\omega_{\Delta P}\right)^2+\left(\frac{\delta K}{\delta \rho_c}\times\omega_{\rho_c}\right)^2+\left(\frac{\delta K}{\delta D_o}\times\omega_{D_o}\right)^2+\left(\frac{\delta K}{\delta D_p}\times\omega_{D_p}\right)^2\right)} \tag{F.25}$$

where:

Q = volumetric flow rate of air as measured by a mass flow controller, m^3/h, and,

ρ_c = density of air as measured during calibration of orifice meter, kg/m^3.

The values of known (manufacturer reported) uncertainties have been compiled in Table F.1. Table F.2 lists the calculated sensitivity coefficients of all variables, calculated uncertainties of the dependent variables as well as the reported uncertainties of independent variables. It also breaks down the contribution of each variable's measurement uncertainty to the total uncertainty. For the uncertainty analysis performed on one of the low-volume sampling systems used in this study, the uncertainty in the measurement of volumetric flow rate (Q) was calculated to be 0.166 m^3/h for a target volume flow rate of 1 m^3/h. Thus the uncertainty in the measurement was found to be 16.6%. The measurement of pressure drop across the orifice meter was the leading contributor (70.28%) to the overall uncertainty. Thus in order to achieve a higher degree of certainty in the volume flow rate calculations, the uncertainty in the measurement of pressure drop should be decreased.

References

Holman, J. P. 2001. *Experimental Methods for Engineers*. 7th ed. Boston MA: McGraw Hill.

Table F.1. Instrument uncertainty specifications.

Parameter	Notation	Instrument	Reported Uncertainty
P_b	ω_{Pb}	Davis Perception II	0.01in of mercury = 33.9 Pa
P_s	ω_{Ps}	Steam Table (Silver and Nydahl)	0.0001 psia= 0.6894757 Pa
RH	ω_{RH}	TSI Veloicalc Model 8386	± 3% of value
t_{db}	ω_{tdb}	TSI Veloicalc Model 8386	0.3 °C
Q	ω_{Qmfc}	Omega FMA 5424 mass flow controller	1.5% FS =0.018 m^3/h
ΔP_T	$\omega_{\Delta PT}$	Omega PX 274 pressure transducer + HOBO	1% FS + 2.5%FS =90.2625 Pa
ΔP_m	$\omega_{\Delta Pm}$	Dwyer Mark III digital manometer	0.5% FS = 24.9 Pa
D_o	ω_{Do}	End mill specs	0.005 in = 0.000127 m
D_p	ω_{Dp}	End mill specs	0.005 in = 0.000127 m

Table F.2. Volumetric flow rate sensitivity analysis for uncertainty propagation

	Variable	Units	Nominal value used	Sensitivity coefficient (θ)	Uncertainty (ω)	% of partial uncertainty	% of total uncertainty
Q	K	dimensionless	0.644346	1.56	0.045	17.85	17.85
	ΔP	Pa	318.96	1.57E-03	90.2625	70.28	70.28
	ρ_a	kg/m^3	1.1538	-0.435	1.24E-03	0.03	0.03
	D_o	m	4.76E-03	450.16	1.27E-04	11.84	11.84
	Dp	m	9.53E-03	14.08	1.27E-04	0	0
ρ_a	RH	%	60	-1.85E-04	1.5	5.02	0.0015
	P_s	Pa	4250	-2.61E-06	0.689	0	0
	P_b	Pa	101325	1.15E-03	33.9	9.9	0.00297
	t_{db}	℃	30	-3.80E-03	0.3	85.08	0.0255
K	Q	m^3/h	1.005	0.64143	0.018	6.45	1.1513
	ΔP	Pa	325.83	-9.83E-04	24.9	29	5.1765
	ρ_c	kg/m^3	1.1775	0.2726	1.27E-03	0.06	0.0107
	D_o	m	4.76E-03	286.86	1.27E-03	64.4	11.4954
	D_p	m	9.53E-03	8.976	1.27E-03	0.09	0.016
ρ_c	RH	%	50	-0.000185	1.5	2.763	0.0003
	P_s	Pa	3167.5	-0.000002614	0.689	0	0
	P_b	Pa	101325	0.001149	33.9	9.782	0.001
	t_{db}	°C	25	-0.003804	0.3	87.455	0.0094

APPENDIX G

MALVERN MASTERSIZER ANALYSIS PROCEDURE FOR DETERMINATION OF PARTICLE SIZE DISTRIBUTION (PSD) OF DUST

Malvern (Mastersizer 2000) Procedures

1. **Turning On the Instrument**

The switch is on the right side of the Malvern. The blue light on the top right side will come on when the instrument is on. Make sure the computer is connected and turned on.

2. Hooking Up the Unit You Want to Run Samples on.

a. The left side unit is for dry samples (**Scirocco 2000A**) and the right side unit is for running samples wet (in methanol) and is called the **HYDRO 2000SM (A)**.

b. You remove the unit you want to run by lifting it out of its cradle using the handle located on top of the unit.

c. Insert the unit into the center cradle (the middle) carefully. Lock it into place by turning the handle into the locking position.

d. Once you have the unit securely in position, you must hook up the tubing. For the **Scirocco** (dry) unit, there is one large tube that must be connected to the right side of the dry sampler (the one with the window). Fit the tube snuggly over the outlet. For the **HYDRO** (wet) unit, there are two connection tubes (one is blue and one is red). The two tubes are attached to the SVDU or *Small Volume Dispersion Unit*. Plug the blue tube into the 'cell out' which has a matching blue outlet. Plug the red tube into the 'cell in' which has a matching red outlet. You should feel a slight 'click' when they are firmly attached.

2. Begin the Program for Running Samples.

a. Click on the '**Mastersizer 2000**' program icon on the computer's desktop.

b. The user name should be 'aircrew' and will already be entered in unless you delete it. Just click 'okay' to continue.

c. The 'tip of the day' will display unless you change the settings. I find these hints helpful, but you can decide whether or not you want them displayed when you start up. Click 'close' on the pop-up window.

3. Choose your SOP (Standard Operating Procedure).

a. Several SOP's are already saved for you to use when running samples, but you may need to create new ones when using different materials (samples) because the instrument will need a different refractive index to obtain accurate results.

b. The most commonly used SOP's are **Silica wet** and **Silica dry**. Most of the samples we run are from cattle feed yards and dairies which consist primarily of sand and dirt so the best option under materials is 'silica'. For samples that are mixed materials, chose the material that the sample has the greatest amount of. The great thing about this program is that if you get it wrong, you can go back later and edit the 'material' which changes the refractive index and adjusts the sample results according to the new refractive index. (You can fix it!)

c. After you close out of the ‘tip of the day’, a new pop-up window will ask you if you want to ‘Run an existing SOP’, ‘Edit an existing SOP’, ‘Use the SOP creation wizard’, or ‘Make a manual measurement’.

d. If you know the SOP you would like to run choose ‘Run an existing SOP’. If you know the SOP you would like to run but need to adjust a few parameters click ‘Edit an existing SOP’. If you are working with new materials which will require a new refractive index click ‘Use the SOP creation wizard’ and this will take you on a step-by-step process to set up a new SOP. Once you have made your selection click ‘okay’.

e. If you happen to ‘cancel’ out of the pop-up window, that’s okay. There are icons at the top located on the tool bar that allow you to do the same things. You can also click on ‘Configure’ tab and choose ‘New SOP’ or ‘Edit SOP’ to create a new SOP or edit an existing SOP.

f. If you need help deciding what material you are using, always ask a professor or graduate student in the department for their opinion.

4. Beginning the SOP – Running your Samples

a. Make sure your unit is properly connected. The dry sampler must also be turned on when running dry samples. The switch is located at the back of the unit (with the window).

b. For dry samples, make sure the sample tray is dusted out using the (paint) brush provided. The tray can be removed using the screw on the front. The ‘gates’ at the

front of the tray can be adjusted using the two screws on the top right side of the tray. Normally, you won't have to remove the sample tray or adjust the gates. You may need to remove the tray occasionally to clean the hair or debris out of the mesh filter located just below the tray. For the wet samples, you must clean out the SVDU by removing the mouth and pouring in ethanol. Make sure the handle on the right side of the SVDU is pointing up so the methanol doesn't drain out right away! After a few seconds, lower the handle on the right side of the SVDU to drain the ethanol. Repeat this one or two more times to make sure the SVDU is properly cleaned. You will need to ***drain out the SVDU with ethanol 2-3 times before every run*** to ensure accurate results. The SOP should prompt you to clean it out every time in case you forget.

c. Before you start measuring with the **dry sampler** you must place the sample in the tray. The SOP for the **wet sampler** will give you instruction in the yellow box to tell you when to add the sample.
d. Before you start the SOP for the dry sampler, make sure the air is turned on. The pressure gauge should be about 80-90 psi. Also make sure the vacuum is on and connected. For the wet sampler, make sure there is proper drainage for the ethanol and it isn't spilling out onto the floor.
e. To begin the measurements click on 'Measure' and 'Start SOP' at the top. Select the SOP you want to run.
f. The **dry sampler** will start up and the vacuum will come on. The SOP will start a 'background run' to leave out particles in the test that may still be in the unit. After

the background run is finished, it will begin the run and suck the material through the 'gates' and into the unit. Observe if the entire sample goes into the unit and how fast. You may have to adjust the time or vibration in the SOP. All of the sample should go into the unit at a steady rate; not too fast or too slow. The results will be incorrect if some of the particles are left behind in heterogeneous mixtures (the larger particles may be left out).

g. The dry sampler only runs one sample at a time, so three runs must be executed for each sample.

h. Your supervisor will designate what the samples should be named. Behind each of the dry runs it helps to label each one behind the name – '_1', '_2', or '_3' so you know if it is run 1, 2, or 3 for the **dry samples**.

i. The wet sampler will also begin running a 'background' to check for particles left over, but unlike the dry sampler, it will perform all three runs in one measurement. Just make sure it is designated to perform 3 measurements. You can check this by clicking on the 'Measurement Cycles' tab in the SOP and see if it has 'Measurements **3** per aliquot' in the box before running the SOP.

j. When the SOP tells you to 'add sample' in the yellow box for the **wet sampler**, make sure you add the sample slowly. There should be a small 'spoon' or scooper beside the machine to use for adding the samples. Usually you don't need any more than half a scoop to get into the green area. Make sure the sample is within the green area of the bar so you don't add too much or too little sample. If you add too much and the bar goes above the green into the red area, start over. You will have to flush

out the SVDU again and restart the SOP. It only takes a little of the sample to perform the run. If you have added plenty of the sample and nothing is showing up on the bar, you might try turning up the RPM's on the *Dispersion Unit Controller*. This stirs up the sample making it more detectable. The controller is located on top of the Malvern and is a small box with a knob to adjust the RMP speed manually. You will have to set the RPM speed before running **wet samples** to ensure proper dispersion of the samples in the SVDU. The SOP will automatically recommend a stirring speed, but this sometimes needs to be adjusted for different samples.

k. ***Be careful not to set the stirrer speed too high** because this may form bubbles and severely mess up your data because the unit detects the bubbles as sample particles.

l. The **dry sampler** will complete the run and ask you if you want to run the SOP again. Click 'yes' if you want to continue running the same type of samples and 'no' if you are done or want to view the results. Make sure you clean out the tray before starting the SOP again. The **wet sampler** will take you through the process step-by-step giving you instructions in the yellow box in the SOP pop-up window. The instructions will tell you when to add the sample so DO NOT add the sample before beginning. Once the sampler is done it will ask you if you want to run the same SOP and you can respond as stated above.

m. Do not forget that the **wet sampler** needs to be flushed out with ethanol 2-3 times after each run as in the beginning.

5. View your Results

a. To view the results, highlight the samples you want to view and click on the tab '**Result Analysis (M)**'. If you want to see more than one, just hold down the shift or control keys to highlight multiple samples.

b. You can also create an average of several different runs. Highlight the samples you want an average for and click on the '**Edit'** menu and select '**Create average result**'.

c. The parameters for the um in the result analysis should be **d(.159)**, **d(.5)**, **d(.841)** which is the same as 15.9%, 50%, and 84.1%.

6. When you are done running samples for the day

a. It is okay to leave the Mastersizer on. It is built to run nonstop but if you prefer to shut it down, that is okay too. I do recommend turning the computer off or at least turning the screen off. There should be a surge protector for all the equipment in case of an electrical storm.

7. Exporting files

a. The Mastersizer 2000 can export files into Excel or Access automatically or you can do it after you finish running samples.

b. You must first set up a file in the program you want to export to so the data has a place to go.

c. Make sure you are on the '**Results**' tab. Highlight the samples you want to export.

d. Click on '**File**' and '**Export Data**'.

e. A pop-up box will appear. You should choose '**Use commas as separators**' and '**Include header row**' under '**Format Options**'.

f. '**Overwrite**' to file means it will completely replace what is currently in the file you are exporting to. '**Append**' to file means it will just add what you have selected to the file you are exporting to without replacing what is already there.

8. What else do you need to know?

Cleaning the lenses:

a. You will need to clean the lenses on the insertable units occasionally. The program should tell you when it needs to be cleaned but you may have to check it anyway if the SOP does not want to start running.

b. You clean the lenses using camera or lens cleaning tissues.

c. The outside of the lenses can be cleaned by taking the unit out of its holder (cradle) and gently wiping of the lens on both sides. This will usually suffice for getting the SOP to run. The inside of the lenses can be cleaned but you have to carefully remove them using the special tool provided.

d. The tool is located on the inside of the HYDRO unit's case in the front. It is shaped like a cylinder.

e. One end of the tool has two notches in it. Insert the notches into the holes on the sides of the lens and turn it counter-clockwise. Turn the unit with the lens on its side

so that the lens falls out onto the tool (don't drop it!). Clean the inside of the lens by gently wiping it off also. Try to remove as many of the particles as possible.

f. After cleaning, gently reinsert the lens into the unit using the tool. Tighten the lens by turning it clock-wise with the tool about a forth of a turn. DO NOT OVER-TIGHTEN – THIS WILL CRACK THE LENS!

g. Put the cleaning tool back in its holder.

Other Settings & Calculations:

a. The most common calculation you may have to perform is finding the GSD or Geometric Standard Deviation. 1) First find the MMD (Mass Median Diameter) in the 'Results Analysis' which is the d(.5) and also use the d(.841) and d(.159). The formula is simple:

$$\frac{[d(.841)/d(.5)]+[d(.5)/d(.1)]}{2} = GSD$$

b. The blue bar on the SOP represents the obscuration (range). When running smaller particles (2 micron) you want to keep the obscuration low (1-2%). When running large particles (1000 micron), you can have obscuration limits higher (30%).

c. In a multiple compound, it is more important to use the smaller particles refractive index.

d. A good indicator of RI (refractive index) is the “weighted residual” which should be less than 1. “Fit” is also a good indicator.

e. 10-12 seconds is usually an adequate amount of time for the dry sampler setting regarding running time for pulling the sample into the unit. Change this using ‘Edit SOP’.

f. You may need to adjust the **Vibration Feed Rate** and the **Dispersive Air Pressure** when using the dry sampler which is found under the **Sampler Settings** tab in ‘Edit SOP’.

g. Make sure you enter a **sample name** and **source type** when saving results. You can change the sample name each time, but the source type remains fixed unless you edit the SOP.

h. The **Report/Saving** tab lets you set up whether you want to automatically export the results of the measurements. You can also change this using ‘Edit SOP’.

i. When using the **wet sampler** you will most likely need to select Silica 1.0 as your material and Ethanol as the dispersant. This can be adjusted in the ‘Edit SOP’ under the **Materials** tab.

j. A 10 second background and measurement time should be adequate for the **wet sampler**.

APPENDIX H

RESULTS OF ANALYSIS OF DATA FROM WIND TUNNEL EXPERIMENTS

Table H.1. Cut-points, slopes and concentrations of flat-head PM_{10} sampler.

Independent Parameters			Cut-point (um)			Slope			Concentration (ug/m3)		
Dust type	**Wind Speed (kph)**	**Target Concentration ($\mu g/m^3$)**	**Rep 1**	**Rep 2**	**Rep 3**	**Rep 1**	**Rep 2**	**Rep 3**	**Rep 1**	**Rep 2**	**Rep 3**
Ultrafine ARD	2	150	9.21	10.31	10.47	2.16	1.71	2.25	130.96	145.28	145.7404
Ultrafine ARD	2	300	10.92	12.22	11.89	1.32	1.56	2.24	321.295	194.364	276.5946
Ultrafine ARD	2	500	14.86	13.13	14.43	2.53	2.27	2.47	445.39	472.976	479.049
Ultrafine ARD	2	1000	25.67	18.56	18.19	4.26	1.76	1.93	1226.39	542.096	953.146
Ultrafine ARD	2	1500	23.59	17.45	22.97	2.27	2.16	2.26	1805.845	1447.86	1710.776
Ultrafine ARD	8	150	10.63	13.43	14.42	1.34	1.54	2.36	161.567	155.5505	167.9118
Ultrafine ARD	8	300	16.8	17.32	15.8	2.2	2.56	2.23	336.98	321.146	345.6781
Ultrafine ARD	8	500	9.58	12.56	13.21	1.63	4.5	1.78	287.1155	425.2535	366.9557
Ultrafine ARD	8	1000	8.64	8.34	11.6	1.61	1.87	1.93	983.01	1335.485	1192.496
Ultrafine ARD	8	1500	7.94	7.89	9.52	1.6	2.01	1.83	1744.593	1807.085	1846.8
Ultrafine ARD	24	150	13.47	15.73	14.25	1.82	3.15	1.42	141.585	176.391	166.5213
Ultrafine ARD	24	300	14.59	16.21	17.11	1.18	1.35	1.21	302.892	233.166	284.6278
Ultrafine ARD	24	500	18.19	16.74	18.14	1.2	1.14	1.44	608.49	683.058	670.9894
Ultrafine ARD	24	1000	20.99	20.99	20.75	2.23	2.23	1.5	642	1042.923	860.8584
ARD	2	150	12.99	12.25	13.49	2.19	1.33	2.34	93.92	96.283	96.43787
ARD	2	300	8.54	9.28	9.3	2.1	1.85	2.12	226.04	218.757	229.1497
ARD	2	500	7.89	7.77	9.53	2.43	3.38	2.44	392.8	271.887	340.3493
ARD	2	1000	6.41	6.15	6.83	1.71	2.72	2.72	1080	392.2765	743.8935
ARD	2	1500	8.79	8.95	7.57	4.12	3.6	3.4	1070	515.2015	807.2168
ARD	8	150	18.21	15.5	14.82	2.33	2.3	2.37	94.303	84.12	89.87507
ARD	8	300	17.68	12.92	12.42	1.29	2.1	2.11	185.295	183.144	189.4195
ARD	8	1000	14.89	9.57	9.08	2.82	2.63	2.44	679.0355	699.4944	717.9268
ARD	8	1500	9.57	7.08	8.64	2.53	3.43	2.75	804.7435	771.4896	819.481
ARD	24	150	8.71	11.99	10.52	5.78	3.24	3.37	73.9035	96.42	86.70582

Table H.1. Continued

Independent Parameters			Cut-point (um)			Slope			Concentration (ug/m3)		
Dust type	**Wind Speed (kph)**	**Target Concentration ($\mu g/m^3$)**	**Rep 1**	**Rep 2**	**Rep 3**	**Rep 1**	**Rep 2**	**Rep 3**	**Rep 1**	**Rep 2**	**Rep 3**
ARD	24	300	7.47	11.02	9.21	8.25	2.49	2.44	141.948	235.84	197.4257
ARD	24	500	5.5	8.65	6.76	2	3.51	3.21	312.5025	313.444	324.0676
ARD	24	1000	6.5	7.83	6.13	8.5	3.64	3.64	479.655	596.864	563.2705
Cornstarch	2	150	17.09	7.76	9.13	2.94	3.01	2.83	75.93	113.214	101.7309
Cornstarch	2	300	13.97	7.36	8.42	3.16	1.37	1.82	95.454	122.37	116.3153
Cornstarch	2	500	7.93	6.19	6.48	2.33	3	3.07	153.516	144.456	156.7046
Cornstarch	2	1000	8.14	7.09	6.27	2.64	3.81	2.83	211.134	165.462	196.2566
Cornstarch	2	1500	8.05	8.35	5.87	4.8	2.44	2.54	234.21	335.7	305.9558
Cornstarch	8	150	7.11	7.81	8.92	2.41	2.17	2.02	93.21	72.52	94.73635
Cornstarch	8	300	7.9	8.9	13.45	2.17	4.5	2.94	220	202.307	230.2381
Cornstarch	8	500	8.14	13.01	12.98	2.21	2.32	2.19	254.55	314.027	311.4469
Cornstarch	8	1000	11.22	16.3	15.31	2.17	2.1	2.07	474.28	334.509	427.6982
Cornstarch	8	1500	19.64	16.37	18.86	2.42	1.41	2.33	443.23	459.69	485.5545
Cornstarch	24	150	10.38	15.49	12.73	2.62	1.51	2.41	82.275	94.305	109.7775
Cornstarch	24	300	15.03	18.38	14.32	2.17	1.39	1.83	122.12	237.5	211.757
Cornstarch	24	500	19.79	18.37	17.89	1.41	1.47	1.63	200.68	308.39	290.1892

Table H.2. Cut-points, slopes and concentrations of louvered PM_{10} sampler.

Independent Parameters			Cut-point (um)			Slope			Concentration (ug/m3)		
Dust type	**Wind Speed (kph)**	**Target Concentration ($\mu g/m^3$)**	**Rep 1**	**Rep 2**	**Rep 3**	**Rep 1**	**Rep 2**	**Rep 3**	**Rep 1**	**Rep 2**	**Rep 3**
Ultrafine ARD	2	150	8.81	11.32	11.12	2.30	1.63	2.62	123.45	144.04	140.91
Ultrafine ARD	2	300	11.15	12.57	12.23	1.44	1.64	6.48	305.00	178.86	260.02
Ultrafine ARD	2	500	14.36	13.81	14.78	2.55	2.71	2.69	483.92	530.81	528.29
Ultrafine ARD	2	1000	17.70	16.03	17.23	1.91	1.45	4.13	1350.51	557.55	1030.61
Ultrafine ARD	2	1500	22.43	19.11	21.03	2.86	1.24	2.54	1775.45	1301.46	1624.06
Ultrafine ARD	8	150	11.67	12.26	14.60	1.69	1.74	2.10	162.34	162.17	171.50
Ultrafine ARD	8	300	18.53	14.57	15.66	2.34	3.20	2.88	330.11	295.00	329.38
Ultrafine ARD	8	500	12.99	13.83	12.69	1.61	2.51	2.86	287.13	487.68	396.62
Ultrafine ARD	8	1000	7.11	9.87	12.81	1.38	1.67	3.32	1144.71	1406.11	1317.40
Ultrafine ARD	8	1500	9.58	8.93	8.60	1.71	1.68	1.80	1739.79	1904.88	1890.54
Ultrafine ARD	24	150	14.94	17.77	14.66	1.52	2.13	2.94	133.20	191.51	168.96
Ultrafine ARD	24	300	13.88	15.54	16.24	1.41	1.42	2.50	299.88	228.62	280.77
Ultrafine ARD	24	500	16.73	16.31	17.93	2.02	1.15	1.28	588.57	599.62	620.10
Ultrafine ARD	24	1000	21.10	19.73	20.21	1.22	2.02	1.34	619.60	1015.55	835.20
ARD	2	150	11.02	12.20	12.65	2.32	1.41	2.41	93.85	82.72	88.88
ARD	2	300	9.19	7.92	8.79	1.99	3.03	2.25	242.79	210.16	232.58
ARD	2	500	8.20	10.14	10.86	2.87	1.98	2.75	396.72	249.65	329.93
ARD	2	1000	7.78	6.68	7.35	3.33	2.87	3.03	790.00	402.50	607.47
ARD	2	1500	8.43	8.61	7.25	4.22	3.75	3.15	1080.00	506.14	807.09
ARD	8	150	18.25	12.79	14.71	2.34	2.00	2.42	98.42	59.07	77.99

Table H.2. Continued

ARD	8	300	17.51	14.20	12.22	1.69	1.90	2.16	210.07	164.22	191.06
ARD	8	500	13.47	16.50	12.33	2.55	2.54	2.92	551.84	228.51	394.21
ARD	8	1000	14.61	9.12	9.73	3.54	5.80	2.57	653.37	663.20	685.21
ARD	8	1500	9.12	6.35	8.25	2.44	3.50	2.93	783.97	737.20	790.27
ARD	24	150	7.87	12.59	10.02	5.43	5.96	3.32	73.08	85.57	80.28
ARD	24	300	6.10	12.05	9.41	5.20	2.95	2.66	139.03	210.51	181.94
ARD	24	500	5.43	9.12	5.83	2.05	2.32	3.05	309.88	254.88	290.28
ARD	24	1000	6.60	7.35	6.24	7.80	3.77	3.33	481.32	490.75	505.19
Cornstarch	2	150	18.01	8.51	9.34	3.35	2.12	3.09	86.21	75.98	85.02
Cornstarch	2	300	14.47	8.16	8.21	1.79	1.54	1.96	103.51	118.94	118.15
Cornstarch	2	500	9.21	5.80	6.76	3.33	3.54	3.22	157.64	110.89	139.19
Cornstarch	2	1000	6.81	6.51	6.84	2.71	3.45	2.93	218.07	156.88	194.57
Cornstarch	2	1500	8.01	8.99	6.12	4.75	2.13	2.36	233.10	337.81	306.65
Cornstarch	8	150	7.52	9.84	9.13	1.85	1.63	2.57	107.93	76.79	104.20
Cornstarch	8	300	7.93	8.93	15.22	1.63	3.15	2.85	260.00	181.38	237.10
Cornstarch	8	500	8.62	14.39	13.79	2.07	3.17	2.37	344.71	356.80	379.08
Cornstarch	8	1000	10.03	13.82	15.64	2.13	1.94	1.95	524.79	377.18	476.44
Cornstarch	8	1500	16.45	16.94	19.21	3.33	1.61	1.99	477.94	306.81	413.37
Cornstarch	24	150	9.35	14.61	11.27	2.29	1.56	2.21	86.38	86.53	107.22
Cornstarch	24	300	18.19	18.45	14.76	2.66	1.33	1.85	146.87	139.10	166.44
Cornstarch	24	500	20.22	21.47	19.10	1.36	1.45	1.66	244.79	319.26	317.44

Table H.3. MMDs, GSDs and concentrations of dome-top TSP sampler.

Independent Parameters			MMD (µm)			GSD			Concentrations (µg/m^3)		
Dust type	**Wind Speed (kph)**	**Target Concentration (µg/m^3)**	**Rep 1**	**Rep 2**	**Rep 3**	**Rep 1**	**Rep 2**	**Rep 3**	**Rep 1**	**Rep 2**	**Rep 3**
Ultrafine ARD	2	150	4.40	5.25	4.84	2.04	2.18	2.14	162.50	180.06	180.08
Ultrafine ARD	2	300	4.15	4.70	4.53	2.62	2.04	2.34	390.52	256.79	345.36
Ultrafine ARD	2	500	4.88	5.20	5.27	1.99	2.26	2.15	602.14	628.14	641.31
Ultrafine ARD	2	1000	3.71	5.10	4.47	1.99	2.08	2.06	1487.14	755.00	1201.60
Ultrafine ARD	2	1500	4.40	5.00	4.81	2.05	2.06	2.08	2178.78	1658.36	2021.47
Ultrafine ARD	8	150	4.53	4.80	4.79	2.04	1.99	2.03	162.45	185.59	182.68
Ultrafine ARD	8	300	4.62	4.90	4.89	2.09	2.09	2.11	365.98	365.68	383.22
Ultrafine ARD	8	500	4.77	4.75	4.56	2.00	2.02	2.03	417.14	563.84	506.25
Ultrafine ARD	8	1000	4.48	5.18	4.94	1.95	1.98	1.99	1196.30	1632.62	1454.14
Ultrafine ARD	8	1500	4.30	5.03	4.77	1.97	2.02	2.02	2006.17	2287.03	2222.56
Ultrafine ARD	24	150	4.04	4.86	4.55	1.93	2.16	2.07	159.27	204.66	189.94
Ultrafine ARD	24	300	4.10	4.80	4.55	2.00	2.01	2.03	308.33	319.90	328.90
Ultrafine ARD	24	500	4.32	4.49	4.43	1.99	2.12	2.08	615.79	769.65	716.24
Ultrafine ARD	24	1000	4.13	4.84	4.60	2.00	2.01	2.03	671.44	1167.20	936.52
ARD	2	150	6.55	9.89	9.77	2.70	2.50	2.62	158.66	173.82	171.19
ARD	2	300	8.02	9.57	8.66	2.84	2.85	2.87	520.85	254.31	393.34
ARD	2	500	6.37	10.35	9.85	3.68	2.85	3.27	851.07	419.81	647.00
ARD	2	1000	5.89	10.91	8.87	2.30	2.80	2.59	1748.89	710.93	1248.50
ARD	2	1500	5.05	6.02	5.75	2.58	2.38	2.50	1838.07	939.29	1418.94
ARD	8	150	7.12	17.86	11.15	2.38	3.35	2.92	158.63	195.44	183.18
ARD	8	300	6.08	8.09	11.22	2.84	2.62	2.75	304.36	428.51	383.94
ARD	8	500	7.25	5.73	10.09	3.04	2.36	2.71	717.92	543.85	650.59

Table H.3. Continued

Dust type	Wind Speed (kph)	Target Concentration (µg/m^3)	Rep 1	Rep 2	Rep 3	Rep 1	Rep 2	Rep 3	Rep 1	Rep 2	Rep 3
ARD	8	1000	7.25	5.95	9.19	2.55	2.29	2.44	1289.00	1736.44	1592.31
ARD	8	1500	6.00	6.05	9.32	2.50	2.22	2.38	1234.94	1301.75	1324.57
ARD	24	150	6.68	9.96	10.06	2.70	2.88	2.82	148.73	204.54	183.38
ARD	24	300	5.95	9.66	9.68	2.19	3.26	2.78	332.03	460.76	415.40
ARD	24	500	5.10	12.98	10.59	2.58	2.84	2.74	809.91	559.54	704.38
ARD	24	1000	5.64	10.56	10.11	2.44	2.90	2.71	1017.69	1318.11	1227.20
Cornstarch	2	150	16.20	21.38	15.10	1.67	2.24	1.99	190.36	218.00	216.86
Cornstarch	2	300	15.74	13.10	15.23	1.56	1.88	1.75	319.47	314.00	333.87
Cornstarch	2	500	14.80	12.40	14.36	1.62	2.88	2.31	471.46	462.18	492.01
Cornstarch	2	1000	16.00	15.26	15.77	1.72	1.95	1.86	663.30	617.08	672.98
Cornstarch	2	1500	16.45	12.80	14.45	1.70	1.83	1.79	601.36	1149.97	952.63
Cornstarch	8	150	13.30	9.90	12.30	1.83	2.50	2.21	158.87	192.59	195.57
Cornstarch	8	300	14.30	11.80	13.79	1.82	2.22	2.05	310.51	491.24	440.81
Cornstarch	8	500	13.05	10.00	12.21	2.03	2.08	2.08	485.04	670.83	627.88
Cornstarch	8	1000	20.20	13.85	18.10	1.60	2.99	2.36	603.22	858.88	793.08
Cornstarch	8	1500	20.95	11.50	17.37	2.32	2.00	2.17	805.25	919.68	924.31
Cornstarch	24	150	20.88	14.90	18.86	1.68	1.75	1.73	220.35	317.09	304.58
Cornstarch	24	300	16.25	13.90	17.99	2.03	1.76	1.91	274.33	417.15	388.25
Cornstarch	24	500	17.52	15.05	18.69	1.78	1.68	1.74	495.68	635.46	620.01

Table H.4. MMDs, GSDs and concentrations of cone-top TSP sampler.

Independent Parameters			MMD (µm)			GSD			Concentrations (µg/m^3)		
Dust type	**Wind Speed (kph)**	**Target Concentration (µg/m^3)**	**Rep 1**	**Rep 2**	**Rep 3**	**Rep 1**	**Rep 2**	**Rep 3**	**Rep 1**	**Rep 2**	**Rep 3**
Ultrafine ARD	2	150	2.79	4.5	3.68	2.14	2.06	2.16	122.125	155.628	145.6639
Ultrafine ARD	2	300	4.4	4.7	4.67	2.32	2.1	2.27	344.71	202.94	293.8977
Ultrafine ARD	2	500	4.73	5.05	5.02	2.02	2.13	2.14	395.365	581.472	502.3204
Ultrafine ARD	2	1000	3.7	4.95	4.40	1.98	2.02	2.06	1208.545	765.84	1049.342
Ultrafine ARD	2	1500	4.25	4.75	4.61	1.93	2.04	2.05	1560.775	1525.908	1609.384
Ultrafine ARD	8	150	4.21	4.7	4.57	2	2.31	2.23	136.71	151.998	152.1802
Ultrafine ARD	8	300	4.36	4.95	4.77	2.02	1.97	2.05	308.3955	321.3315	329.6159
Ultrafine ARD	8	500	4.4	4.3	4.49	2	1.87	1.99	267.267	466.6585	375.4086
Ultrafine ARD	8	1000	4.62	4.5	4.70	2.08	2.05	2.13	909.468	1159.123	1067.173
Ultrafine ARD	8	1500	4.77	4.5	4.79	2.03	2.05	2.10	1297.744	1610	1500.715
Ultrafine ARD	24	150	4.52	4.84	4.81	1.98	2.38	2.25	91.41	120.726	111.7315
Ultrafine ARD	24	300	3.93	4.75	4.43	2	2.3	2.22	257.757	276.444	279.6836
Ultrafine ARD	24	500	4.51	4.38	4.58	2.11	2.1	2.17	504.174	769.83	653.2676
Ultrafine ARD	24	1000	4.37	4.4	4.52	2.04	2.04	2.10	853.245	985.926	953.1383
ARD	2	150	5.05	8.67	7.61	3.29	3.49	3.50	192.65	153.23	176.4212
ARD	2	300	5.54	9.4	8.30	2.45	3.24	2.95	432.95	379.3075	419.6412
ARD	2	500	5.4	9.45	8.22	2.62	3.08	2.94	698.3	471.955	601.082
ARD	2	1000	8.66	8.47	10.04	3.94	3.02	3.57	1736.29	729.7455	1252.771
ARD	2	1500	6.2	5.75	7.04	2.96	2.6	2.86	1198.49	845.6745	1053.589
ARD	8	150	6.65	6.75	7.83	2.74	3.38	3.16	119.0035	105.4992	113.8438
ARD	8	300	4.6	10.6	8.20	2.74	3	2.96	248.9905	218.2272	240.1014

Table H.4. Continued

ARD	8	500	4.6	5.55	5.83	2.74	2.69	2.80	650.485	346.728	508.1517
ARD	8	1000	5.05	6.4	6.54	2.47	2.86	2.75	944.1355	869.8176	942.3552
ARD	8	1500	4.66	5.65	5.92	2.36	2.64	2.58	1101.254	1450.666	1341.714
ARD	24	150	5.67	11.68	7.11	2.37	2.66	2.60	41.805	147.472	99.31141
ARD	24	300	6.24	8.33	8.28	2.92	3.41	3.27	276.309	286.096	291.1547
ARD	24	500	4.48	14.64	5.32	2.42	3.24	2.93	588.5505	442.528	530.9728
ARD	24	1000	5.03	5.25	5.99	2.97	2.25	2.67	769.815	1203.896	1042.352
Cornstarch	2	150	15.1	12.3	13.87	2.11	2.24	2.24	151.734	75.444	115.8312
Cornstarch	2	300	17.4	14.9	16.40	1.79	2.04	1.98	176.574	189.87	193.9973
Cornstarch	2	500	18	13.8	16.04	1.65	2.59	2.20	266.136	465.342	396.313
Cornstarch	2	1000	18.47	12.5	15.50	1.85	2.09	2.03	383.616	545.862	498.8176
Cornstarch	2	1500	13.4	12.9	13.45	1.91	2.9	2.50	455.442	658.776	598.425
Cornstarch	8	150	12.56	13.2	13.24	1.54	2.02	1.84	133.1	139.44	152.4977
Cornstarch	8	300	15.65	12.6	14.29	1.88	2.53	2.28	237.62	199.507	236.9836
Cornstarch	8	500	14.2	12.8	13.75	2.69	2.51	2.67	335.4	250.831	313.197
Cornstarch	8	1000	39.3	13.2	25.28	2.52	1.91	2.27	589.08	380.38	508.8334
Cornstarch	8	1500	14.8	12.9	14.08	1.82	2.21	2.08	466.84	445.662	488.633
Cornstarch	24	150	17.7	13.25	15.58	1.99	1.85	1.97	148.805	161.195	180.1755
Cornstarch	24	300	16.45	14.4	15.68	2.05	2.08	2.13	189.795	290.49	274.6368
Cornstarch	24	500	17.7	13.9	15.96	1.8	1.86	1.89	258.74	259.715	289.5362

Table H.5. MMDs, GSDs and concentrations of Isokinetic sampler.

Independent Parameters			MMD (µm)			GSD			Concentrations (µg/m^3)		
Dust type	**Wind Speed (kph)**	**Target Concentration (µg/m^3)**	**Rep 1**	**Rep 2**	**Rep 3**	**Rep 1**	**Rep 2**	**Rep 3**	**Rep 1**	**Rep 2**	**Rep 3**
Ultrafine ARD	2	150	4.3	6.8	4.23	2.09	3.93	2.11	181.54	196.61	198.70
Ultrafine ARD	2	300	4.52	5	4.67	2.14	2.41	2.1	422.38	288.65	378.49
Ultrafine ARD	2	500	4.61	4.9	4.54	2.09	1.99	2.11	664.50	705.26	713.18
Ultrafine ARD	2	1000	3.97	5.05	4.02	2.03	2.04	2.09	1859.35	857.14	1460.41
Ultrafine ARD	2	1500	4.57	4.9	4.49	1.98	2.09	1.95	1752.68	1697.58	1799.36
Ultrafine ARD	8	150	4.62	5.35	4.75	2.04	2.07	2.01	171.16	262.16	223.97
Ultrafine ARD	8	300	4.5	5.3	4.33	2.12	2.13	2.13	431.58	503.14	485.57
Ultrafine ARD	8	500	5.05	5	5.08	2.12	1.86	2.08	538.56	650.44	615.98
Ultrafine ARD	8	1000	4.5	5.2	4.56	2.1	2.11	2.2	1545.66	2035.93	1843.10
Ultrafine ARD	8	1500	4.83	5.08	4.73	2	2.07	2.1	2363.61	2958.58	2743.50
Ultrafine ARD	24	150	4.5	5.2	4.5	2.16	2.46	2.19	175.64	196.50	195.32
Ultrafine ARD	24	300	4.62	5.35	4.62	1.96	2.07	1.94	335.33	649.97	500.94
Ultrafine ARD	24	500	4.34	5.75	4.31	2.07	3.48	2.01	614.77	1402.82	1016.42
Ultrafine ARD	24	1000	3.97	5.2	4.08	2.03	1.95	2.04	1376.47	2260.98	1854.41
ARD	2	150	6.05	11.45	10.23	2.27	4.42	3.48	177.10	189.31	188.83
ARD	2	300	7.24	10.6	9.72	2.52	2.86	2.83	471.78	480.13	494.63
ARD	2	500	6.11	11.65	11.07	2.85	3.22	3.15	794.92	530.73	681.05
ARD	2	1000	6.24	11.8	11.46	2.67	3.27	3.2	1358.37	829.86	1123.15
ARD	2	1500	4.76	6.41	10.45	2.65	2.4	2.38	1695.36	1165.50	1474.56
ARD	8	150	8.02	19.58	12.23	3.74	4.29	4.34	225.39	206.70	222.14
ARD	8	300	6.6	9.6	12.03	2.92	3.18	3.18	453.73	453.02	470.74
ARD	8	500	6.56	6	11.49	2.59	2.67	2.7	873.73	746.07	839.18
ARD	8	1000	6.27	6	10.88	2.84	2.69	2.65	1541.32	2010.04	1867.80

Table H.5. Continued

ARD	8	1500	6.15	7	10.76	2.86	2.72	2.74	1801.44	2267.64	2138.23
ARD	24	150	6.05	11.25	11.22	2.92	3.17	3	222.99	198.96	216.67
ARD	24	300	6.9	10.38	10.94	2.43	2.93	2.87	353.51	415.50	400.80
ARD	24	500	4.21	14.9	12.23	2.69	3.8	3.14	824.03	1098.00	1010.15
ARD	24	1000	4.62	11.45	11.56	3.01	3.36	3.24	1362.29	998.51	1218.68
Cornstarch	2	150	15.72	23.8	16.44	1.76	2.48	1.84	268.91	220.03	255.35
Cornstarch	2	300	14.85	14.2	14.52	1.62	1.79	1.61	339.01	568.82	490.95
Cornstarch	2	500	15.7	13.9	13.81	1.79	1.867	1.56	497.09	514.97	534.80
Cornstarch	2	1000	17.45	17.5	17.33	1.9	2.07	1.93	633.32	780.43	753.48
Cornstarch	2	1500	17.35	14	15.5	1.94	1.61	1.94	1284.50	1115.86	1257.34
Cornstarch	8	150	14.52	13.9	14.12	1.75	2.19	1.69	212.08	203.40	227.11
Cornstarch	8	300	15.7	12.75	15.65	2	2	2.09	549.78	391.71	496.74
Cornstarch	8	500	12.86	15.7	13.76	1.89	2.31	1.93	758.54	637.50	738.46
Cornstarch	8	1000	18.36	14.6	16.97	1.73	1.8	1.72	1032.96	844.62	988.94
Cornstarch	8	1500	19.21	12.8	15.66	1.69	1.98	1.65	2195.60	1084.49	1680.31
Cornstarch	24	150	22.18	15.4	21.34	2.05	1.77	2	305.50	212.90	284.59
Cornstarch	24	300	17.41	17	20.6	2	2.36	2.04	380.35	447.10	455.98
Cornstarch	24	500	18.81	31.1	22.21	1.72	2.42	1.62	504.33	588.38	596.82

Table H.6. Cut-points and slopes of dome-top TSP sampler.

Independent Parameters			Cut-point (µm)			Slope		
Dust type	**Wind Speed (kph)**	**Target Concentration (µg/m^3)**	**Rep 1**	**Rep 2**	**Rep 3**	**Rep 1**	**Rep 2**	**Rep 3**
Ultrafine ARD	2	150	29.89	25.68	27.96	1.24	1.62	1.28
Ultrafine ARD	2	300	22.98	24.21	22.41	1.5	1.38	1.35
Ultrafine ARD	2	500	20.44	32.56	23.24	1.35	1.32	1.32
Ultrafine ARD	2	1000	26.34	22.83	25.24	1.22	1.23	1.28
Ultrafine ARD	2	1500	28.33	18.56	26.68	1.04	1.05	1.21
Ultrafine ARD	8	150	21.86	12.62	23.21	1.86	1.89	2.2
Ultrafine ARD	8	300	28.57	34.18	21.08	1.32	1.4	1.49
Ultrafine ARD	8	500	29.89	22.01	22.01	2.41	1.31	1.21
Ultrafine ARD	8	1000	23.21	19.23	22.96	1.53	1.22	1.29
Ultrafine ARD	8	1500	29.66	25.45	27	2.05	1.35	1.31
Ultrafine ARD	24	150	22.38	19.87	22.86	2.11	1.58	2.11
Ultrafine ARD	24	300	28.49	21.34	29.47	2.09	2.19	2.29
Ultrafine ARD	24	500	23.88	14.5	24.53	2.29	2.23	2.41
Ultrafine ARD	24	1000	27.67	13.21	28.29	2.09	3.37	3.12
ARD	2	150	24.5	28.73	24.61	1.36	1.35	1.36
ARD	2	300	36.6	35.76	34.6	2.07	1.72	1.27
ARD	2	500	41.8	35.21	41.87	1.9	1.91	1.69
ARD	2	1000	34.29	34.3	34.29	1.89	1.34	1.88
ARD	2	1500	35.01	27.64	40.03	1.29	2.31	2.31
ARD	8	150	28.6	25.3	26.64	1.27	3.07	2.95

Table H.6. Continued

ARD	8	300	45.01	26.9	29.61	1.38	1.64	1.64
ARD	8	500	23.31	29.99	29.4	2.48	1.65	1.62
ARD	8	1000	37.22	34.29	31.23	1.43	1.46	1.57
ARD	8	1500	21.27	35.47	24.21	1.62	1.63	1.61
ARD	24	150	35.01	27.52	25.45	2.93	2.3	2.65
ARD	24	300	33.09	43.21	32.21	1.45	1.65	1.59
ARD	24	500	31.52	23.14	34.21	2.06	2.22	2.21
ARD	24	1000	25.32	27.73	28.97	2.4	1.67	2.81
Cornstarch	2	150	25.99	24.72	22.69	1.53	1.49	1.59
Cornstarch	2	300	25.11	24.11	24.56	1.68	1.63	1.55
Cornstarch	2	150	25.99	24.72	22.69	1.53	1.49	1.59
Cornstarch	2	300	25.11	24.11	24.56	1.68	1.63	1.55
Cornstarch	2	1500	36.43	34.23	37	1.38	2.23	2.21
Cornstarch	8	150	41.85	27.43	25.94	1.11	2.13	2.26
Cornstarch	8	300	29.5	23.21	23.64	1.45	2.16	2.13
Cornstarch	8	500	37.44	23.8	28.81	1.43	1.82	1.75
Cornstarch	8	1000	30.43	42.32	34.32	1.66	1.21	1.15
Cornstarch	8	1500	42.61	42.6	32.12	2.31	2.25	2.51
Cornstarch	24	150	56.22	24.98	24.56	2.05	1.22	1.26
Cornstarch	24	300	28.88	31.99	29.92	1.38	2.43	1.25
Cornstarch	24	500	24.45	26.58	26.54	1.59	1.5	1.46

Table H.7. Cut-points and slopes of cone-top TSP sampler.

Independent Parameters			Cut-point (µm)			Slope		
Dust type	**Wind Speed (kph)**	**Target Concentration (µg/m^3)**	**Rep 1**	**Rep 2**	**Rep 3**	**Rep 1**	**Rep 2**	**Rep 3**
Ultrafine ARD	2	150	24.42	23.32	23.49	2.43	1.54	1.46
Ultrafine ARD	2	300	23.32	29.82	22.89	2.45	1.33	1.34
Ultrafine ARD	2	500	27.35	37.99	37.98	2.4	1.36	1.38
Ultrafine ARD	2	1000	27.34	22.08	26.99	2.29	1.32	1.33
Ultrafine ARD	2	1500	23.73	23.51	22.87	2.82	1.78	1.78
Ultrafine ARD	8	150	22.79	45.98	31.16	2.6	1.54	1.55
Ultrafine ARD	8	300	23.39	24.66	28.81	2.84	1.61	1.64
Ultrafine ARD	8	500	28.12	26.72	30.6	2.27	1.28	2.21
Ultrafine ARD	8	1000	21.09	16.78	34.13	1.5	1.87	2.04
Ultrafine ARD	8	1500	22.32	18.98	25.92	1.91	2.03	2.09
Ultrafine ARD	24	150	23.09	18.56	27.87	2.04	2.14	2.41
Ultrafine ARD	24	300	20.87	24.93	22.91	2	2.54	2.26
Ultrafine ARD	24	500	24.54	14.87	25.89	2.05	2.63	2.28
Ultrafine ARD	24	1000	29.73	12.77	28.11	3.43	3.65	3.41
ARD	2	150	46.65	41.55	46.5	1.27	1.28	1.27
ARD	2	300	48	45.32	38.06	2.63	2.43	2.33
ARD	2	500	54.21	46.09	57.12	2.45	2.46	2.16
ARD	2	1000	43.13	41.23	44.13	2.19	2.19	2.29
ARD	2	1500	30.67	32.67	53.06	2.09	2.41	2.31
ARD	8	150	23.57	24.74	24.16	2.81	3.23	3.18
ARD	8	300	35.41	24.89	44.23	1.58	1.67	1.78

Table H.7. Continued

ARD	8	500	27.26	38.23	58.21	2.74	2.32	2.34
ARD	8	1000	34.65	73.2	42.13	3.92	1.23	1.18
ARD	8	1500	22.86	23.44	28.21	2.85	1.86	1.82
ARD	24	150	42.17	42.33	42.29	1.14	2.31	1.24
ARD	24	300	37.51	57.21	44.18	1.56	1.75	1.54
ARD	24	500	33.58	53.87	64.21	1.36	1.44	1.41
ARD	24	1000	35.74	31.57	40.03	1.87	2.12	2.31
Cornstarch	2	150	37.08	25.43	23.41	1.64	1.32	1.51
Cornstarch	2	300	26.01	28.19	28.1	1.56	1.42	1.42
Cornstarch	2	500	19.65	25.43	22.31	1.94	1.7	1.76
Cornstarch	2	1000	19.12	22.35	22.96	2.48	2.06	2.13
Cornstarch	2	1500	34.81	41.11	45.21	2.28	2.34	2.24
Cornstarch	8	150	46.51	32.48	35.51	1.25	2.29	2.13
Cornstarch	8	300	33.54	38.88	38.79	1.23	1.85	1.54
Cornstarch	8	500	37.19	43.33	42.21	1.47	1.54	1.36
Cornstarch	8	1000	35.02	37.76	35.41	2.28	1.19	1.21
Cornstarch	8	1500	69.54	49.28	49.61	2.37	1.38	1.39
Cornstarch	24	150	44.27	32.3	33.61	2.41	3.01	2.61
Cornstarch	24	300	32.25	41.23	42.21	2.66	1.52	1.56
Cornstarch	24	500	25.09	22.43	22.38	1.95	1.66	1.54

VITA

Abhinav Guha graduated from University of Mumbai (Bombay), India with a Bachelor of Engineering (B.E) degree in Civil Engineering in June 2006. He then entered the Biological and Agricultural Engineering graduate program at Texas A&M University in January 2007 and received his Master of Science (M.S) degree in May 2009. During his graduate study, he served as the Vice President of the India Association, an organization promoting cultural and social activities amongst graduate Indian students in the campus for the year 2007-08. His research interests include air pollution engineering and the interaction between science and policy surrounding air quality issues. He plans to publish the findings of his research in a peer-reviewed journal.

In January 2009, Abhinav began working towards a Doctoral degree at the Department of Environmental Science, Policy and Management at the University of California, Berkeley. He may be reached at 250B, Hilgard Hall, University of California Berkeley, CA 94720. His e-mail is abhinavguha@berkeley.edu.